MITOPHAGY AND ITS SIGNALLING MECHANISMS IN SKELETAL MUSCLE

By

ALEX SEABRIGHT

A thesis submitted to

The School of Sport, Exercise and Rehabilitation Sciences

The University of Birmingham

For the Degree of

DOCTOR OF PHILOSOPHY

School of Sport, Exercise and Rehabilitation Sciences

University of Birmingham

September 2020

ACKNOWLEDGEMENTS

Firstly, I would like to thank Dr Yu-Chiang Lai for the first-class training that he has provided me with during my PhD. Without your enthusiasm and drive to produce high quality work, I am not sure that I would have achieved as much as I have over the past 3 years had I have taken a different path. To begin with, your hands-on approach to wet-lab-based skills training was exactly what I needed and for that I will be forever grateful. Since then, you have instilled in me a growing passion for research, and in doing so, you have helped me to realise my scientific potential.

To all my colleague's past (Ben Stocks, Jessica Dent, Nathan Hodson, Sophie Joanisse & Stephen Ashcroft) and present (Ibrahim Musa, Peter Dawson, Samuel Lord & Yusuke Nishimura) thank you for your continued support and guidance. Specifically, I would like to thank Stephen Ashcroft and Nathan Hodson for their contributions to my early training in cell culture. More recently, Ibrahim Musa and Samuel Lord, your willingness to assist me with projects alongside your own research has been commendable. I wish you all the very best with respect to your own careers and personal lives.

I would like to thank everyone in the Exercise Metabolism Research Group (EMRG) for giving me a platform to present my work throughout my PhD. A special mention also goes to Ryan Marshall whose willingness to discuss ideas and the latest and greatest research papers has provided me with endless entertainment.

Lastly, I would like to thank my immediate family and friends for their continued support and interest in my work. In particular, Katherine Britnell for the level of understanding that you have displayed over the past two years.

DECLARATIONS

I declare that all the work contained within this thesis is my own with the following exceptions:

1. The mito-QC mitophagy reporter construct was kindly provided by Dr Ian Ganley from the Medical Research Council (MRC) Protein Phosphorylation and Ubiquitylation Unit (PPU) at the University of Dundee.
2. Professor Miratul Muqit from MRC PPU at the University of Dundee kindly provided the PINK1 antibody and HEK293 FT cells.
3. MRC PPU Reagents and Services kindly shared the HALO-UBA^{UBQLN1} TUBE construct for bacterial expression.
4. Professor Richard Youle from the National Institute of Health, Bethesda, USA generously provided the PINK1 knockout cell line.
5. AMPK α1/α2 HEK293 deficient cells were kindly provided by Professor Grahame Hardie and were initially generated by Dr Alexander Gray. Both Professor Hardie and Dr Gray are based at the University of Dundee.
6. Figure 1.2 was obtained from "Mammalian mitophagy - from in vitro molecules to in vivo models". This is an open access article under the terms of the Creative Commons Attribution License, which permits use, distribution and reproduction in any medium, provided the original work is properly cited.
7. Permissions for the re-use of Figure 1.3 taken from "Visualizing and Modulating Mitophagy for Therapeutic Studies of Neurodegeneration" were obtained from Elsevier (publisher) - License Number: 4962550402239

8. Permissions for the re-use of Table 1.1 taken from “Investigating Mitophagy and Mitochondrial Morphology In Vivo Using *mito*-QC: A Comprehensive Guide” were obtained from Springer Nature (publisher) - License Number: 4960720373215
9. Dr Yu-Chiang Lai, as my supervisor, provided intellectual input throughout.

ABSTRACT

The reasons why skeletal muscle health undergoes unfavourable decline with increasing age are not well understood. One hypothesis that may explain the demise of skeletal muscle during ageing is linked to a reduced ability to selectively remove damaged and dysfunctional mitochondria in a process called mitophagy. At present, much of our understanding of the molecular mechanisms that regulate mitophagy is derived from work conducted in immortalised, cancer cell lines made to overexpress non-native proteins. Conversely, far less is known about the endogenous mechanisms that coordinate mitophagy in skeletal muscle. Thus, the aim of this thesis is to gain a deeper understanding of the endogenous signalling mechanisms that govern mitophagy in skeletal muscle. Herein, after making a stable C2C12 mito-QC skeletal muscle cell line, we discover that 5'-AMP-activated protein kinase (AMPK) activation by a small molecule, 991, promotes mitochondrial fission and induces mitophagy. From a mechanistic perspective, we demonstrate that AMPK mediates the phosphorylation and activation of mitochondrial fission factor (MFF), unc-51-like autophagy activating kinase 1 (ULK1) and TANK-binding kinase 1 (TBK1). Activation of MFF facilitates mitochondrial fission while activation of ULK1 and TBK1 helps to coordinate autophagosomal engulfment. Both of these steps are vital for efficient mitophagy. Meanwhile, having developed a ubiquitin pull-down assay to examine the most widely studied signalling nodes known to regulate mitophagy in immortalised cell lines, PTEN-induced kinase 1 (PINK1) and Parkin, we reveal some interesting findings. While it is possible to stimulate endogenous PINK1 kinase and Parkin E3 ligase activity in C2C12 skeletal muscle cells, we demonstrate that such activation requires prolonged, non-physiological treatment with the chemical protonophore carbonyl cyanide m-

chlorophenyl hydrazone (CCCP). Lastly, we integrate the findings contained within this thesis into the current literature while evaluating how mitophagy is regulated in muscle through the steps of mitochondrial fission, ubiquitylation and autophagosomal engulfment. In doing so, we identify the most critical questions within the field that are yet to be answered. Altogether, this thesis improves understanding of the molecular signalling mechanisms that regulate mitophagy in skeletal muscle.

LIST OF CONFERENCE ABSTRACTS AND COMMUNICATIONS

1. **Keystone Symposia: New insights into the Biology of Exercise, Keystone, USA, March 2020** - Poster Communication - AMPK activation induces mitophagy and promotes mitochondrial fission while activating TBK1 in a PINK1-Parkin independent manner.

2. **European Congress on Sports Science (ECSS), Czech Republic, July 2019 -** Oral YIA Communication - Investigating mechanisms of mitophagy in skeletal muscle cells.

3. **Life Sciences: Post-Translational Modifications and Cell Signalling, Nottingham, UK March 2019** - Flash Poster Communication - Investigating phosphorylation and ubiquitylation crosstalk in skeletal muscle mitophagy.

LIST OF PUBLICATIONS

1. **Seabright AP**, Fine NHF, Barlow JP, Lord SO, Musa I, Gray A, Bryant JA, Banzhaf M, Lavery GG, Hardie DG, Hodson DJ, Philp A, Lai YC. AMPK activation induces mitophagy and promotes mitochondrial fission while activating TBK1 in a PINK1-Parkin independent manner. FASEB Journal, 2020 Mar 23.

2. **Seabright AP**, Lai YC. Regulatory roles of PINK1-Parkin and AMPK in skeletal muscle mitophagy. Frontiers in Physiology, 2020 (Under review).

3. Elhassan YS, Kluckova K, Fletcher RS, Schmidt MS, Garten A, Doig CL, Cartwright DM, Oakey L, Burley CV, Jenkinson N, Wilson M, Lucas SJE, Akerman I, **Seabright A**, Lai YC, Tennant DA, Nightingale P, Wallis GA, Manolopoulos KN, Brenner C, Philp A, Lavery GG. Nicotinamide Riboside Augments the Aged Human Skeletal Muscle NAD^+ Metabolome and Induces Transcriptomic and Anti-inflammatory Signatures. Cell Reports, 2019 Aug 13.

4. Fenton CG, Webster JM, Martin CS, Fareed S, Wehmeyer C, Mackie H., Jones R, **Seabright AP**, Lewis JW, Lai Y. C, Goodyear CS, Jones SW, Cooper MS, Lavery GG, Langen R, Raza K, Hardy RS. Arthritis Research & Therapy, 2019 Aug 1.

LIST OF TABLES

Chapter 1

Table 1.1 Comparison of the methods available to assess mitophagy 23

Chapter 4

Supplementary Table 4.10 List of antibodies used 92

LIST OF FIGURES

Chapter 1

Figure 1.1 A schematic illustrating ubiquitin-dependent, receptor-dependent and lipid-dependent mitophagy 15

Figure 1.2 A schematic illustrating how the mito-QC, mt-Keima and mitoTimer reporters assess mitophagy 19

Figure 1.3 A schematic illustrating how mito-SRAI reports mitophagy 21

Chapter 3

Figure 3.1 Visualisation and quantification of mitophagy and mitochondrial morphology using C2C12 cells stably expressing mito-QC 45

Figure 3.2 Validation of ubiquitin pull-down technique in murine skeletal muscle cells and tissue 50

Figure 3.3 CCCP treatment induces endogenous PINK1 kinase activity and Parkin E3 ligase activity in skeletal muscle cells 51

Chapter 4

Figure 4.1 CCCP treatment induces mitophagy and promotes mitochondrial fission in skeletal muscle cells 66

Figure 4.2 CCCP treatment does not reduce markers of mitochondrial protein content in skeletal muscle cells despite inducing mitochondrial membrane depolarisation and impairing mitochondrial respiration 68

Figure 4.3 CCCP treatment induces endogenous PINK1 kinase activity and Parkin E3 ligase activity in skeletal muscle cells 71

Figure 4.4 CCCP treatment induces phosphorylation of endogenous TBK1 in a PINK1-Parkin independent manner 73

Figure 4.5 AMPK activation induces mitophagy and promotes mitochondrial fission in skeletal muscle cells 75

Figure 4.6 AMPK activation is responsible for MFF phosphorylation at Ser 146 in skeletal muscle cells 76

Figure 4.7 AMPK activation by 991 induces TBK1 activation in a PINK1-Parkin independent manner 79

Figure 4.8 A working model of the mechanisms regulating mitophagy processing in skeletal muscle cells 89

Supplementary Figure 4.9 Quantification of Figure 4.2A - CCCP treatment does not reduce markers of mitochondrial protein content in skeletal muscle cells 91

Chapter 5

Figure 5.1 A working model of the four step mitophagy process in skeletal muscle . . 113

LIST OF ABBREVIATIONS

AA	antimycin A
ACC	acetyl-CoA carboxylase
ADP	adenosine diphosphate
afCFP	acid fast cyan fluorescent protein
AICAR	5-aminoimidazole-4-carboxamide
AMP	adenosine monophosphate
AMPK	5’ adenosine monophosphate-activated protein kinase
AMPKα1/2	AMPK alpha 1 and alpha 2 subunits
ANOVA	analysis of variance
ARIH1	ariadne RBR E3 ubiquitin protein ligase 1
ATP	adenosine triphosphate
BCL2L1	BCL-2-like protein 1
BCL2-L-13	BCL-2-like protein 13
BH3	BCL2-homology 3
BNIP3	BCL-2 interacting protein 3
BNIP3L/NIX	BCL-2 interacting protein 3-like
BSA	bovine serum albumin
°C	degrees Celsius
CCCP	carbonyl cyanide m-chlorophenyl hydrazone
CK2	casein kinase 2
CISD1	CDGSH iron sulphur domain 1
CO_2	carbon dioxide
CRISPR	clustered regularly interspaced short palindromic repeats

CTRL	control
DMEM	Dulbecco’s modified eagles’ medium
DMSO	dimethyl sulfoxide
DNA	deoxyribonucleic acid
DRP1	dynamin-related protein 1
ER	endoplasmic reticulum
ETC	electron transport chain
FCCP	carbonyl cyanide-p-trifluoromethoxyphenylhydrazone
FKBP8	Peptidyl-prolyl cis-trans isomerase FKBP8
FIS1	mitochondrial fission 1 protein
FUNDC1	FUN14 domain-containing protein 1
GAPDH	glyceraldehyde 3-phosphate dehydrogenase
GFP	green fluorescent protein
GTP	guanosine-5'-triphosphate
h	hours
HCl	hydrochloric acid
HEPES	4-(2-hydroxyethyl)-1-piperazineethanesulfonic acid
IBR	Institute of Biomedical Sciences
IMM	inner mitochondrial membrane
IMS	intermembrane space
kDa	kilodalton
KI	knock in
KO	knock out
LC3	microtubule-associated protein 1A/1B-light chain 3

LIR	LC3 interacting region
MARCH5	mitochondrial ubiquitin ligase
MFF	mitochondrial fission factor
MFN1	mitofusin 1
MFN2	mitofusin 2
mg	milligram
MID49	mitochondrial dynamics protein 49
MID51	mitochondrial dynamics protein 51
mL	millilitre
mmol	millimolar
MPC	mitochondrial profiling centre
mRNA	messenger ribonucleic acid
mtDNA	mitochondrial DNA
$mtFIS1_{101-152}$	mitochondrial targeting sequence of FIS1 (amino acids 101-152)
mTOR	mammalian target of rapamycin
MUL1	mitochondrial E3 ubiquitin protein ligase 1
NBR1	next to BRCA1 gene 1 protein
NDP52	nuclear dot protein 52
O_2	oxygen
OCR	oxygen consumption rate
OMM	outer mitochondrial membrane
OPA1	optic atrophy protein 1
OPTN	optineurin
OXPHOS	oxidative phosphorylation

PAGE	polyacrylamide gel electrophoresis
PBS	phosphate buffered saline
PGAM5	serine/threonine-protein phosphatase PGAM5, mitochondrial
PGC1α	peroxisome proliferator-activated receptor gamma coactivator 1-alpha
pH	potential of hydrogen
PINK1	PTEN-induced kinase 1
PVDF	polyvinylidene fluoride
RIPK3	receptor interacting serine/threonine kinase 3
Rot	rotenone
SDS	sodium dodecyl sulphate
SEM	standard error of the mean
Ser	serine
SRAI	signal retaining autophagy indicator
Src	proto-oncogene tyrosine-protein kinase Src
SQSTM1/p62	sequestosome-1
TAX1BP1	tax1-binding protein 1
TBST	tris-buffered saline Tween-20
TBK1	TANK-binding kinase 1
TEM	transmission electron microscopy
Thr	threonine
TIM	translocase of the inner membrane
TOLLES	TOLerance of Lysosomal EnvironmentS
TOM	translocase of the outer membrane

TOM70	translocase of the outer membrane 70 kDa subunit
TUBE	tandem ubiquitin binding entity
Ub	ubiquitin
UBL	ubiquitin like
UBA^{UBQLN1}	his-halo-ubiquilin1 UBA domain tetramer
µg	microgram
µL	microlitre
µM	micromolar
ULK1	unc-51 like autophagy activating kinase 1
VDAC1	voltage-dependent anion channel 1
YFP	yellow fluorescent protein
991	AMPK activator 991

TABLE OF CONTENTS

CHAPTER 1: GENERAL INTRODUCTION. 1

1.1 A brief introduction to mitochondria 2

1.1.1 Evolution 2

1.1.2 Structure 2

1.1.3 Function 2

1.1.4 Mechanisms of mitochondrial quality control 3

1.1.4.1 Mitochondrial biogenesis 3

1.1.4.2 Mitochondrial fission/ fusion 4

1.1.4.3 Mitochondrial degradation 5

1.2 Mitophagy in non-muscle cells and tissues: what do we already know? 5

1.2.1 The history of mitophagy 5

1.2.2 Mitophagy at rest and under stress 6

1.2.3 Signalling mechanisms 7

1.2.3.1 Ubiquitin-dependent mitophagy 8

1.2.3.1.1 PINK1-Parkin 8

1.2.3.1.2 TBK1 9

1.2.3.1.3 MUL1 10

1.2.3.1.4 ARIH1 10

1.2.3.2 Receptor-dependent mitophagy 11

1.2.3.2.1 BNIP3 & BNIP3L/NIX 11

1.2.3.2.2 FUNDC1 11

1.2.3.2.3 BCL2-L-13 12

1.2.3.2.4 FKBP8 13

1.2.3.3 Lipid-dependent mitophagy 13

1.2.3.3.1 Cardiolipin 13

1.2.3.4 Other mitophagy activating signals 14

1.2.3.4.1 AMPK-ULK1 14

1.3 Measuring mitophagy 16

1.3.1 Transmission electron microscopy (TEM) 16

1.3.2 Fluorescence-based approaches 17

1.3.2.1 Mito-QC 17

1.3.2.2 Mt-Keima 17

1.3.2.3 Mito-Timer 18

1.3.2.4 Mito-SRAI 20

1.3.2.5 Colocalisation of mitotracker and lysotracker 21

1.3.2.6 Immunofluorescence-based colocalisation of mitochondria with LC3-positive autophagosomes 21

1.3.2.7 Anti-DNA antibodies 22

1.3.3 Other approaches 22

1.3.3.1 Biochemical analysis of mitophagic flux 22

1.4 Skeletal muscle health and mitophagy in ageing 27

1.5 Mitophagy in skeletal muscle: what do we already know? 28

1.5.1 Measurement models 28

1.5.2 Mitophagy at rest 29

1.5.3 Signalling mechanisms 29

1.5.3.1 PINK1-Parkin 30

1.5.3.2 AMPK-ULK1 31

1.5.3.3 FUNDC1 31

1.5.3.4 BNIP3 & BNIP3L/NIX 31

1.6 Specific aims of the thesis 32

CHAPTER 2: GENERAL METHODS. 34

2.1 Cell lines and culture 35

2.1.1 C2C12 35

2.1.2 HeLa 35

2.1.3 HEK293 Flp-In 35

2.2 Drug reconstitution and cell treatment 36

2.3 Cell lysis 36

2.4 Tissue powdering and homogenisation 36

2.5 Protein assay 37

2.6 Sample preparation 37

2.7 Western blotting 37

2.7.1 Gel electrophoresis 37

2.7.2 Transfer and blocking 37

2.7.3 Primary antibody 38

2.7.4 Secondary antibody 38

2.7.5 Imaging 38

2.7.6 Analysis 38

2.8 Respirometry 39

2.9 Statistics 39

CHAPTER 3: DEVELOPING TOOLS TO STUDY MITOPHAGY AND ITS SIGNALLING MECHANISMS IN SKELETAL MUSCLE 40

3.1 Generating a stable skeletal muscle mito-QC reporter cell line 41

3.1.1 Background 41

3.1.2 Method 41

3.1.2.1 DNA construct 41

3.1.2.2 Transfection & viral harvesting. 41

3.1.2.3 Viral infection and selection of mito-QC positive C2C12 myoblasts . . 42

3.1.2.4 Cell sorting 42

3.1.2.5 Cell treatment and fixation. 43

3.1.2.6 Image capture 43

3.1.2.7 Quantification of mitophagy and mitochondrial fission. 44

3.2 Assessing endogenous PINK1 kinase and Parkin E3 ligase activity in skeletal muscle 46

3.2.1 Background 46

3.2.2 Method 48

3.2.2.1 Bacterial expression of HALO-UBA^{UBQLN1} tandem ubiquitin binding entity (TUBE). 49

3.2.2.2 Ubiquitin enrichment 49

3.2.2.3 Sample preparation 49

3.2.2.4 Western blotting 49

CHAPTER 4: AMPK ACTIVATION INDUCES MITOPHAGY AND PROMOTES MITOCHONDRIAL FISSION WHILST ACTIVATING TBK1 IN A PINK1-PARKIN INDEPENDENT MANNER 52

4.1 Abstract 55

4.2 Introduction 56

4.3 Materials & Methods 58

4.3.1 Cell lines and culture 58

4.3.2 Drug reconstitution and cell treatment 59

4.3.3 Cell lysis 59

4.3.4 Ubiquitin pull-down 59

4.3 5 Western blotting 60

4.3.6 DNA construct and expression 61

4.3.7 Generation of AMPK α1/α2 deficient HEK293 Flp-In cells 61

4.3.8 Mitophagy assay 62

4.3.9 Mitophagy and mitochondrial morphology quantitation 63

4.3.10 Respirometry 63

4.3.11 Statistical analysis 64

4.4 Results 64

4.4.1 CCCP treatment induces mitophagy and promotes mitochondrial fission in skeletal muscle cells 64

4.4.2 CCCP treatment does not alter mitochondrial protein content despite depolarising the mitochondrial membrane and impairing mitochondrial respiration 67

4.4.3 CCCP treatment induces PINK1 kinase activity and Parkin E3 ligase activity in skeletal muscle cells 70

4.4.4 CCCP treatment induces phosphorylation of TBK1 in a PINK1-Parkin independent manner 68

4.4.5 AMPK activation by 991 induces mitophagy and promotes mitochondrial fission via phosphorylation of MFF in skeletal muscle cells 74

4.4.6 AMPK activation by 991 induces endogenous TBK1 activation in PINK1-Parkin independent manner in skeletal muscle cells 77

4.5 Discussion 81

4.6 Limitations and future directions 87

4.6 Conclusion 90

CHAPTER 5: REGULATORY ROLES OF PINK1-PARKIN AND AMPK IN SKELETAL MUSCLE MITOPHAGY 93

5.1 Abstract 95

5.2 Introduction 96

5.3 PINK1-Parkin-mediated mitophagy 99

5.3.1 PINK1-Parkin-mediated mitophagy in non-muscle cell lines 99

5.3.2 PINK1-Parkin-mediated mitophagy in skeletal muscle 100

5.3.3 PINK1-Parkin mediated mitochondrial fission 101

5.3.3.1 Non-muscle cells lines 101

5.3.3.2 Skeletal muscle 101

5.3.4 PINK1-Parkin-mediated mitochondrial ubiquitylation 102

5.3.4.1 Non-muscle cells lines 102

5.3.4.2 Skeletal muscle 102

5.3.5 PINK1-Parkin-mediated autophagosomal engulfment 104

5.3.5.1 Non-muscle cells lines 104

5.3.5.2 Skeletal muscle 105

5.3.6 A summary of PINK-Parkin signalling pathway in skeletal muscle mitophagy 105

5.4 AMPK-mediated mitophagy 106

5.4.1 AMPK in skeletal muscle 106

5.4.2 AMPK-mediated mitophagy in non-muscle cell lines. 107

5.4.3 AMPK-mediated mitophagy in skeletal muscle 107

5.4.4 AMPK-mediated mitochondrial fission 107

5.4.4.1 Non-muscle cells lines 107

5.4.4.2 Skeletal muscle 108

5.4.5 AMPK and mitochondrial ubiquitylation 109

5.4.5.1 Non-muscle cells lines 109

5.4.5.2 Skeletal muscle 109

5.4.6 AMPK and autophagosomal engulfment 110

5.4.6.1 Non-muscle cells lines 110

5.4.6.2 Skeletal muscle 110

5.4.7 A summary of AMPK-mediated mitophagy in skeletal muscle 111

5.5 Mitophagy is not homogeneous between tissues 111

5.6 A working model of mitophagy in skeletal muscle 112

5.7 Future directions 114

CHAPTER 6: FINAL REMARKS 115

6.1 Main findings 116

6.2 Limitations 119

6.3 Conclusion 121

CHAPTER 7: REFERENCES. 123

CHAPTER 1

GENERAL INTRODUCTION

1.1 A brief introduction to mitochondria

1.1.1 Evolution

Mitochondria are small double-membrane-bound organelles that are found in almost all eukaryotic cells. In 1967, Lynn Margulis (formerly Sangan) famously published the theory that mitochondria evolved from endosymbiotic prokaryotic bacteria (1). Approximately 10 years later, phylogenetic analyses of mitochondrial genes and proteins revealed that mitochondria are indeed of prokaryotic origin with a unique ancestry (2-4).

1.1.2 Structure

Mitochondria are comprised of four compartments, including: the outer membrane (OMM), the inner membrane (IMM), the intermembrane space (IMS), and the matrix (5). Classic textbook illustrations display mitochondria as bean-shaped structures, with a highly folded inner membrane encased by an outer membrane (6). More recently, the development of three-dimensional viewing technologies, has enabled a more detailed picture of mitochondrial morphology to be generated (7). It is now widely accepted that the mitochondria exist inside cells and tissues as a highly dynamic tubular network (8).

1.1.3 Function

Mitochondria are important metabolic hubs that perform a wide range of functions. While mitochondria are the main source of adenosine triphosphate (ATP) via oxidative phosphorylation (OXPHOS), they also provide molecules for fatty acid, hormone and amino acid synthesis (9). From a signalling perspective, mitochondria help to regulate intracellular calcium levels (10), the innate immune response (11) as well as being the primary source of reactive oxygen species (ROS) (12). Interestingly, mitochondria also

play a vital role in the intrinsic apoptotic pathway that leads to cell death (13). Critically, in order to perform these functions, several mechanisms of mitochondrial quality control are needed to keep mitochondria healthy (14).

1.1.4 Mechanisms of mitochondrial quality control

The mitochondrial network is maintained by several mechanisms of mitochondrial quality control, namely: biogenesis (formation of new mitochondrial material), fission (splitting of the mitochondrial network), fusion (joining of separate mitochondria) and degradation (breakdown of mitochondria) (14, 15).

1.1.4.1 Mitochondrial biogenesis

The formation of new mitochondrial material during mitochondrial biogenesis helps to rejuvenate the mitochondrial network in order to maintain mitochondrial quality (15). Mitochondrial biogenesis involves synchronised transcription and translation of both nuclear and mitochondrial genes. While more than 98% of mitochondrial proteins are nuclear-encoded (16), it is well known that both nuclear and mitochondrial encoded proteins are required to build the electron transport chain for OXPHOS (17). Nuclear encoded mitochondrial proteins are made in the cytoplasm and are imported into mitochondria via translocase of the outer membrane (TOM) and translocase of the inner membrane (TIM) complexes (17). Conversely, mitochondrial DNA (mtDNA) encoded proteins are transcribed and translated in the mitochondria (17). Both nuclear and mitochondrial-encoded proteins are directed to one of the four mitochondrial compartments through their amino acid pre-sequence (16).

1.1.4.2 Mitochondrial fission/ fusion

Mitochondria undergo continuous fission and fusion events in response to cellular stress (18) which helps to maintain a healthy mitochondrial population (19). Fission results in morphologically and functionally separate mitochondria whereas fusion helps to mix different compartments of the mitochondrial network.

Mitochondrial fission has several different purposes, including the generation of transportable mitochondrial units for movement along the cytoskeleton, the release of cytochrome c during apoptosis and the separation of damaged mitochondria for mitophagy (20). On the other hand, fused mitochondrial networks are important for the dissipation of metabolic energy via the transmission of membrane potential as well as the continuous exchange of mtDNA and its products to supress mitochondrial defects (21).

The core molecular machinery controlling mitochondrial fission and fusion processes are large guanosine triphosphatases (GTPases) in the dynamin family (22). The actions of these GTPases facilitate the division and fusion of the OMM and IMM. Specifically, the cytosolic GTPase dynamin related protein 1 (DRP1) mediates mitochondrial fission (23). The key receptors of DRP1 on the OMM are: mitochondrial fission factor (MFF), mitochondrial fission protein 1 (FIS1) and mitochondrial dynamics proteins 49/51 (MID49/51) (24). During mitochondrial fission, DRP1 is recruited from the cytosol to the OMM where it assembles into a helical ring around mitochondria and severs both membranes via GTP-dependent constriction (25). Conversely, fusion of the OMM is controlled by membrane-anchored dynamin family members called mitofusins (MFN1 and MFN2) (26). Fusion of the IMM is mediated by a single dynamin family member called optic atrophy protein 1 (OPA1) (26).

1.1.4.3 Mitochondrial degradation

Superfluous/ damaged mitochondria or mitochondrial proteins can be removed through several different mechanisms, including: mitochondrial proteases, proteasomal degradation, mitochondrial derived vesicles (MDVs) and mitophagy (15, 27). Each of these mechanisms helps to keep the mitochondrial population healthy. However, the main advantage mitophagy is that it enables entire mitochondria (including its membrane, proteins and nucleic acids) to be recycled in one go.

In simple terms, mitophagy refers to mitochondrial specific autophagy which is comprised of several different stages. Following separation of damaged mitochondria via fission, mitochondria are primed for engulfment by double membraned autophagosomes. Autophagosomes subsequently fuse with lysosomes which contain enzymes that degrade mitochondria.

1.2 Mitophagy in non-muscle cells and tissues: what do we already know?

1.2.1 The history of mitophagy

In 1914, Margret and Warren Lewis first proposed the idea that mitochondria can be degraded (28). Many years after, in the late 1950's and early 1960's, the use of electron microscopy helped to reveal mitochondria encapsulated inside vesicles and lysosomes (29-31).

After Christian de Duve proposed the concept of cellular autophagy in the mid 1960's, the idea that mitochondria undergo autophagy gathered significant momentum (32, 33) and was subsequently reported in several different animal models (34-36). Some years later in the early 2000s, mitochondrial autophagy was revealed to be selective through

the observation that depolarised mitochondria are targeted for degradation. Around this time, the word mitophagy was popularised through the work of Lemasters in 2005 (37) after first being used by Scott and Klionsky in 1998 (38).

Mechanistically, the way in which mitochondria are primed for mitophagy first started to be uncovered in the late 2000s by the Klionsky, Ohsumi, Ney and Youle laboratories. In yeast, ATG32 (mammalian homologue BCL2-L-13) was identified as an important mitophagy receptor (39) while BNIP3L/NIX was also shown to play a critical role in mitophagy during red blood cell differentiation (40, 41). Furthermore, the ubiquitin E3-ligase Parkin was shown to regulate mitophagy in response to mitochondrial depolarisation (42). Understanding of Parkin-mediated mitophagy was further strengthened following the identification of PTEN induced kinase 1 (PINK1) as an upstream regulator of Parkin (43-47). Since these studies, our knowledge of mitophagy has expanded rapidly.

1.2.2 Mitophagy at rest and under stress

While the exact function of mitophagy under basal conditions is not well understood, this phenomena has been well demonstrated in numerous studies (48-50). The widely accepted view is that cells undergo basal mitophagy as a general housekeeping mechanism. Interestingly, mitophagy is neither homogenous across tissues nor between cells within the same tissue (48, 49). This is supported by the fact that levels of basal mitophagy are greater in cells with high metabolic activity, such as retina photoreceptor neurons and cardiomyocytes (51). Based on these data, it seems as though the physiological function and metabolism of a specific tissue determines its level of mitophagy in the basal state.

Over the years, mitophagy has been studied in response to a range of different stresses, including: nutrient starvation (52), hypoxia (53, 54) and mitochondrial depolarisation (42, 46). Each of these stimuli have been shown to markedly increase mitophagy beyond baseline resting levels. Among the most commonly used mitophagy inducers are chemical protonophores that depolarise mitochondria (e.g. CCCP, FCCP) and electron transport chain inhibitors (e.g., rotenone, antimycin A or oligomycin). While these chemicals lack physiological relevance, they are extremely effective at impairing mitochondria (55, 56). As a result, their use has greatly advanced mechanistic understanding of how mitochondrial damage activates mitophagy.

1.2.3 Signalling mechanisms

Much of our knowledge regarding the molecular signalling mechanisms that govern mitophagy is derived from work in immortalised, cancer cells lines. In these cells, it has become clear that ubiquitin-dependent, receptor-dependent and lipid-dependent mechanisms are capable of regulating mitophagy (57) (Figure 1.1). Several signalling pathways and molecules have been implicated in the control of ubiquitin-dependent mitophagy, such as PTEN-induced kinase 1 (PINK1)-Parkin and TBK1 as well as other E3 ubiquitin ligases, including MUL1 and ARIH1. Conversely, BNIP3, BNIP3L/NIX, FUNDC1, BCL2-L-13 and FKBP8 are all suggested to regulate receptor-dependent mitophagy while cardiolipin helps to facilitate lipid-dependent mitophagy. The master energy sensing kinase 5'-AMP-activated protein kinase (AMPK) and its direct downstream substrate ULK1 are also reported to be potent mitophagy activating signals (52, 58, 59).

1.2.3.1 Ubiquitin-dependent mitophagy

1.2.3.1.1 PINK1-Parkin

The PTEN induced kinase 1 (PINK1)-Parkin signalling axis is considered to be the classical mitophagy pathway. This mechanism has been studied extensively in the context of neurodegeneration because mutations in human PINK1 (PARK6) (60, 61) and Parkin (PARK2) (62) are assumed to be causative for early-onset Parkinson's disease. Furthermore, abnormal mitophagy processing is thought to contribute towards the pathophysiology of Parkinson's disease (63).

Under basal conditions, PINK1 is continuously degraded through the N-end-rule pathway (64). However, insults such as: a) the loss of the mitochondrial membrane potential (42, 46); b) excessive production of reactive oxygen species (ROS) (65, 66); and, c) mutations in mitochondrial DNA (mtDNA) (67), can activate PINK1 kinase activity. PINK1 then activates Parkin's ubiquitin E3 ligase activity, which labels damaged mitochondria prior to autophagosomal engulfment and mitochondrial degradation (15, 68).

Upon loss of mitochondrial membrane potential, for example, following depolarisation with the protonophore carbonyl cyanide m-chlorophenyl hydrazone (CCCP), PINK1 is stabilised and activated on the outer mitochondrial membrane (OMM) (46). This facilitates PINK1-dependent ubiquitin (Ub) phosphorylation at Ser 65 (69-71) leading to the recruitment of Parkin E3 Ub ligase to the OMM (46). Allosteric activation of Parkin through phospho-Ub binding (72), along with PINK1 mediated Parkin phosphorylation (73) maximally activates Parkin (74). This enables Parkin to polyubiquitylate OMM proteins such as: CDGSH iron sulphur domain 1 (CISD1); mitofusin1/2 (MFN1/2); translocase of outer membrane 70 kDa subunit (TOM70); mitochondrial fission 1 protein

(FIS1); and, voltage-dependent anion channel 1 (VDAC1) (75, 76). The formation of poly-ubiquitin chains on damaged mitochondria leads to the recruitment of autophagy receptors, including NDP52, NBR1, OPTN, SQSTM1/p62 and TAX1BP1 (77). Because these autophagy receptors possess a ubiquitin-binding domain as well as a LC3-interacting region (LIR) motif, they have the capacity to link ubiquitylated mitochondria to autophagosomal LC3 via their LIR motif. Mechanistically, NDP52 and OPTN are the essential receptors for mitophagy with some contribution from TAX1BP1, whereas NBR1 and SQSTM1/ p62 are dispensable (78). Ultimately, activation of autophagy receptors promotes autophagosomal engulfment of damaged mitochondria (77) prior to lysosome-dependent degradation.

1.2.3.1.2 TBK1

TANK-binding kinase 1 (TBK1) plays an important regulatory role in innate immunity via the cGAS-STING-TBK1 signalling axis (79). More recently, TBK1 has been implicated in mitophagy (80-82). Interestingly, TBK1's activation following its phosphorylation at Ser 172 (83) is suggested to require PINK1-Parkin signalling which in turn, generates poly-ubiquitin chains on depolarised mitochondria (78, 84). Mechanistically, TBK1 is suggested to activate autophagy receptors, such as nuclear dot protein 52 (NDP52) (82), optineurin (OPTN) (81) and sequestosome-1 (SQSTM1/ p62) (80). More specifically, TBK1 enhances binding capacity of both OPTN and p62/SQSTM1 with poly-ubiquitin chains via phosphorylation of multiple serine residues (80, 81). Vargas and colleagues (82) have also shown that TBK1 activation promotes NDP52-mediated recruitment of the ULK1 complex during autophagosomal engulfment in the lead up to mitochondrial degradation.

1.2.3.1.3 MUL1

Mitochondrial E3 ubiquitin protein ligase 1 (MUL1) resides on the OMM and ubiquitylates proteins, such as MFN2 (85). As a small ubiquitin-like modifier (SUMO) E3 ligase, MUL1 also SUMOylates DRP1 to enhance its stability on mitochondria (86, 87). As well as regulating mitochondrial fission and fusion events (86, 88), MUL1 is reported to mediate mitophagy via ULK1 in response to selenite-induced reactive oxygen species (ROS) production (89). Furthermore, despite sharing some of the same substrates as Parkin (e.g. MFN2), MUL1 is reported not to affect PINK1-Parkin-mediated mitophagy in HeLa cells (85). Interestingly, however, MUL1 possess an LIR-like motif in its ring domain which raises the possibility that MUL1 may be able to induce mitophagy by directly tethering to autophagic membranes (90).

1.2.3.1.4 ARIH1

Ariadne RBR E3 ubiquitin protein ligase 1 (ARIH1) has recently been implicated in PINK1-dependent mitophagy following it overexpression in HeLa cells (91). Although ARIH1-dependent mitophagy requires PINK1 as well as the ubiquitylation of mitochondrial proteins, none of Parkin's known substrates are suggested to be involved in ARIH1-mediated mitophagy. These data indicate that ARIH1 may well ubiquitylate proteins substrates than are not targeted by Parkin in order to induce mitophagy (91). However, beyond these data, the regulatory role of ARIH1 in mitophagy has not been thoroughly explored.

1.2.3.2 Receptor-dependent mitophagy

1.2.3.2.1 BNIP3 & BNIP3L/NIX

BCL-2 interacting protein 3 (BNIP3) and BCL-2 interacting protein 3-like (BNIP3L), otherwise known as NIX, are proteins from the BCL2 family that induce both autophagy and apoptosis (92). BNIP3L is a homologue of BNIP3 and shares ~55% of the same amino acid sequence (93). Structurally, BNIP3 and BNIP3L both contain the same LIR motif. This characteristic enables both proteins to interact with LC3 which helps to recruit autophagosomes for the engulfment of damaged mitochondria, particularly under hypoxic conditions (94-96). Mutation of BNIP3 and BNIP3L's LIR motif prevents their interaction with LC3 and attenuates the clearance of damaged mitochondria in mitophagy (95-97). Conversely, phosphorylation of BNIP3 and BNIP3L's LIR motif enhances their interaction with LC3 to promote mitophagy (97, 98).

Interestingly, a number of studies have started to investigate crosstalk between receptor-dependent mitophagy through BNIP3/BNIP3L and ubiquitin-dependent mitophagy via PINK1-Parkin signalling. For example, Parkin is reported to ubiquitylate BNIP3 in order promote the recruitment of autophagy receptors to damaged mitochondria (99). Furthermore, not only has BNIP3 been shown to inhibit the degradation of PINK1, but it also helps to stabilise PINK1 on OMM (100). This was also shown to lead to the recruitment of Parkin to the mitochondria for subsequent mitophagy (100).

1.2.3.2.2 FUNDC1

FUN14 domain-containing protein 1 (FUNDC1) is an OMM protein that orchestrates mitophagy (53). Structurally, FUNDC1 possesses an LC3 interacting region (LIR) motif in its N-terminus which is exposed to the cytosol and interacts with LC3 to recruit

autophagosomes prior to mitochondrial degradation (53, 54). Both phosphorylation and ubiquitylation are suggested to regulate FUNDC1's involvement in mitophagy. Under basal conditions, FUNDC1's interaction with autophagosomal LC3 is blocked by Tyr 18 (53) and Ser 13 (101) phosphorylation by Src kinase and CK2 respectively. Conversely, dephosphorylation of FUNDC1 at Ser 13 by PGAM5, a mitochondrial phosphatase, promotes the tethering of mitochondria to autophagosomal LC3 (102). The activity of PGAM5 is regulated through its interaction with BCL2L1 which is degraded under hypoxic conditions (102). This results in increased PGAM5 phosphatase activity, which in turn, encourages linkage of mitochondria to LC3-decorated autophagosomes (102). In another study, ULK1-mediated phosphorylation of FUNDC1 at Ser 17 is reported to enhance mitophagy by promoting FUNDC1-LC3 binding in response to hypoxia and FCCP treatment (54). Since then, it has been reported that the mitochondria E3 ubiquitin ligase MARCH5 is able to ubiquitylate FUNDC1 prior to its dephosphorylation, to prevent excessive mitophagy in response to hypoxic stress (103).

1.2.3.2.3 BCL2-L-13

The outer mitochondrial membrane (OMM) protein BCL2-L-13 plays multifunctional role in mitophagy as it mediates both mitochondrial fission and degradation in response to CCCP treatment (104). In mt-Keima-expressing HEK293 cells, knockdown of endogenous BCL2-L-13 attenuated CCCP-induced mitochondrial fission and mitophagy, indicating that BCL2-L-13 plays a key role in both of these processes (104). Structurally, BCL2-L-13 possesses several BH domains and an LC3 interacting region (LIR) that are vital for its function. To demonstrate this, mitochondrial fission is reported to be abolished in HEK293 cells transfected with deletion mutants for BH1-4, indicating that BH1-4 domains are important for BCL2-L-13-induced mitochondrial fission (104).

Furthermore, mutation of BCL2-L-13's LIR motif prevented interaction with LC3, whereas full length BCL2-L-13 tethers itself to autophagosomal LC3 to promote mitophagy (104). More recently, an updated model of mitophagy involving BCL2-L-13 has been proposed whereby BCL2-L-13 recruits the ULK1 complex, which in turn, connects BCL2-L-13 to LC3-decorated autophagosomes via its own LIR (105).

1.2.3.2.4 FKBP8

FKBP8 resides on the OMM and is associated with several cellular processes including apoptosis, the regulation of mammalian target of rapamycin (mTOR) (106) and mitophagy (107). In response to CCCP treatment, previous work has demonstrated that FKBP8 translocates away from the mitochondria to the endoplasmic reticulum (ER) in order to evade degradation (107, 108). This property of FKBP8 is unique compared to the other mitochondrial receptors involved in mitophagy, such as FUNDC1 and BCL2-L-13. Mechanistically, FKBP8 mediates LIR-dependent recruitment of LC3 to damaged mitochondria and overexpression of both FKBP8 and LC3 induces mitophagy (107). At an endogenous level, FKBP8 is indicated to contribute towards both mitochondrial fission and mitophagy under hypoxic conditions (109).

1.2.3.3 Lipid-dependent mitophagy

1.2.3.3.1 Cardiolipin

Cardiolipin is a mitochondrial anionic phospholipid that resides almost exclusively on the inner mitochondrial membrane. While cardiolipin is known to help regulate mitochondrial function through its association with electron transport chain subunits (110), it is also capable of acting as a receptor in mitophagy. In response to mitophagy inducers, such as rotenone (ETC complex I inhibitor) and CCCP (mitochondrial

uncoupler), cardiolipin is suggested to translocate to the OMM, enabling its interaction autophagosomal LC3 (111). This helps to promote the capture of damaged mitochondria in autophagosomes prior to their degradation (111). Recent work has shown that cardiolipin's translocation to the OMM depends upon the mitochondrial nucleoside diphosphate kinase (NDPK-D), an intermembrane space- localised kinase, that binds to cardiolipin in response to CCCP treatment (112).

1.2.3.4 Other mitophagy activating signals

1.2.3.4.1 AMPK-ULK1

Egan and colleagues (52) first revealed that AMPK is involved in mitophagy. In their study, not only did cells expressing non-phosphorylatable ULK1 mutants contain more mitochondria, but a higher proportion of these mitochondria were enlarged with altered cristae. Others have subsequently shown that AMPK-mediated phosphorylation of ULK1 at Ser 555 regulates its activation and translocation to mitochondria for its involvement in mitophagy (52, 59). These early studies indicate that AMPK-mediated phosphorylation of ULK1 helps to orchestrate mitophagy.

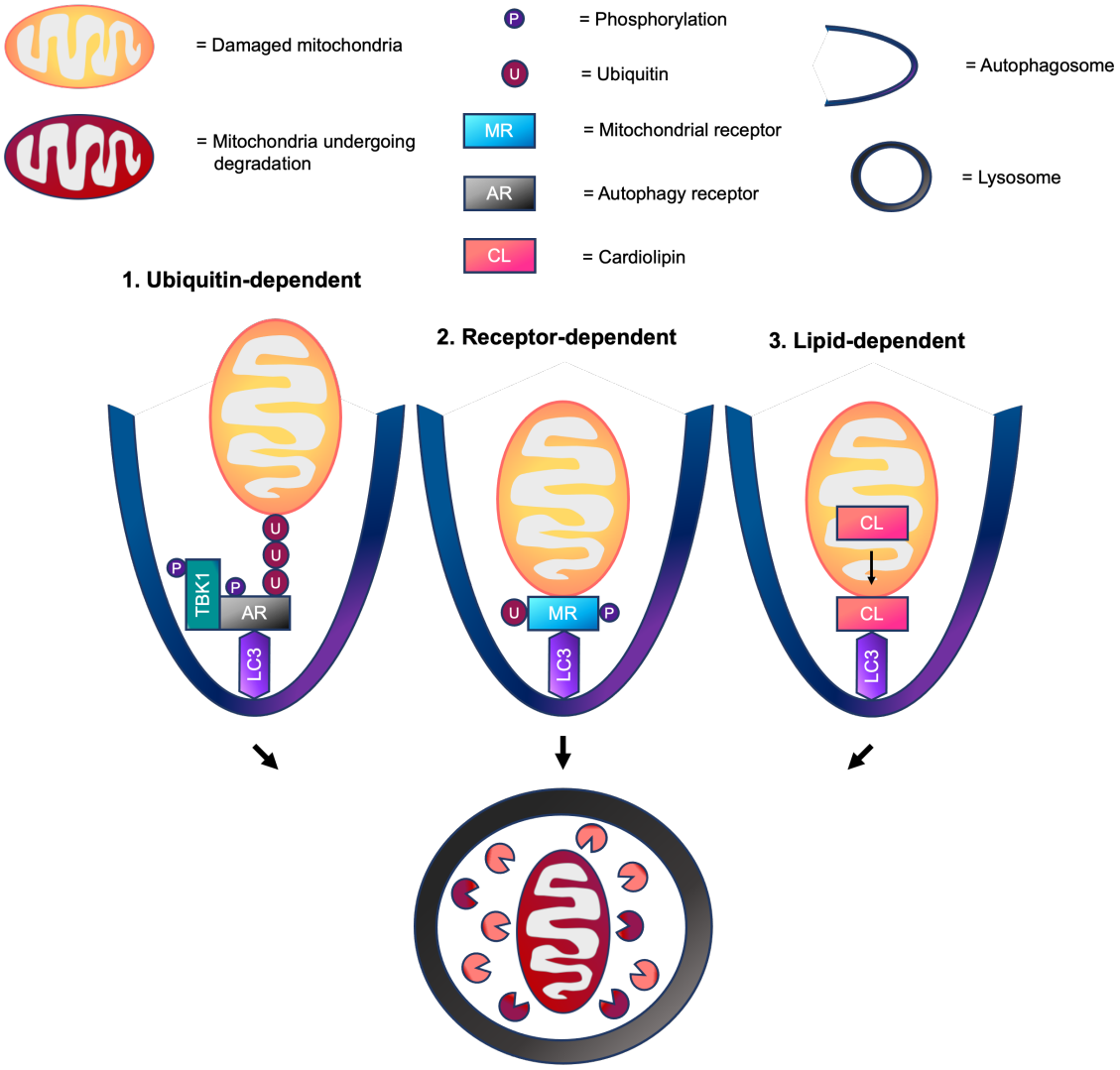

Figure 1.1 A schematic illustrating ubiquitin-dependent, receptor-dependent and lipid-dependent mitophagy. 1 - During ubiquitin-dependent mitophagy, outer mitochondrial membrane (OMM) proteins on damaged mitochondria are marked with ubiquitin molecules by E3 ubiquitin ligases, such as Parkin and mitochondrial E3 ubiquitin protein ligase 1 (MUL1). Next, ubiquitylated OMM proteins are recognised by autophagy receptors, such as optineurin (OPTN) and nuclear dot protein 52 (NDP52), which in turn, tether ubiquitylated mitochondria to the autophagosome through their LC3 interacting region (LIR). Several studies have shown that phosphorylation and activation of multiple autophagy receptors is controlled, at least in part, by TANK-binding kinase 1 (TBK1). 2 - During receptor-dependent mitophagy, mitochondrial receptors, such as BCL-2 interacting protein 3 (BNIP3), BCL-2 interacting protein 3-like (BNIP3L/NIX) and FUN14 domain-containing protein 1 (FUNDC1), that reside on the OMM, directly tether damaged mitochondria to LC3-decorated autophagosomal membranes via their LIR. Linkage of damaged

mitochondria to autophagosomes encourages mitophagy. Both phosphorylation and ubiquitylation are suggested to regulate the involvement of various mitochondrial receptors in mitophagy. 2 - During lipid-dependent mitophagy, the mitochondrial phospholipid cardiolipin translocates away from the inner mitochondrial membrane (IMM), where it normally resides, to the OMM. Here, cardiolipin interacts with autophagosomal LC3 to promote mitophagy. Lastly, in ubiquitin-dependent, receptor-dependent and lipid-dependent mitophagy, fully formed autophagosomes fuse with lysosomes enabling mitochondrial degradation.

1.3 Measuring mitophagy

In recent years, tremendous progress has been made with respect to our understanding mitophagy through the development of new tools. As such, it is now possible to monitor mitophagy with enhanced resolution both in vitro and in vivo. The advantages and disadvantages of these tools including the recently developed mito-SRAI are discussed herein.

1.3.1 Transmission electron microscopy (TEM)

Transmission electron microscopy (TEM) is considered to be the gold standard for assessing mitophagy (113) because it enables mitochondria to be visualised inside autophagic and lysosomal membranes. However, as described in Table 1.1, TEM has several drawbacks (113). To circumvent the disadvantages associated with TEM, over the past decade a number of fluorescence-based models have been developed to study mitophagy.

1.3.2 Fluorescence-based models

1.3.2.1 Mito-QC

The mito-QC reporter construct as first described by Allen and colleagues (114) uses a functionally inert, tandem mCherry-GFP tag fused to the mitochondrial targeting sequence of the OMM protein FIS1. The mito-QC reporter construct (mCherry-GFP-mt-FIS1$^{101-152}$) takes advantage of the fact that green fluorescence protein (GFP), unlike mCherry, cannot withstand the acidic proteolytic conditions of the lysosome (114). Under steady-state basal conditions, in cells and tissues expressing mito-QC, mitochondria fluoresce both red (mCherry) and green (GFP) making the mitochondrial network appear gold in colour when these spectra are merged. However, upon mitophagy, the acidic conditions of the lysosome quench the GFP signal, but not mCherry. As a result, punctate structures that fluoresce red only form within the mitochondrial network and the appearance of these red puncta indicate sites of ongoing mitophagy (Figure 1.2).

1.3.2.2 Mt-Keima

The coral derived fluorescent protein Keima was first tethered to the mitochondrial targeting sequence of cytochrome c oxidase subunit VIII (mt-Keima) to help assess mitophagy (115). Unlike most fluorescent proteins, Keima does not undergo proteolytic degradation in low pH conditions. Instead, the excitation peak of Keima shifts from 458 nm (green light signal) in the neutral pH environment of the autophagosome for example to 561 nm (red light signal) under low pH conditions such as those inside the lysosome. The sensitivity of Keima to changes in pH make it a useful tool to report lysosome-dependent mitochondrial degradation during mitophagy (115). However, a major limitation of mt-Keima is that its signal is sensitive to fixation and therefore not very

suitable for largescale high-throughput screening assays, that require samples to be stored (see Table 1.1).

1.3.2.3 Mito-Timer

Targeting of the fluorescent protein Timer to the mitochondria (mito-Timer) to monitor mitochondrial turnover was first described by Hernandez and colleagues (116). The fluorescent properties of mito-Timer mean that it is now used to report: a) the synthesis of new mitochondria; b) mitochondrial structure; c) mitochondrial oxidative stress, and when combined with lysosomal imaging, is capable of evaluating mitophagy (58, 117). To engineer the mito-Timer construct, Hernandez and colleagues (116) tethered the mitochondrial targeting sequence of the cytochrome c oxidase subunit VIII gene to the N terminus of DsRed mutant (DsRed1-E5). DsRed1-E5 is aptly named Timer because its fluorescence changes over time (118). When newly synthesised, mitochondria-targeted Timer fluoresces green, but following a form of oxidation (dehydrogenisation) on the Tyr 67 residue, Timer fluorescence shifts irreversibly to red (119, 120). However, until mito-Timer is combined with staining or fluorescent labelling of the lysosome, it is only capable of making indirect measurements of mitophagy. This is because general (non-mitophagic) autophagosomes are capable of forming at endoplasmic reticulum (ER)-mitochondria contact sites (121-123) and mitochondria themselves can directly contact lysosomes (124). Therefore, until mitochondria can be shown to be inside the acidic microenvironment of the lysosome, direct assessment of mitophagy is not possible using this reporter (see Table 1.1).

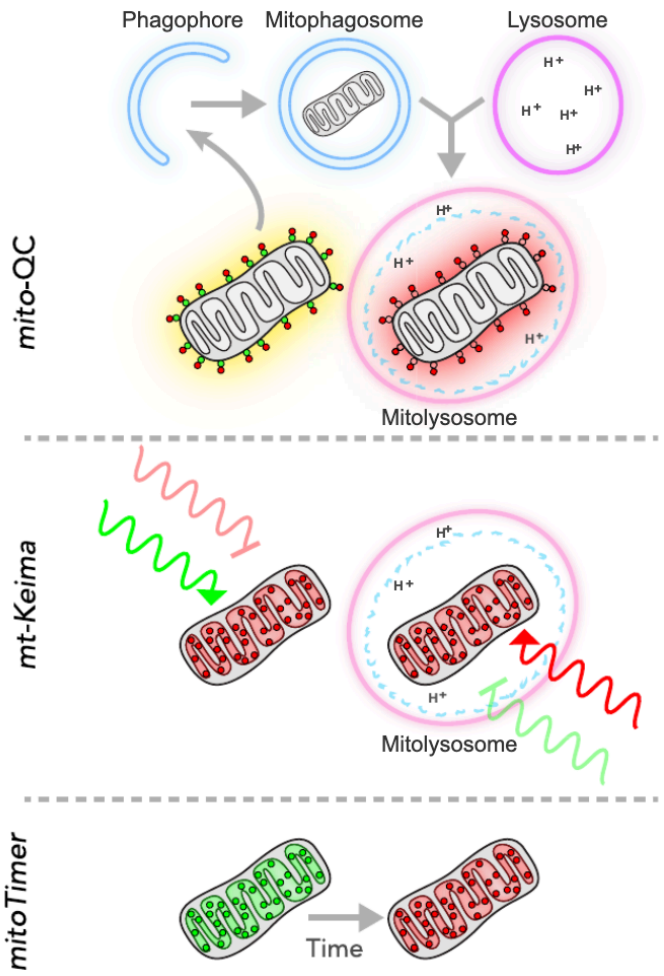

Figure 1.2 A schematic illustrating how the mito-QC, mt-Keima and mitoTimer reporters assess mitophagy. Using mito-QC, under steady-state basal conditions, a tandem mCherry-GFP tag targeted to the outer mitochondrial membrane makes the mitochondrial network appear gold in colour when red (mCherry) and green (GFP) spectra are merged. Upon mitophagy, the low pH of the lysosome quenches the GFP, but not mCherry, signal. Using mt-Keima, Keima is expressed in the mitochondrial matrix because of its fusion with cytochrome c oxidase subunit VIII. Under basal conditions, mt-Keima is excited by light peaking at 458 nm, whereas this increases to 561 nm under lysosomal conditions, i.e. upon mitophagy. Importantly, mt-Keima's emission spectra stays at 620 nm regardless of a change in pH. Using mitoTimer, the fluorophore DsRed1-E5 was targeted to the mitochondrial matrix. MitoTimer was initially designed to monitor the age of mitochondria as fluorescence shifts from green to red over a 48 h period. However, assessment of mitophagy is possible when combined with staining or fluorescent labelling of the lysosome. Taken from Rodger and colleagues (125).

1.3.2.4 Mito-SRAI

In recent months, the same group that engineered mt-Keima have developed a novel fluorescent based mitophagy reporter called mitochondrial targeted signal retaining autophagy indicator (mito-SRAI) (126). Much like mt-Keima, the reporter system in mito-SRAI is fused to cytochrome c oxidase subunit VIII and is resistant to lysosomal environments. However, in contrast to mt-Keima, mito-SRAI uses a tandem fluorescent tag consisting of a yellow-emitting fluorescence protein (YFP) termed YPet, tethered to acid fast cyan-emitting fluorescence protein (afCYP) renamed TOLerance of Lysosomal EnvironmentS (TOLLES). In addition, the mito-SRAI construct includes degrons (127, 128) that clear mistargeted SRAI, promoting effective labelling of the mitochondria. In neutral pH environments, YPet and TOLLES remain stable, however in low pH conditions, for example in the acidic microenvironment of the lysosome, YPet is completely degraded but TOLLES is not (Figure 1.3). As a result, punctate structures reflecting mitolysosomes appear in the TOLLES image and the ratio of TOLLES/YPet can be calculated as a read out of mitophagy (Figure 1.3). Importantly, mito-SRAI is resistant to fixation which circumvents the major drawback associated with mt-Keima.

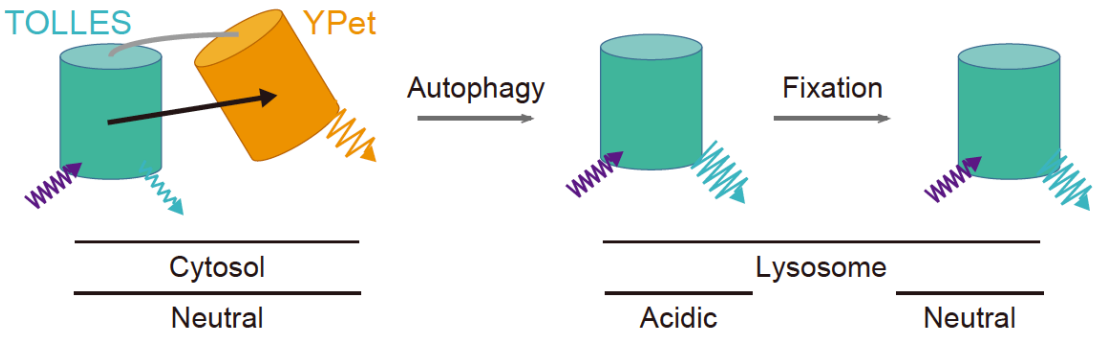

Figure 1.3 A schematic illustrating how mito-SRAI reports mitophagy. Using mito-SRAI, in neutral pH conditions SRAI fluoresces both YPet and TOLLES. However, after lysosomal delivery, YPet is quenched resulting in the appearance of TOLLES puncta, indicating sites of ongoing mitophagy. TOLLES signal is fully retained in fixed cells. Taken from Katayama and colleagues (126).

1.3.2.5 Colocalisation of mitotracker and lysotracker

Both mitotracker and lysotracker staining can be used concurrently to assess mitophagy without spectral overlap. For example, visualisation of colocalised mitotracker green and lysotracker red signals can be used to indicate ongoing sites of mitophagy (mitolysosomes). While this technique is very easy to employ, it is incapable of detecting mitophagy in vivo, thus restricting its use to cells.

1.3.2.6 Immunofluorescence-based colocalisation of mitochondria with LC3-positive autophagosomes

Colocalisation of the mitochondrial network with LC3-decorated autophagosomes is a technique commonly used to indirectly assess mitophagy. Although this method is easy to employ, and has been widely used in cell-based models, it does not provide the most accurate assessment of mitophagy compared to other techniques. This is because non-specific autophagosomes are known to form at endoplasmic reticulum-mitochondria

contact sites (121-123) and mitochondria themselves can directly contact lysosomes (124).

1.3.2.7 Anti-DNA antibodies

Mitochondrial DNA (mtDNA) is commonly assessed as marker of mitochondrial content. Loss of mtDNA reflects a reduction in mitochondrial content, indicating mitochondrial degradation. While some studies have used this method to indirectly assess mitophagy, a major limitation of this approach is that not possible to determine whether mitochondria have been degraded by lysosomes or by other means, such as mitochondrial proteases.

1.3.3 Other approaches

1.3.3.1 Biochemical analysis of mitophagic flux

Assessing rates of mitophagy turnover by blocking lysosome-dependent degradation, with and without use of selective inhibitors, provides a read-out of mitophagy via so-called 'mitophagic flux' (129-133). Fusion of autophagosomes with lysosomes can be prevented using drugs, such as bafilomycin A1 and colchicine. Following treatment, mitochondrial proteins are isolated from cell and tissue lysates prior to western blotting with antibodies that are specific to proteins implicated in autophagy, such as LC3II and SQSTM1/ p62 (129-131, 133). Mitophagic flux can then be determined by subtracting the values of protein abundance obtained before the use of the drug inhibitor from those acquired afterwards. While this technique provides some insight into mitophagy, it lacks sensitivity (113). Moreover, bafilomycin A1 is highly toxic and not suitable for use in vivo while colchicine is known to induce unwanted off target effects, such as DNA damage (134).

Table 1.1

Comparison of the methods available to assess mitophagy in vitro and in vivo. Taken from McWilliams and Ganley (113)

Method/ Technique	Advantages	Disadvantages
Transmission electron microscopy (TEM)	• Gold-standard method of detection • Enables direct visualisation of autophagosomal membranes, autophagic bodies, and other cellular compartments • Immunolabeling can localise proteins of interest to mitophagosomes	• Laborious - many steps where error/inconsistencies can be introduced • Requires high degree of technical expertise to implement and execute • Requires depth of experience to interpret • Not adaptable for high throughput screening • Difficult to optimise for tissues • Often requires perfusion fixation for tissues • Immunolabeling can be challenging due to loss of epitopes during sample processing
Mito-QC	• Provides end-point readout of mitophagy in vitro and in vivo • OMM labelling enables monitoring/characterisation of mitochondrial network and study of dynamics • Constitutive expression facilitates constant monitoring • Compatible with tissue fixation • Immunolabeling enables resolution of mitophagy in a vast array of cell subtypes in vivo • Compatible with freezing and samples stored long-term	• Fixation must be conducted using formaldehyde at pH 7.0: any deviation in pH of fixative will result in de-quenching of GFP (yellow/gold mitolysosomes instead of red-only). • LAMP1 immunostaining can be used to easily verify the lysosomal nature of presumptive mitophagic structures. For fluorescent immunolabeling, secondary fluorophores limited to those outside of GFP/mCherry spectra • Incompatible with heat-mediated antigen retrieval - SDS-mediated antigen retrieval possible • Level of reporter expression must be controlled to prevent mislocalisation • mCherry and GFP signals are suggested to be susceptible to

	• No specialist microscopy setup required- compatible with simple and sophisticated systems • Ease of measurement enables multiparametric quantitation- mitolysosome number, size, mitochondrial shape, etc	proteasome-dependent degradation (126)
Mt-Keima	• Provides end-point readout of mitophagy in vitro and in vivo • Compatible with intravital imaging	• mt-Keima protein is incompatible with fixation and thus directs immunolabeling, only enables a regional analysis of mitophagy in complex tissues • Analysis must be conducted in live tissue slices, not amenable to high-throughput in vivo analysis and may necessitate further verification • mt-Keima signal is lost upon freezing/ cryosectioning not possible • Long-term storage of tissue specimens and slices for reference is not possible • No antibodies yet available to Keima protein, thus electron microscopy-based verification not possible • Spectral overlap can complicate interpretation and quantitation • Level of reporter expression must be controlled to prevent mislocalisation
Mt-SRAI	• Provides end-point readouts of mitophagy under both live and fixed conditions • Compatible with high-throughput screening of mitophagy inducers	• No antibodies yet available to label SRAI proteins, thus electron microscopy-based verification is not possible

	• Untargeted cytosolic SRAI is cleared via degrons encoded within the SRAI construct	
MitoTimer	• Enables a pulse-chase monitoring of mitochondrial half-life and mitophagy in vitro and in vivo • Useful model to understand biogenesis • Compatible with fixation and immunolabeling	• Direct measurements of mitophagy not possible until MitoTimer red puncta are shown to colocalise with staining or fluorescent labelling of the lysosome • Conditional model requires the use of doxycycline to activate in vitro • Constitutive mito-Timer expression in mice reported to be heterogeneous in tissue (the heart: expression in ventricles, reduced in aorta) • Maturation of mito-Timer protein may be different across cells and tissues in vivo
Colocalisation of mitotracker and lysotracker	• Rapid, easy to use	• Incompatible to detect mitophagy in vivo • Documented problems with specificity and variability in labelling • Off-target effects in other membrane-bound organelles
Immunofluorescence-based co-localisation of mitochondria with LC3-positive Autophagosome	• Rapid, easy to use	• Difficult to implement for in vivo mitophagy • Non-specific autophagosomes thought to form at mitochondria • Not all mitophagy may be LC3-dependent

Anti-DNA antibodies	• Enables visualisation of loss of mtDNA nucleoids following stimulus-induced mitophagy in vitro	• Direct measurements of mitophagy not possible • Expensive • Antibody used in field (Progen) is highly inefficient in tissues: manufacturer recommends 1:10 dilution • Yields variable results in vivo
Biochemical analysis of mitophagic flux	• Rapid, easy to use	• Low sensitivity, i.e., high levels of mitophagy required • Lysosomal inhibitors required to interpret flux (e.g., Bafilomycin A1, hydroxychloroquine) and can have detrimental effects in vivo

1.4 Skeletal muscle health and mitophagy in ageing

Skeletal muscle makes up ~40% of total body mass (135) and its primary functions are to; enable movement, maintain posture, generate heat and store and move substances within the body. During ageing, skeletal muscle health declines, often progressing into a condition known as sarcopenia (136). From a clinical standpoint, sarcopenia is defined by low muscle strength and low muscle quantity/quality and it is considered to be severe when these characteristics are accompanied by impaired physical performance (136). As sarcopenia manifests the likelihood of functional impairment and disability increases (137) meaning that individuals cannot perform tasks that are essential for daily living. This places a significant financial burden on healthcare systems (138).

The reasons why sarcopenia manifests during ageing are not well understood. One hypothesis is that mitochondrial quality control becomes disrupted (139). As mentioned previously, mitochondrial clearance via mitophagy is an important mechanism of mitochondrial quality control and recent work suggests that this process is compromised in aged muscle (140). To support this, skeletal muscle mitochondria accrue protein damage (141) and become functionally impaired (142-145) in humans during ageing. The accumulation of damaged and dysfunctional mitochondria reported in these studies is consistent with the notion that mitochondrial clearance via mitophagy is compromised in aged muscle. Furthermore, Ryu and colleagues (146) have also shown that activating mitophagy with the bioactive metabolite Urolithin A improves muscle function in rodent models. Taken together, these studies suggest that age-related impairments in mitophagy may play a role in aged skeletal muscle dysfunction and sarcopenia.

At present, the molecular signalling pathways that drive mitophagy in skeletal muscle are not well understood. Thus, gaining a deeper understanding of molecular mechanisms that control mitophagy in skeletal muscle will help to identify important signalling molecules that regulate this process. Such knowledge can then be used to help develop novel therapies, including pharmacological strategies, to combat defective mitophagy in muscle and therefore promote healthy ageing.

1.5 Mitophagy in skeletal muscle: what do we already know?

1.5.1 Measurement models

As discussed previously, transmission electron microscopy (TEM) is the gold standard technique for detecting mitophagy occurrence because it enables direct visualisation of mitochondria inside autophagic and lysosomal membranes (113). However, it is not widely used in skeletal muscle research, mainly because operating TEM requires a high degree of technical expertise (113). Without TEM, it is not currently possible to directly assess skeletal muscle mitophagy in humans. As a result, in-vivo fluorescence-based models, such as mito-QC (48, 49, 58, 147), mito-Timer (58), and mt-Keima (50, 148, 149) are starting to be used. Furthermore, immortalised rodent and primary human muscle cells can be used to study mitophagy when combined with mitochondria-lysosome imaging tools. Because of the relative ease of culturing immortalised rodent muscle cells, such as C2C12 and L6 compared to primary muscle cells, immortalised cells are more commonly used (132, 150-152). However, when using immortalised cell lines to study skeletal muscle mitophagy, it is important to recognise that differences in mitophagy and its signalling mechanisms may exist between species. This is supported by differences in the transcriptome and metabolism of immortalised rodent compared to human primary

muscle cells (148). As such, immortalised rodent skeletal muscle cells do not fully represent human skeletal muscle.

1.5.2 Mitophagy at rest

Moderate levels of mitophagy have been shown to occur in skeletal muscle under resting conditions compared to other tissues. In skeletal muscle cross sections obtained from mice stably expressing mito-QC, levels of mitophagy are similar to cardiac muscle, more than the spleen, but less than the liver and kidneys (48). Because these data have only recently been generated, the reasons why levels of mitophagy are different between tissues is not well understood. Nevertheless, subsequent work from the same group has demonstrated that mitophagy occurrence in skeletal muscle correlates with its glycolytic activity (147). In this study, the highly oxidative soleus muscle obtained from mito-QC knock-in mice displayed fewer mitophagy events per tissue area compared to the more glycolytic gastrocnemius (147). Furthermore, red gastrocnemius fibres displayed far fewer mitophagy events compared to the more glycolytic mixed and white gastrocnemius muscle fibres (147).

1.5.3 Signalling mechanisms

At present, our understanding of the molecular mechanisms that regulate mitophagy in skeletal muscle lags well behind what is known in non-muscle cell lines. So far, the regulatory roles of PINK1-Parkin, AMPK-ULK1 and FUNDC1 have been studied the most thoroughly. In contrast, the roles of BNIP3 and BNIP3L/NIX have not been studied as comprehensively. Furthermore, other signalling molecules implicated in mitophagy, such as TBK1, MUL1 ARIH1, BCL2-L-13, FKBP8 and cardiolipin are yet to be investigated in skeletal muscle.

1.5.3.1 PINK1-Parkin

Only a few studies in the literature have evaluated the role of PINK1 and Parkin in skeletal muscle mitophagy. As a result, whether PINK1-Parkin signalling is a potent regulator of mitophagy in skeletal muscle is debated. Borgia and colleagues (153) reported that patients with spinal and bulbar muscular atrophy (SBMA) have increased PINK1 protein in mitochondria isolated from skeletal muscle (153). Consistently, indirect measurements of mitophagy (co-localisation of LC3 and ATPase) are also increased in SBMA patients, suggesting that the PINK1-mediated mitophagy may be activated under conditions of severe pathological stress in human skeletal muscle. Furthermore, Chen and colleagues (130) reported that LC3-II flux in mitochondrial enriched skeletal muscle lysates is attenuated following endurance exercise in Parkin knock-out (KO) mice, suggesting that Parkin is required for exercise-induced mitophagy. Interestingly, recent work from the Yan laboratory has also shown that acute endurance exercise induces mitophagy in mice expressing the pMitoTimer reporter (58). However, using the same exercise protocol, the authors reported that PINK1 is not present in mitochondria enriched muscle lysates, suggesting that PINK1 is dispensable for mitophagy under these conditions (154). McWilliams and colleagues (49) have also demonstrated that basal mitophagy occurs in muscle from both PINK1 KO and wild type mice on a mito-QC background, suggesting that under healthy, rested conditions, PINK1 is not required for mitophagy.

1.5.3.2 AMPK and ULK1

Laker and colleagues were the first to demonstrate that AMPK is involved in skeletal muscle mitophagy using mice expressing a muscle-specific dominant-negative form of the catalytic α2 subunit of AMPK (dnTG) (58). Interestingly, mitophagy was shown to be transiently elevated 6 h after a bout of treadmill running in wild type, but not dnTG, mice (58). Downstream of AMPK, the authors also showed that ULK1 is required for exercise-induced mitophagy using muscle-specific ULK1 knock-out mice (58).

1.5.3.3 FUNDC1

Fu and colleagues (155) have shown that FUNDC1 mediates skeletal muscle mitophagy. In their study, levels of mitophagy as assessed via mt-Keima were reported to be significantly attenuated in primary murine FUNDC1 muscle KO cells following FCCP treatment (155).

1.5.3.4 BNIP3 & BNIP3L/NIX

In humans, previous work has shown that patients with spinal and bulbar muscular atrophy (SBMA) have increased BNIP3 protein levels in mitochondria isolated from skeletal muscle (153). Consistently, indirect measurements of mitophagy (co-localisation of LC3 and ATPase) are also increased in SBMA patients, suggesting that BNIP3 may be activated for mitophagy under conditions of pathological stress. In addition to this, others have measured BNIP3 mRNA expression and protein content in skeletal muscle without making direct, quantifiable measurements of mitophagy (156, 157). While observational investigations such as these provide some insight, there is a need for more thorough mechanistic research to elucidate the roles of BNIP3 and BNIP3L/NIX in skeletal muscle mitophagy.

1.6 Thesis aim and objectives

The overarching aim of this thesis is to improve understanding of the molecular signalling mechanisms that regulate mitophagy in skeletal muscle. Because there are very few studies investigating PINK1-Parkin signalling in the context of skeletal muscle mitophagy, this pathway will be a focal point of this thesis. In addition, because activation of AMPK has been indicated to induce mitophagy skeletal muscle tissue under physiological conditions, it is important to identify downstream signalling molecules that are involved in this process.

In parallel, as has been highlighted throughout Chapter 1, several fluorescent-based tools have been developed in recent years to provide quantitative read-outs of mitophagy. Through collaboration with Dr Ian Ganley's laboratory at the University of Dundee, we managed to gain access to the mito-QC mitophagy reporter construct. Crucially, utilising this construct means that it is possible to align molecular signalling events with the end-point process of mitophagy.

Thus, the specific objectives of this thesis in the context of skeletal muscle are to:

1) Develop a C2C12 cell line that stably expresses mito-QC.

2) Determine whether endogenous PINK1-Parkin signalling is functionally active.

3) Determine whether pharmacological activation of AMPK induces mitophagy.

4) Identify AMPK substrates that help to orchestrate mitophagy.

5) Determine whether AMPK cooperates with PINK1-Parkin signalling.

Herein:

Chapter 2 describes the general methodology and analytical techniques used in the thesis.

Chapter 3 describes the development of a stable skeletal muscle cell line as well as a ubiquitin pull-down technique to assess the activities of PINK1 kinase and Parkin E3 ligase in skeletal muscle.

Chapter 4 provides mechanistic insight into AMPK-mediated mitophagy and PINK1-Parkin signalling in skeletal muscle.

Chapter 5 integrates the findings of Chapter 4 into the current literature while highlighting the most important questions that are yet to be addressed within this field.

Chapter 6 then provides additional written analysis focussing on the main findings of this thesis as well as its limitations.

CHAPTER 2

GENERAL METHODS

2.1 Cell lines and culture

All cells were seeded on 100mm dishes and cultured in Dulbecco's Modified Eagle Medium (DMEM) containing GlutaMAX, 25 mM glucose, 1 mM sodium pyruvate, supplemented with 10% (v/v) foetal bovine serum (GE Healthcare, Buckinghamshire, UK) and 1% (v/v) Penicillin-Streptomycin (10 000 Units/mL-ug/mL). Medium (10 mL) was changed every other day. Cultures were maintained in a humidified incubator at 37°C with an atmosphere of 5% CO2 and 95% air.

2.1.1 C2C12

Mouse skeletal muscle C2C12 myoblast cells were obtained from the American Type Culture Collection (ATCC, Manassas, VA, USA). C2C12 myoblasts were grown until 90% confluent when media was changed to elicit differentiation into myotubes (high glucose DMEM supplemented with 2% (v/v) horse serum (Sigma-Aldrich, Cambridgeshire, UK) and 1% (v/v) Penicillin-Streptomycin (10 000 Units/mL-ug/mL). Differentiation was allowed to occur for 5-7 days, until myotubes were fully formed and experimental procedures began.

2.1.2 HeLa

Wild type and PINK1 knockout (KO) HeLa cells were kindly provided by Professor Richard Youle (National Institutes of Health, USA).

2.1.3 HEK293 Flp-In

Wild type and AMPK α1/α2 deficient HEK293 Flp-In (KO) cells were kindly provided by Professor Grahame Hardie (University of Dundee, UK).

2.2 Drug reconstitution and cell treatment

Carbonyl cyanide m-chlorophenyl hydrazine (CCCP) (Sigma-Aldrich, Cambridgeshire, UK) and adenosine monophosphate (AMP)–activated protein kinase (AMPK) activator 991 (Aobious, MA, USA) were reconstituted as 10 mM and 20 mM (1000x) stocks in DMSO, respectively.

2.3 Cell lysis

Following drug treatment, cells were washed twice in ice-cold Dulbecco's phosphate buffered saline (DPBS) without calcium and magnesium ThermoFisher Scientific, Leicestershire, UK). Cells were lysed in ice-cold sucrose lysis buffer (500 µL) containing: 250 mM sucrose, 50 mM Tris-base (pH 7.5), 50 mM sodium fluoride, 10 mM sodium β- glycerolphosphate, 5 mM sodium pyrophosphate, 1 mM EDTA, 1 mM EGTA, 1 mM benzamidine, 1 mM of sodium orthovanadate, 1 x complete Mini EDTA-free protease inhibitor cocktail, 1% (v/v) Triton X-100, and 100 mM 2-chloroacetamide. Cell lysates were centrifuged for 15 minutes at 18 000 g (4°C) and stored at -80ºC until further analysis.

2.4 Tissue powdering and homogenisation

Snap-frozen mouse muscle tissue was powdered using a Cellcrusher tissue pulveriser (Cellcrusher, Co. Cork, Ireland) on dry ice. Thereafter, ~50mg of powdered muscle was homogenised in a 10-fold volume excess ice-cold sucrose lysis buffer (see section "2.3 Cell lysis") using a hand-held Polytron homogeniser. The resulting homogenate was centrifuged for 15 minutes at 18 000 g (4°C) to pellet insoluble material before lysates were stored at -80ºC until further analysis.

2.5 Protein assay

Analysis of total protein was made using the Bradford protein assay (ThermoFisher Scientific, Leicestershire, UK). Briefly, 10 µL of cell or tissue lysate was diluted in 90 µL or 190 µL ddH2O respectively. Diluted samples were loaded in duplicate into a 96- well microplate containing 300 µL Bradford protein reagent. Absorbance was measured at 595 nm using the FLUOstar OMEGA microplate reader. Protein in each sample was quantified from a standard curve using BSA standards ranging from 1-100 µg.

2.6 Sample preparation

Cell and tissue lysates were prepared in 1x NuPAGE LDS sample buffer containing 2- mercaptoethanol (final concentration 1.5%) and left to denature overnight at room temperature.

2.7 Western blotting

2.7.1 Gel Electrophoresis

Prepared samples (25-75 µg of total protein) were loaded into 4%-12% Bis/Tris precast gels (ThermoFisher Scientific, Leicestershire, UK) prior to sodium dodecyl sulphate–polyacrylamide gel electrophoresis (SDS-PAGE). Gels were run in 1x MOPS buffer (ThermoFisher Scientific, Leicestershire, UK) for approximately 80 minutes at 150V.

2.7.2 Transfer and Blocking

Proteins were transferred onto PVDF membranes (Millipore, Hertfordshire, UK) via wet transfer for 1 hour at 100V. Membranes were blocked in 3% of BSA diluted in Tris-

buffered saline Tween-20 (TBST): 20 mM Tris-base pH 7.5, 137 mM sodium chloride, 0.1% (v/v) Tween-20, for 1 hour.

2.7.3 Primary Antibody

Primary antibodies were diluted in 3% of BSA made up in TBST. The list of primary antibodies used are described in 4.8 -Supplementary Table 1. Membranes were left to incubate overnight in primary antibody at 4°C.

2.7.4 Secondary Antibody

Membranes were washed in TBST three times for 10 minutes prior to incubation in horse radish peroxidase conjugated secondary antibodies for 1 h at room temperature. The list of secondary antibodies used are described in 4.8 -Supplementary Table 1. Prior to imaging, membranes were washed a further three times for 10 minutes in TBST to removal residual secondary antibody.

2.7.5 Imaging

Antibody binding was detected using enhanced chemiluminescence horseradish peroxidase substrate detection kit (Millipore, Hertfordshire, UK). Imaging was undertaken using a G:BOX Chemi-XR5 (Syngene, Cambridgeshire, UK).

2.7.6 Analysis

Manual band quantification was performed using ImageJ/Fiji (National Institutes of Health, USA). Corrections were performed to remove the effects of background signal. Proteins of interest were normalised to vinculin or glyceraldehyde 3-phosphate dehydrogenase (GAPDH) loading controls.

2.8 Respirometry

C2C12 myoblasts were seeded at 20 000 cells per well on XFe24 microplates and cultured as previously described in “2.1 Cell lines and culture”. At 90% confluency, myoblasts were differentiated for 5 days as described in “2.1.1 C2C12”. Fully differentiated myotubes were exposed to 10 μM CCCP or 0.1% DMSO as a vehicle control for 24 hours. Treated cells were washed in Agilent Seahorse XF Base DMEM (Agilent Technologies, Manchester, UK) supplemented with 25 mM glucose, 1 mM sodium pyruvate, and 2 mM L-Glutamine. C2C12 myotubes incubated in Agilent Seahorse XF Base DMEM were inserted into a Seahorse XFe24 extracellular flux analyser (controlled at 37°C) for a 10-minute equilibration, and four measurement cycles to record basal cellular respiration. Oligomycin (1 μM), FCCP (3 μM), and a mixture of rotenone (1 μM) plus antimycin A (2 μM) were then added sequentially to establish ADP phosphorylation and proton leak rates of respiration; maximum electron transfer capacity, and residual oxygen consumption, respectively. After each addition of these compounds a further four measurement cycles were recorded. For all respirometry experiments, each measurement cycle consisted of a 1-minute wait, 2-minute mix, and 3-minute measurement period and all data were normalized to total protein as quantified by Bradford protein assay.

2.9 Statistical analysis

All statistical analyses were performed using GraphPad Software Inc Prism version 8. For time course and dose response experiments, a one-way analysis of variance (ANOVA) was performed with Dunnett's or Sidak's multiple comparisons test where appropriate. For microscopy and seahorse extracellular analyser experiments, unpaired t tests were performed. Data are presented as mean ± SEM.

CHAPTER 3

DEVELOPING TOOLS TO STUDY MITOPHAGY AND ITS SIGNALLING MECHANISMS IN SKELETAL MUSCLE

3.1 Generating a stable skeletal muscle mito-QC reporter cell line

3.1.1 Background

As discussed previously, the mito-QC reporter construct as first described by Allen and colleagues (114) uses a functionally inert, tandem mCherry-GFP tag fused to the mitochondrial targeting sequence of the outer mitochondrial membrane (OMM) protein mitochondrial fission 1 (FIS1). This mito-QC mitophagy reporter (mCherry-GFP-mt-$FIS1_{101-152}$) takes advantage of the fact that green fluorescence protein (GFP), unlike mCherry, cannot withstand the acidic proteolytic conditions of the lysosome (114). After identifying that the mito-QC reporter provides direct and reliable end-point read-outs of mitophagy, through collaboration with Dr Ian Ganley's laboratory at the University of Dundee, we managed to gain access to this construct. Thereafter, our aim was to generate a stable C2C12 mito-QC skeletal muscle cell line to study mitophagy and its signalling mechanisms in muscle.

3.1.2 Method

3.1.2.1 DNA construct

A pBABE.hygro vector containing cDNA for mCherry, GFP, and residues 101-152 of mouse mitochondrial fission 1 protein (FIS1), otherwise known as mito-QC, was kindly provided by Dr Ian Ganley (MRC PPU, University of Dundee, UK).

3.1.2.2 Transfection & viral harvesting

HEK293 FT cells were kindly provided by Professor Miratul Muqit (MRC PPU, University of Dundee, UK) and cultured as previously described in "2.1 Cells lines and culture". The mito-QC construct was co-transfected into HEK293FT cells with

GAG/POL and VSV-G expression plasmids (Clontech, Saint- Germain-en-Laye, France) for retrovirus production using lipofectamine LTX reagent (ThermoFisher Scientific, Leicestershire, UK) in accordance with manufacturer's instructions. Media containing the resulting retrovirus was collected 48 h after transfection before being aliquoted into 1.5 mL eppendorf tubes and stored at -80°C.

3.1.2.3 Viral infection and selection of mito-QC positive C2C12 myoblasts

A volume of 5 mL of collected media containing the retrovirus was applied to C2C12 myoblasts in the presence of 10 μg/mL polybrene for 24 h (Sigma-Aldrich, Cambridgeshire, UK). Cells were selected with 500 μg/mL of hygromycin for 48 h (Sigma-Aldrich, Cambridgeshire, UK). Cells were subsequently placed in fresh culture medium and allowed to reach 80% confluency prior to a further 48 h round of hygromycin selection. Surviving cells indicating mito-QC positive C2C12 myoblasts were placed in fresh culture medium and allowed to recover to 80% confluency prior to cell sorting.

3.1.2.4 Cell sorting

To obtain a stable homogenous cell line, infected C2C12 myoblasts were sorted and collected based on their expression of mCherry and GFP using FACSAria (BD Biosciences, Berkshire, UK). These procedures were carried out by specialists in the flow cytometry core facility based in the Institute of Biomedical Research (IBR) at the University of Birmingham. Sorted C2C12 myoblasts stably expressing the highest relative mCherry-GFP-mtFIS1$_{101\text{-}152}$ signal were reseeded and further expanded for characterisation and cryopreservation.

3.1.2.5 Cell treatment and fixation

C2C12 myoblasts stably expressing mCherry-GFP-mt-FIS1$_{101\text{-}152}$ were seeded on imaging dishes (Ibidi, Grfelfing, Germany) and treated with either 10 μM of CCCP. Following treatment, cells were washed twice with PBS and fixed in 3.7% of formaldehyde with 200 mM of HEPES (pH 7.0) for 10 minutes. After fixing, cells were washed and incubated for 10 minutes in DMEM supplemented with 10 mM of HEPES (pH 7.0), and then washed with PBS before applying Prolong gold mounting solution containing 4′,6-diamidino-2-phenylindole (ThermoFisher Scientific, Leicestershire UK).

3.1.2.6 Image capture

Imaging was performed using a Crest X-Light spinning disk system coupled to a Nikon Ti-E base, 60x/1.4 NA (CFI Plan Apo Lambda) air objective and Photometrics Delta Evolve EM-CCD. For GFP, excitation was delivered at λ = 458- 482 nm using a Lumencor Spectra X light engine, with emitted signals detected at λ = 500-550 nm. For mCherry, the wavelengths used for excitation and detection were λ = 563-587 nm and λ = 602-662 nm, respectively.

3.1.2.7 Quantification of mitophagy and mitochondrial fission

In cells expressing the mito-QC construct, under basal conditions, mitochondria fluoresce both red (mCherry) and green (GFP) making the mitochondrial network appear gold in colour when these spectra are merged (Figure 3.1 A: CTRL). However, upon mitophagy, the acidic microenvironment of the lysosome quenches the GFP signal but not mCherry. As a result, punctate structures that fluoresce red only form within the mitochondrial network (Figure 3.1 A: CCCP). The disappearance of GFP signal and the emergence of red puncta indicate sites of ongoing mitophagy (mitolysosomes). Therefore, in C2C12 myoblasts stably expressing mito-QC, mean fluorescence intensity of both mCherry were measured in 25 cells from at least 15 fields of view in each condition using ImageJ/Fiji (NIH, Bethesda, MD, USA). The mCherry/GFP ratio of treated cells were normalised to the DMSO treated control group. In doing so, the relative change in the mCherry/GFP ratio captures alterations in mitophagy at a whole cell level (Figure 3.1 B). For each cell measured, mean circularity and Feret's diameter were calculated using measurements made on four different sections of the mitochondrial network as markers of mitochondrial fission (Figure 3.1 B).

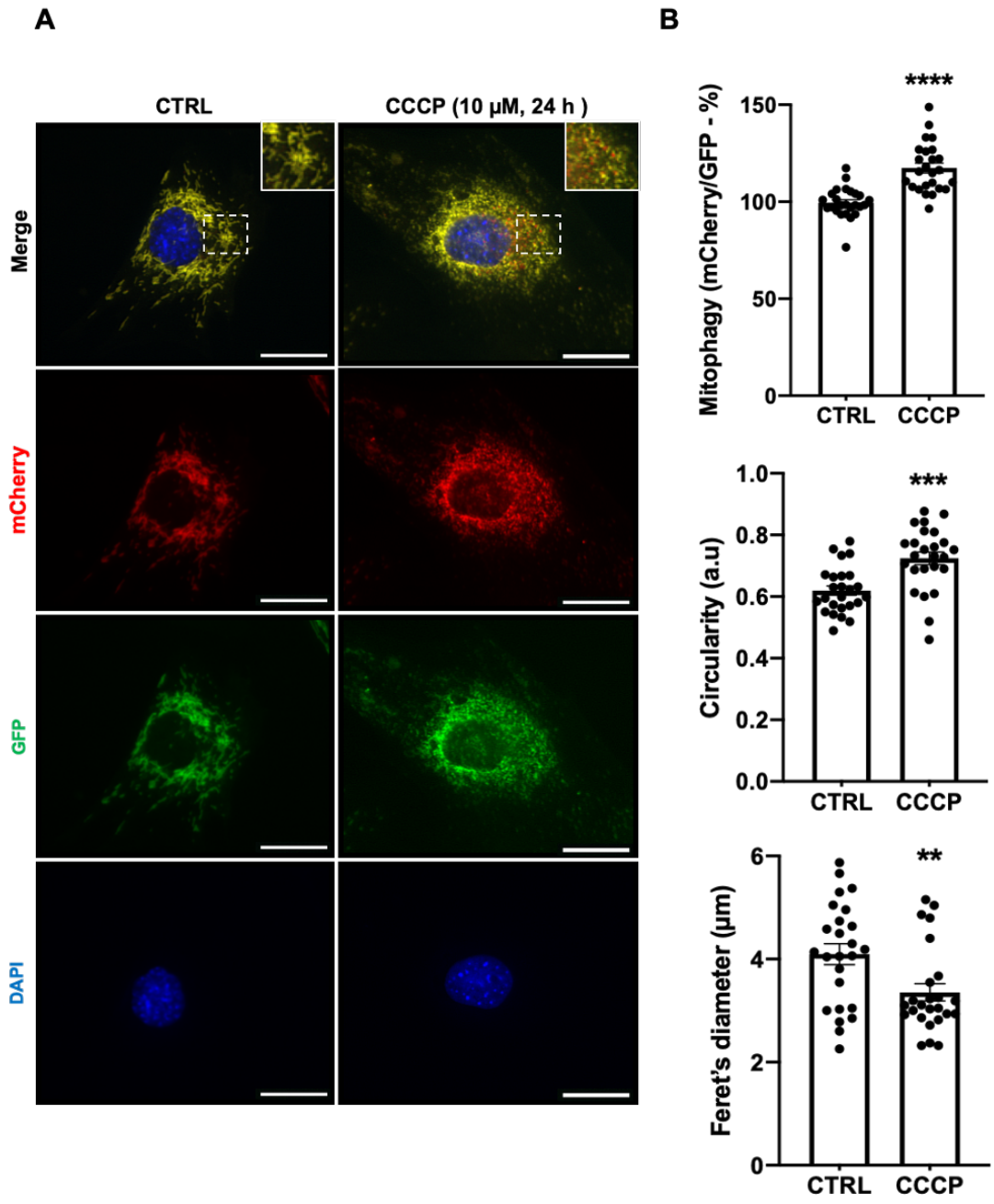

Figure 3.1. Visualisation and quantification of mitophagy and mitochondrial morphology in C2C12 cells stably expressing mito-QC. (A) Representative images illustrating CCCP-stimulated mitophagy and mitochondrial fission in C2C12 myoblasts. C2C12 myoblasts stably expressing mCherry-GFP-FIS1$_{101-152}$ treated with DMSO (0.1%, 24 h) as a vehicle control (CTRL) or CCCP (10 µM, 24 h). Red puncta appearing in the merged image indicate sites of mitophagy. Scale bars = 20 µm. B, Quantification of mitophagy (mCherry/GFP), circularity and Feret's diameter (n = 25 per group). Cells treated as in Figure 1A. Each data point represents one myoblast; mean ± SEM, **P < .01, ***P < .001, ****P <.0001.

3.2 Assessing endogenous PINK1 kinase and Parkin E3 ligase activity in skeletal muscle

3.2.1 Background

As discussed previously, the PINK1-Parkin signalling pathway is the most widely studied axis that regulates mitophagy in non-muscle cells. However, the necessity of this pathway for mitophagy in skeletal muscle is currently undefined. This is primarily due to the lack of appropriate tools to study the activities of PINK1 kinase and Parkin E3 ligase. The main reason why there are so few studies investigating the role of PINK1 in skeletal muscle mitophagy is because many of the commercially available antibodies are insensitive or unspecific when detecting endogenous PINK1 (158). Furthermore, because Parkin is reported to translocate to mitochondria for both mitophagy (42) and mitochondrial biogenesis (159-161) simply measuring mitochondrial Parkin content does not determine which process Parkin is involved in. Thus, developing tools to assess the activities of PINK1 kinase and Parkin E3 ligase will help to improve our understanding of the role of PINK1-Parkin signalling in skeletal muscle mitophagy.

PINK1 phosphorylates ubiquitin at Ser 65 as well as Parkin at Ser 65 within its ubiquitin like (UBL) domain (69-71, 73). The phosphorylation status of both ubiquitin and Parkin at Ser 65 can be used as a read out of PINK1 kinase activity. PINK1-mediated ubiquitin phosphorylation was first discovered using proteomics when PINK1 substrates were profiled in mitochondria isolated from wild-type and PINK1-deficient cells after CCCP treatment (69, 70). In this study, a ubiquitin derived Ser 65 phospho-peptide was identified in mitochondria-associated proteins only in wild-type cells, indicating that PINK1 phosphorylates ubiquitin at Ser 65. The presence of this kinase-substrate

relationship was further verified by in vitro kinase assays, in which recombinant PINK1 phosphorylated wild-type, but not Ser 65A ubiquitin (69-71). It has also been shown that recombinant PINK1 can phosphorylate Parkin at Ser 65 in vitro, and in cells, Parkin phosphorylation at Ser 65 is detected in response to CCCP treatment (73). Allosteric activation of Parkin through phospho-ubiquitin binding (72), along with PINK1-mediated Parkin phosphorylation (73) maximally activates Parkin (74). This enables Parkin to polyubiquitylate OMM proteins, such as CDGSH iron sulphur domain 1 (CISD1) (75, 76). Thus, Parkin's ubiquitin E3 ligase activity can be measured via the detection of polyubiquitin chains on known Parkin substrates.

Even though ubiquitin is the substrate of PINK1 and Parkin is an E3 ligase that tags outer mitochondrial membrane (OMM) proteins with ubiquitin, to our knowledge, a specific ubiquitin pull-down technique has not yet been used to study their intracellular activities in skeletal muscle. To facilitate the study of endogenous PINK1-Parkin signalling, we used immobilised haloalkane dehalogenase (HALO)-tagged-UBA^{UBQLN1} tetramers to capture all ubiquitylated proteins in whole cell and muscle tissue lysates. Successful enrichment of ubiquitin using this technique in whole cell and muscle tissue lysates is shown in Figure 3.2. To explore endogenous PINK1 and Parkin E3 activation, phosphorylation of ubiquitin at Ser 65 and CISD1 ubiquitylation were assessed as intracellular readouts of PINK1 kinase (69-71) and Parkin E3 ligase activity (75, 76) respectively. Interestingly, phosphorylation of Ub at Ser 65 and ubiquitylation of CISD1, were increased after 6, 12, and 24 hours of CCCP treatment (Figure 3.3), indicating this technique to be effective for the assessment of intracellular PINK1 kinase and Parkin E3 ligase activities in skeletal muscle. Although PINK1 is also capable of phosphorylating Parkin at Ser 65, we could not detect endogenous pSer65 Parkin after treating C2C12

muscle cells with CCCP (data not shown), further highlighting the importance of this ubiquitin pulldown technique to assess PINK1 kinase activity. Lastly, having adapted this assay from the work of others (74, 162) the most important consideration to be made when using this assay to measure PINK1-Parkin signalling is that a high amount of starting material (whole muscle lysate) is needed (~1mg per sample) to observe poly-ubiquitin chains.

3.2.2 Method

3.2.2.1 Bacterial expression of HALO-UBA^{UBQLN1} tandem ubiquitin binding entity (TUBE)

pET28a HIS-HALO-TUBE (MRC-PPU, Dundee) were transformed into Escherichia coli BL21 cells. Transformed colonies were selected, grown and expanded in 2000 mL of lysogeny broth LB at 37°C. After reaching an optical density at 600 nm of 0.6, 250 µM of isopropyl β-D-1-thiogalactopyranoside (IPTG) were added to bacterial cultures to induce protein expression. Cultures were left overnight at 18°C before being pelleted and resuspended in lysis buffer (50mM Tris-base (pH 8.0), 150mM NaCL, 50mM Imidazole, 0.5mM tris(2-carboxyethyl)phosphine (TCEP), 1mM phenylmethylsulfonyl fluoride (PMSF)); prior to cell disruption using an Emulsiflex C3 Cell Disruptor (Avestin Europe, Mannheim, Germany). Recombinant proteins were purified by the use of HIS-Trap (GE Healthcare) as per the manufacturer's instructions. Protein concentration measured by nanodrop, and the product stored at -80°C.

3.2.2.2 Ubiquitin enrichment

HaloLink resin (15 µL per sample) (Promega, Hampshire, UK), prewashed with phosphate buffered saline (PBS) was incubated with of HALO-UBA^{UBQLN1} TUBE protein (50 µg per sample) in 750 µL of binding buffer containing: 50 mM of Tris-HCl pH 7.5, 150 mM of sodium chloride, 0.05% of NP-40, 1 mM of dithiothreitol (DTT) for 2 hours at 4°C. Conjugated HaloLink resin and UBA^{UBQLN1} TUBE protein was incubated with 500-1000 µg of protein from lysed muscle and cell samples prior to overnight rotation at 4°C. After three washes in sucrose lysis buffer (see section "2.3 Cell lysis") the enriched Ub and poly-Ub extracts were transferred to a spin column prior to elution.

3.2.2.3 Sample preparation

Eluted samples were prepared in 1x NuPAGE LDS sample buffer containing 2-mercaptoethanol (final concentration 1.5%) and left to denature overnight at room temperature.

3.2.2.4 Western blotting

See Chapter 2 section 2.7. The antibodies used in Figure 3.2 & 3.3 are listed in Supplementary Table 4.10.

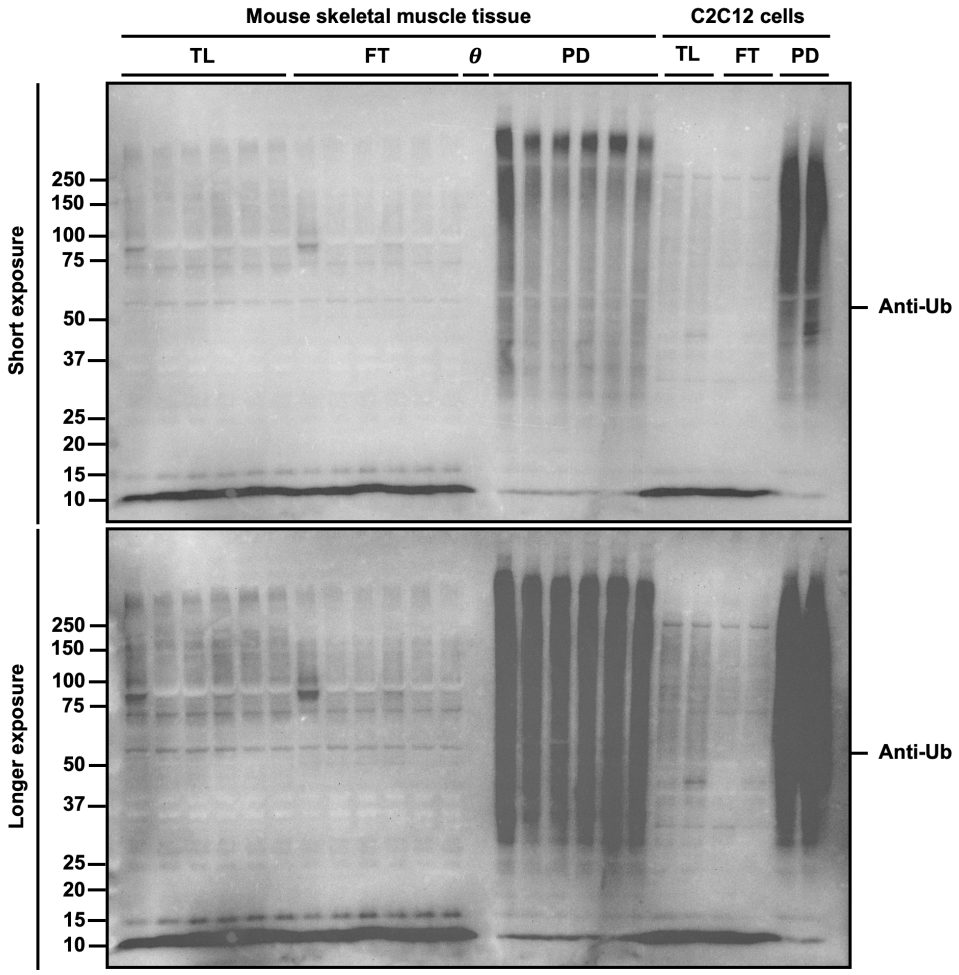

Figure 3.2. Validation of ubiquitin pull-down technique in murine skeletal muscle cells and tissue. Total lysates derived from mouse gastrocnemius muscle (N=6) and C2C12 myotubes (N=2) were incubated with ubiquitin-binding resins derived from his-halo-ubiquilin1 UBA domain tetramer (UBA^{UBQLN1}). Captured ubiquitylated proteins were subject to SDS-PAGE and western blotting with antibodies specific to total ubiquitin (Ub, to verify ubiquitin enrichment). TL = Total lysate, FT = Flow through, θ = Empty lane, PD = Pull-down.

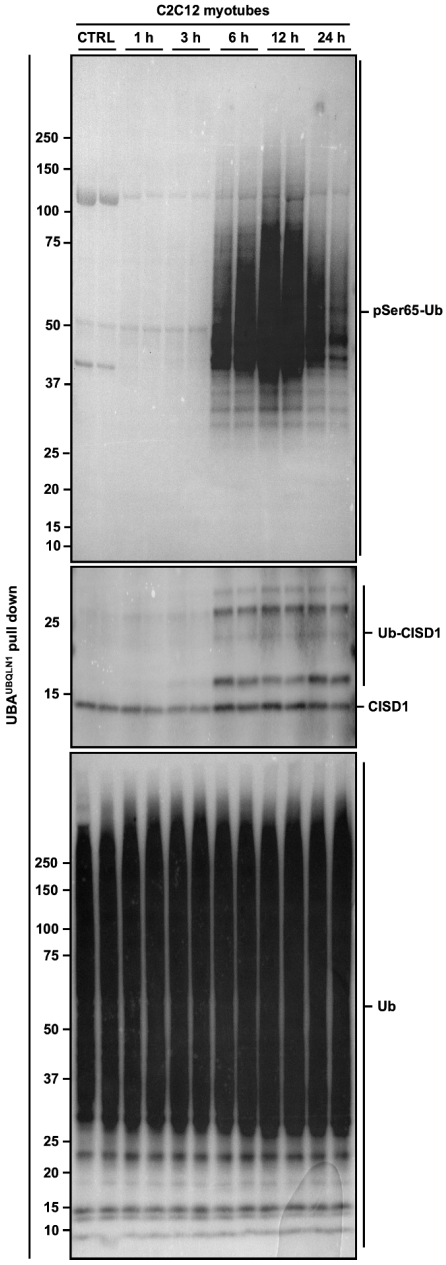

Figure 3.3 CCCP treatment induces endogenous PINK1kinase activity and Parkin E3 ligase activity in skeletal muscle cells. C2C12 myotubes were treated with DMSO (0.1%, 24 h) as a vehicle control (CTRL) or 10 μM of CCCP for up to 24 h. Total lysates were incubated with ubiquitin-binding resins derived from his-halo-ubiquilin1 UBA domain tetramer (UBA^{UBQLN1}). Captured ubiquitylated proteins were subject to SDS-PAGE and western blotting with antibodies specific to: phospho-Ser65 ubiquitin (pSer65 Ub, to determine intracellular PINK1 kinase activity), CDGSH iron sulphur domain 1 (CISD1, to determine intracellular Parkin E3 ligase activity toward its substrate) and total ubiquitin (Ub, to verify ubiquitin enrichment). Representative images of n = 3 independent experiments are shown.

CHAPTER 4

AMPK ACTIVATION INDUCES MITOPHAGY AND PROMOTES MITOCHONDRIAL FISSION WHILE ACTIVATING TBK1 IN A PINK1-PARKIN INDEPENDENT MANNER

4 AMPK activation induces mitophagy and promotes mitochondrial fission while activating TBK1 in a PINK1-Parkin independent manner

Alex P. Seabright[1], Nicholas H. F. Fine[2], Jonathan P. Barlow[3], Samuel O. Lord[1], Ibrahim Musa[1], Alexander Gray[4], Jack A. Bryant[5], Manuel Banzhaf[5], Gareth G. Lavery[2,6,7], D. Grahame Hardie[4], David J. Hodson[2,6,8], Andrew Philp[9,10], Yu-Chiang Lai[1,2,3,7]

1. School of Sport, Exercise and, Rehabilitation Sciences, University of Birmingham, Birmingham, UK
2. Institute of Metabolism and Systems Research, University of Birmingham, Birmingham, UK
3. Mitochondrial Profiling Centre, University of Birmingham, Birmingham, UK
4. Division of Cell Signalling & Immunology, School of Life Sciences, University of Dundee, Dundee, UK
5. Institute of Microbiology and Infection, School of Bioscience, University of Birmingham, Birmingham, UK
6. Centre for Endocrinology, Diabetes and Metabolism, Birmingham Health Partners, Birmingham, UK
7. MRC Versus Arthritis Centre for Musculoskeletal Ageing Research, University of Birmingham, Birmingham, UK
8. Centre of Membrane Proteins and Receptors, University of Birmingham, Birmingham, UK

9. Diabetes & Metabolism Division, Garvan Institute of Medical Research, Sydney, New South Wales, Australia School of Sport, Exercise and Rehabilitation Sciences, University of Birmingham, UK.

Published in: **Seabright AP, Fine NHF, Barlow JP, Lord SO, Musa I, Gray A, Bryant JA, Banzhaf M, Lavery GG, Hardie DG, Hodson DJ, Philp A, Lai YC**. AMPK activation induces mitophagy and promotes mitochondrial fission while activating TBK1 in a PINK1-Parkin independent manner. The FASEB Journal, 2020 Mar 23. https://doi.org/10.1096/fj.201903051R

Author contributions: A.P. Seabright and Y.C. Lai conceived the study and designed experiments. A.P. Seabright performed all experiments with the following exceptions. S.O. Lord was trained by A.P. Seabright to perform the ubiquitin pull down assay before being handed samples already collected by A.P. Seabright. The western blot data generated by S.O. Lord is presented in Figure 4.4C. I. Musa helped to culture, treat and lyse both wild-type and AMPK α1/α2 deficient HEK293 Flp-In cells for one of the three independent experiments in Figure 4.7C. This is because A.P. Seabright was attending a conference (Life Sciences: Post-Translational Modifications and Cell Signalling, Nottingham, UK March 2019). The other two independent experiments in Figure 4.7C were completed by A.P. Seabright. A.P. Seabright and J.P. Barlow analysed the data. N.H.F. Fine, J.A. Bryant, M. Banzhaf, and D.J. Hodson provided microscopy support and expertise. A.P. Seabright and Y.C. Lai wrote the manuscript. A. Gray, M. Banzhaf, D.G. Hardie, G.G. Lavery, D.J. Hodson, and A. Philp helped to review the manuscript. All authors discussed the results and approved the final manuscript.

4.1 - Abstract

Mitophagy is a key process regulating mitochondrial quality control. Several mechanisms have been proposed to regulate mitophagy, but these have mostly been studied using stably expressed non-native proteins in immortalised cell lines. In skeletal muscle, mitophagy and its molecular mechanisms require more thorough investigation. To measure mitophagy directly, we generated a stable skeletal muscle C2C12 cell line, expressing a mitophagy reporter construct (mCherry-GFP-mtFIS1$_{101-152}$). Here, we report that both carbonyl cyanide m-chlorophenyl hydrazone (CCCP) treatment and adenosine monophosphate activated protein kinase (AMPK) activation by 991 promote mitochondrial fission via phosphorylation of MFF and induce mitophagy by ~20%. Upon CCCP treatment, but not 991, ubiquitin phosphorylation, a read-out of PTEN-induced kinase 1 (PINK1) activity, and Parkin E3 ligase activity toward CDGSH iron sulphur domain 1 (CISD1) were increased. Although the PINK1-Parkin signalling pathway is active in response to CCCP treatment, we observed no change in markers of mitochondrial protein content. Interestingly, our data shows that TANK-binding kinase 1 (TBK1) phosphorylation is increased after both CCCP and 991 treatments, suggesting TBK1 activation to be independent of both PINK1 and Parkin. Finally, we confirmed in non-muscle cell lines that TBK1 phosphorylation occurs in the absence of PINK1 and is regulated by AMPK-dependent signalling. Thus, AMPK activation promotes mitophagy by enhancing mitochondrial fission (via MFF phosphorylation) and autophagosomal engulfment (via TBK1 activation) in a PINK1-Parkin independent manner.

4.2 - Introduction

Mitochondria play an important role in maintaining skeletal muscle function (163). The removal of defective mitochondria (known as mitophagy) has been implicated in the sarcopenia of ageing muscle (163). Despite this, our understanding of the molecular mechanisms that regulate skeletal muscle mitophagy remains in its infancy. The lack of tractable tools to study mitophagy and its signalling events in skeletal muscle have made understanding this process difficult. In order to improve our understanding of mitophagy in skeletal muscle, the development of novel tools is required to dissect this process and its signalling at an endogenous level.

Multiple signalling molecules have been implicated in the control of mitophagy, including PTEN-induced kinase 1 (PINK1), Parkin, AMP-activated protein kinase (AMPK), BCL2/adenovirus E1B 19 kDa protein-interacting protein 3 (BNIP3), and BCL2 Interacting Protein 3 Like (BNIP3L, also known as NIX) (57, 58, 68). The PINK1-Parkin signalling axis is the most studied pathway governing mitophagy. In non-muscle cell lines, under basal conditions, PINK1 is continuously degraded through the N-end-rule pathway (64). However, upon loss of mitochondrial membrane potential, for example, following uncoupling with the protonophore carbonyl cyanide m-chlorophenyl hydrazone (CCCP), PINK1 is stabilized and activated on the outer mitochondrial membrane (OMM) (46). This facilitates PINK1-dependent ubiquitin (Ub) phosphorylation at Ser 65 (69-71) leading to the recruitment of Parkin E3 Ub ligase to the OMM (46). Allosteric activation of Parkin through phospho-Ub binding, (72) along with PINK1 mediated Parkin phosphorylation (73) maximally activates Parkin (74), allowing Parkin to ubiquitylate OMM proteins such as mitofusin-1/2 (MFN-1/2) and CDGSH iron sulphur domain 1 (CISD1) (75). Ultimately, ubiquitylation of OMM

proteins provides a docking site for activated autophagy receptors, such as optineurin (OPTN), nuclear dot protein 52 (NDP52), and sequestosome-1 (SQSTM1/p62), to bind, linking ubiquitylated cargo to autophagic membranes (164). TANK-binding kinase 1 (TBK1) is thought to be an important signalling node in this process, activating autophagy receptors that link ubiquitylated cargo to the autophagosome (78, 80-82, 84, 165). TBK1 is known to be activated following phosphorylation at Ser 172 (83) and recent work has suggested that its activation upon mitochondrial depolarization requires both PINK1 and Parkin (78, 84, 166). Despite these advances, much of the research that underpins our current understanding of PINK1-Parkin mediated mitophagy has been conducted in mammalian cells that stably express non-native PINK1 and/ or Parkin (42, 46, 69, 71, 75, 81, 84, 91, 166, 167). Furthermore, murine models have shown that basal mitophagy occurs in skeletal muscle even in the absence of PINK1 (48, 49). These studies highlight the importance of studying mitophagy and its signalling events using endogenous proteins.

5'-AMP-activated protein kinase (AMPK), a critical sensor of cellular energy status, is suggested to be involved in mitophagy (58). AMPK facilitates the clearing of damaged mitochondria by promoting fission through the phosphorylation of mitochondrial fission factor (MFF) (168, 169). This process of fission is required for sequestering damaged mitochondria and is suggested to precede mitophagy (170). Furthermore, AMPK is required for acute exercise-induced mitophagy in mouse skeletal muscle via phosphorylation of unc-51 like autophagy activating kinase 1 (ULK1), which in turn facilitates lysosomal recruitment to damaged mitochondria (58). These studies clearly indicate that in skeletal muscle, AMPK activation promotes mitophagy, possibly by inducing mitochondrial fission and lysosomal recruitment. The important questions in the

field of skeletal muscle mitophagy are: (a) whether the PINK1-Parkin signalling pathway is functionally active; (b) how AMPK is involved in the regulation of mitophagy; and (c) whether it cooperates with PINK1-Parkin signalling. Therefore, the objective of this study was to elucidate the endogenous mechanisms of mitophagy in skeletal muscle cells. To provide linkage between mitophagy and its intracellular signalling events, we generated a stable skeletal muscle cell line expressing a mitophagy reporter construct (mCherryGFP-mtFIS1$_{101-152}$), also known as "mito-QC" (48, 114). Moreover, we employed an Ub pull-down technique to study endogenous ubiquitylation and demonstrate that the PINK1-Parkin signalling pathway is functional in skeletal muscle cells. However, our results also suggest that in skeletal muscle AMPK drives mitophagy by enhancing mitochondrial fission (via MFF phosphorylation) and mitochondrial autophagosome engulfment (via TBK1 phosphorylation), in a PINK1- Parkin independent manner.

4.3 - Materials & Methods

4.3.1 Cell lines and culture

Mouse skeletal muscle C2C12 myoblast cells were obtained from the American Type Culture Collection (ATCC, Manassas, VA, USA). Wild type and PINK1 knockout (KO) HeLa cells were kindly provided by Professor Richard Youle (Biochemistry Section, NIH, Bethesda, MD, USA). Cells were seeded and cultured in DMEM containing GlutaMAX, 25 mM glucose, and 1 mM sodium pyruvate, supplemented with 10% (v/v) foetal bovine serum (GE Healthcare, Buckinghamshire, UK) and 1% (v/v) Penicillin-Streptomycin (100 Units/mL-ug/mL). Myoblasts were differentiated into myotubes at 90% confluency in DMEM supplemented with 2% horse serum (Sigma-Aldrich,

Cambridgeshire, UK). Cultures were maintained in a humidified incubator at 37°C with an atmosphere of 5% CO2 and 95% air.

4.3.2 Drug reconstitution and cell treatment

CCCP (Sigma-Aldrich, Cambridgeshire, UK) and adenosine monophosphate (AMP)–activated protein kinase (AMPK) activator 991 (Aobious, MA, USA) were reconstituted as 10 mM and 20 mM (1000x) stocks in DMSO, respectively. Cells were treated with CCCP and AMPK activator 991 as described in figure legends.

4.3.3 Cell lysis

Cells were lysed in ice-cold sucrose lysis buffer (see section "2.3 Cell lysis"). Cell lysates were centrifuged for 15 minutes at 18 000 g (4°C) and the supernatant stored at -80°C before analysis for total protein using the Bradford protein assay (ThermoFisher Scientific, Leicestershire, UK). Protein in each sample was quantified from a standard curve using BSA standards.

4.3.4 Ubiquitin pull-down

His-halo-ubiquilin1 UBA domain tetramer (UBA^{UBQLN1}) was expressed in Escherichia coli BL21 cells and purified as described previously (74). A 200 µL volume of HaloLink resin (Promega, Hampshire, UK), prewashed with phosphate buffered saline (PBS) was incubated with 1 mg of HALO-UBA^{UBQLN1} TUBE protein in 750 µL of binding buffer: 50 mM Tris-HCl pH 7.5, 150 mM sodium chloride, 0.05% (v/v) NP 40, 1 mM dithiothreitol (DTT) for 2 hours at 4°C. Conjugated HaloLink resin and UBA^{UBQLN1} TUBE protein was incubated with 500-1000 µg of protein from lysed cell samples prior to overnight rotation at 4°C. After three washes in sucrose lysis buffer (see "Cell lysis"),

the enriched Ub and poly-Ub chains were eluted with 1x NuPAGE LDS sample buffer (ThermoFisher Scientific, Leicestershire, UK). Samples were left to denature overnight at room temperature in 1.5% (v/v) 2-mercaptoethanol.

4.3.5 Western blot

Ub pull-down samples and prepared cell lysates (25-75 µg of total protein) were loaded into 4%-12% Bis/Tris precast gels (ThermoFisher Scientific, Leicestershire, UK) prior to sodium dodecyl sulphate–polyacrylamide gel electrophoresis (SDS-PAGE). Gels were run in 1x MOPS buffer for approximately 80 minutes at 150V. Proteins were transferred onto PVDF membranes (Millipore, Hertfordshire, UK) for 1 hour at 100V. Membranes were blocked in 3% of BSA diluted in Tris-buffered saline Tween-20 (TBST): 137 mM of sodium chloride, 20 mM of Tris-base 7.5 pH, 0.1% of Tween-20 for 1 hour and incubated overnight at 4°C with the appropriate primary antibody. Primary antibodies were diluted in 3% of BSA made up in TBST (see Supplementary Table 4.10). Membranes were washed in TBST three times prior to incubation in horse radish peroxidase conjugated secondary antibodies (see Supplementary Table 4.10) at room temperature for 1h. Membranes were washed a further three times in TBST prior to antibody detection using enhanced chemiluminescence horseradish peroxidase substrate detection kit (Millipore, Hertfordshire, UK). Imaging was undertaken using a G:BOX Chemi-XR5 (Syngene, Cambridgeshire, UK). Quantification was performed using ImageJ/Fiji (NIH, Bethesda, MD, USA).

4.3.6 DNA construct and expression

C2C12 myoblasts stably expressing a functionally inert, tandem mCherry-GFP tag fused to the mitochondrial targeting sequence of FIS1 were generated using the methods described by Allen et al (114). Briefly, cDNA for mCherry, GFP, and residues 101-152 of mouse FIS1 were cloned into a pBABE.hygro vector kindly provided by Dr Ian Ganley. The construct was co-transfected into HEK293 FT cells with GAG/POL and VSV-G expression plasmids (Clontech, Saint- Germain-en-Laye, France) for retrovirus production using lipofectamine LTX reagent (ThermoFisher Scientific, Leicestershire, UK) in accordance with manufacturer's instructions. Virus was harvested 48 hours after transfection and applied to C2C12 myoblasts in the presence of 10 μg/mL polybrene (Sigma-Aldrich, Cambridgeshire, UK). Cells were selected with 500 μg/mL of hygromycin (Sigma-Aldrich, Cambridgeshire, UK). In order to obtain a stable homogenous cell line, infected C2C12 myoblasts were sorted and collected based on their expression of mCherry and GFP using FACSAria (BD Biosciences, Berkshire, UK). Sorted C2C12 myoblasts stably expressing the highest relative mCherry-GFP-mtFIS1$_{101-152}$ signal were reseeded and further expanded for characterization and cryopreservation.

4.3.7 Generation of AMPK α1/α2 deficient HEK293 Flp-In cells

AMPK α1 and α2 deficient HEK293 Flp-In cells were generated using the CRISPR-Cas9 technology, as previously described (171). The CRISPR sites were identified using the CRISPR Design Tool (http://tools.genome-engineering.org). The potential targeting oligonucleotides were chosen and a cloning cacc tag was added, as follows: (a) caccGAGTCTGCGCATGGCGCTGC (targets α1 amino acids 1-4, exon1); (b) caccGAAGATCGGCCACTACATTC (targets α1 amino acids 23-29, exon1); 3)

caccGAGGCCGCGCGCCGAAGA (targets α2 intron and ATG start, exon1); 4) caccGAAGCAGAAGCACGACGGGC (targets α2 intron and ATG start, exon1). These oligonucleotides were annealed to their complements containing the cloning tag aaac, and inserted into the back-to-back BbsI restriction sites of pSpCas9(BB)-2A-Puro (PX459) and pSpCas9(BB)-2A-GFP (PX458). HEK293 Flp-In cells were transfected with 2.5 μg of plasmid DNA, consisting of equal amounts of GFP vector containing oligonucleotides 1 and 2, and Puro vector containing oligonucleotides 3 and 4, for α1 and α2, respectively. After 24 hours, cells were trypsinised and plated into 150 mm plates containing DMEM medium supplemented with 10% FBS and 0.4 mg/mL puromycin. After 2 days, the medium was changed, and colonies were allowed to form over the course of 7 days. Individual colonies were harvested and amplified before screening for the presence of AMPK α1/α2 by western blotting.

4.3.8 Mitophagy assay

C2C12 myoblasts stably expressing mCherry-GFP-mt-FIS1$_{101\text{-}152}$ were seeded on imaging dishes (Ibidi, Grfelfing,Germany) and treated with either 10 μM of CCCP or 20 μM of AMPK activator 991. Following treatment, cells were washed twice with PBS and fixed in 3.7% of formaldehyde with 200 mM of HEPES (pH 7.0) for 10 minutes. After fixing, cells were washed and incubated for 10 minutes in DMEM supplemented with 10 mM of HEPES (pH 7.0), and then washed with PBS before mounting with Prolong gold mounting solution containing 4′,6-diamidino-2-phenylindole (DAPI; ThermoFisher Scientific, Leicestershire UK). Images were taken using a Crest X-Light spinning disk system coupled to a Nikon Ti-E base, 60x/1.4 NA (CFI Plan Apo Lambda) air objective and Photometrics Delta Evolve EM-CCD. For GFP, excitation was delivered at λ = 458- 482 nm using a Lumencor Spectra X light engine, with emitted signals

detected at λ = 500-550 nm. For mCherry, the wavelengths used for excitation and detection were λ = 563-587 nm and λ = 602-662 nm, respectively.

4.3.9 Mitophagy and mitochondrial morphology quantitation

Mean fluorescence intensity of both mCherry and GFP, circularity and Feret's diameter were measured in 25 cells from at least 15 fields of view in each condition using ImageJ/ Fiji (NIH, Bethesda, MD, USA). Cells chosen for analysis we selected at random (1 or 2 per field of view) for each condition. The mCherry/GFP ratio of treated cells were normalised to that of their respective DMSO treated control. The relative increase in the mCherry/ GFP ratio provides quantification of mitophagy at a whole cell level. For each of the cells selected for mCherry/GFP analysis, mean circularity and Feret's diameter were also calculated using measurements made on four randomly selected sections of the mitochondrial network.

4.3.10 Respirometry

Cellular bioenergetics was measured in intact attached cells as previously described (172). Briefly, C2C12 myotubes grown on XFe24 microplates exposed to 10 μM of CCCP for 24 hours were washed in Agilent Seahorse XF Base DMEM (Agilent Technologies, Manchester, UK) supplemented with 25 mM of glucose, 1 mM of sodium pyruvate, and 2 mM of L-Glutamine. C2C12 myotubes incubated in Agilent Seahorse XF Base DMEM were inserted into a Seahorse XFe24 extracellular flux analyser (controlled at 37°C) for a 10-minute equilibration, and four measurement cycles to record basal cellular respiration. Oligomycin (1 μM), FCCP (3 μM), and a mixture of rotenone (1 μM) plus antimycin A (2 μM) were then added sequentially to establish ADP phosphorylation and proton leak rates of respiration; maximum electron transfer capacity; and residual

oxygen consumption, respectively. After each addition of these compounds a further four measurement cycles were recorded. For all respirometry experiments, each measurement cycle consisted of a 1-minute wait, 2-minute mix, and 3-minute measurement period and all data were normalized to total protein as quantified by Bradford protein assay.

4.3.11 Statistical analysis

All statistical analyses were performed using GraphPad Software Inc Prism version 8. For time course and dose response experiments, a one-way analysis of variance (ANOVA) was performed with Dunnett's or Sidak's multiple comparisons test where appropriate. For microscopy and seahorse extracellular analyser experiments, unpaired t tests were performed. Data are presented as mean ± SEM.

4.4 - Results

4.4.1 CCCP treatment induces mitophagy and promotes mitochondrial fission in skeletal muscle cells

We generated a mitophagy reporter cell line in C2C12 skeletal muscle cells stably expressing a functionally inert, tandem mCherry-GFP tag fused to the mitochondrial targeting sequence of the OMM protein FIS1 (mCherry-GFP-mt-FIS1$_{101-152}$), as described by Allen et al (114). Under steady-state basal conditions, mitochondria fluoresce both red (mCherry) and green (GFP) making the mitochondrial network appear gold in colour when these spectra are merged (Figure 4.1 A: CTRL). However, upon mitophagy, the acidic conditions of the lysosome quench the GFP signal but not mCherry. As a result, punctate structures that fluoresce red only form within the mitochondrial network (Figure 4.1 A: CCCP). The disappearance of GFP signal and the emergence of red puncta indicate sites of ongoing mitophagy (mitolysosomes). Upon mitochondrial

uncoupling with 10 μM of CCCP treatment for 24 hours, we found that mitophagy increases by 18% in C2C12 myoblasts, as shown by an increase in the ratio of mCherry/ GFP (Figure 4.1 B). Moreover, we demonstrate mitochondrial morphology to be altered in response to CCCP treatment, as indicated by the increase in circularity and decline in Feret's diameter (Figure 4.1 B). Together, these data suggest that CCCP treatment promotes fission of the mitochondrial network.

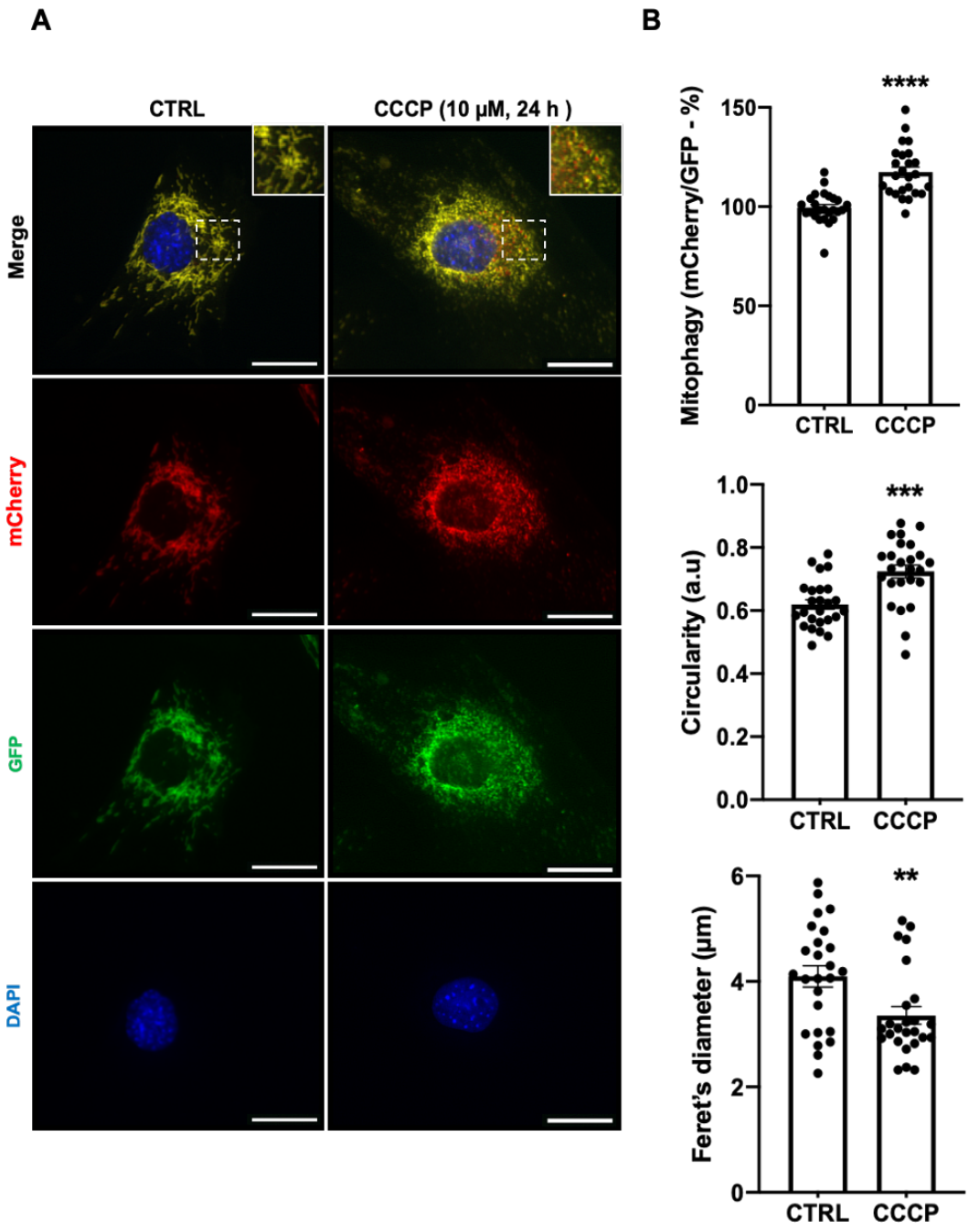

Figure 4.1 CCCP treatment induces mitophagy and promotes mitochondrial fission in skeletal muscle cells. (A) Representative images illustrating CCCP-stimulated mitophagy and mitochondrial fission in C2C12 myoblasts. C2C12 myoblasts stably expressing mCherry-GFP-FIS1$_{101-152}$ treated with DMSO (0.1%, 24 h) as a vehicle control (CTRL) or CCCP (10 µM, 24 h). Red puncta appearing in the merged image indicate sites of mitophagy. Scale bars = 20 µm. B, Quantification of mitophagy (mCherry/GFP), circularity and Feret's diameter (n = 25 per group). Cells treated as in Figure 1A. Each data point represents one myoblast; mean ± SEM, **P < .01, ***P < .001, ****P <.0001.

4.4.2 CCCP treatment does not alter mitochondrial protein content despite depolarising the mitochondrial membrane and impairing mitochondrial respiration.

Despite an 18% increase in mitophagy (Figure 4.1 B), CCCP had no significant effect on markers of mitochondrial protein content, as monitored by the expression of mitofilin and oxidative phosphorylation (OXPHOS) subunits I-V (Figure 4.2 A & Supplementary Figure 4.9). We observed that long isoforms of dynamin-like 120 kDa protein (OPA1) undergo cleavage after 1 hour of CCCP treatment, indicating depolarization of the mitochondrial membrane potential over the 24 h time course (Figure 4.2 B). Furthermore, we found increased phosphorylation of AMPK at Thr 172 and of the AMPK target acetyl-CoA carboxylase (ACC) at Ser 212 after 1 hour of CCCP treatment, indicating increased cellular energy stress (Figure 4.2 B). To confirm deficit in mitochondrial function following prolonged mitochondrial membrane depolarisation, we assessed oxygen consumption rate in myotubes pre-treated with 24 h CCCP using extracellular flux analysis (Figure 4.2 C). We show that 24 h CCCP pre-treatment lowers the basal mitochondrial respiration, ADP phosphorylation, uncoupled mitochondrial respiration, and coupling efficiency, indicating impaired mitochondrial respiration (Figure 4.2 C). Altogether, these data demonstrate that in cells not stably expressing non-native proteins, prolonged mitochondrial membrane depolarisation does not reduce mitochondrial protein content in skeletal muscle cells despite impairing mitochondrial respiration.

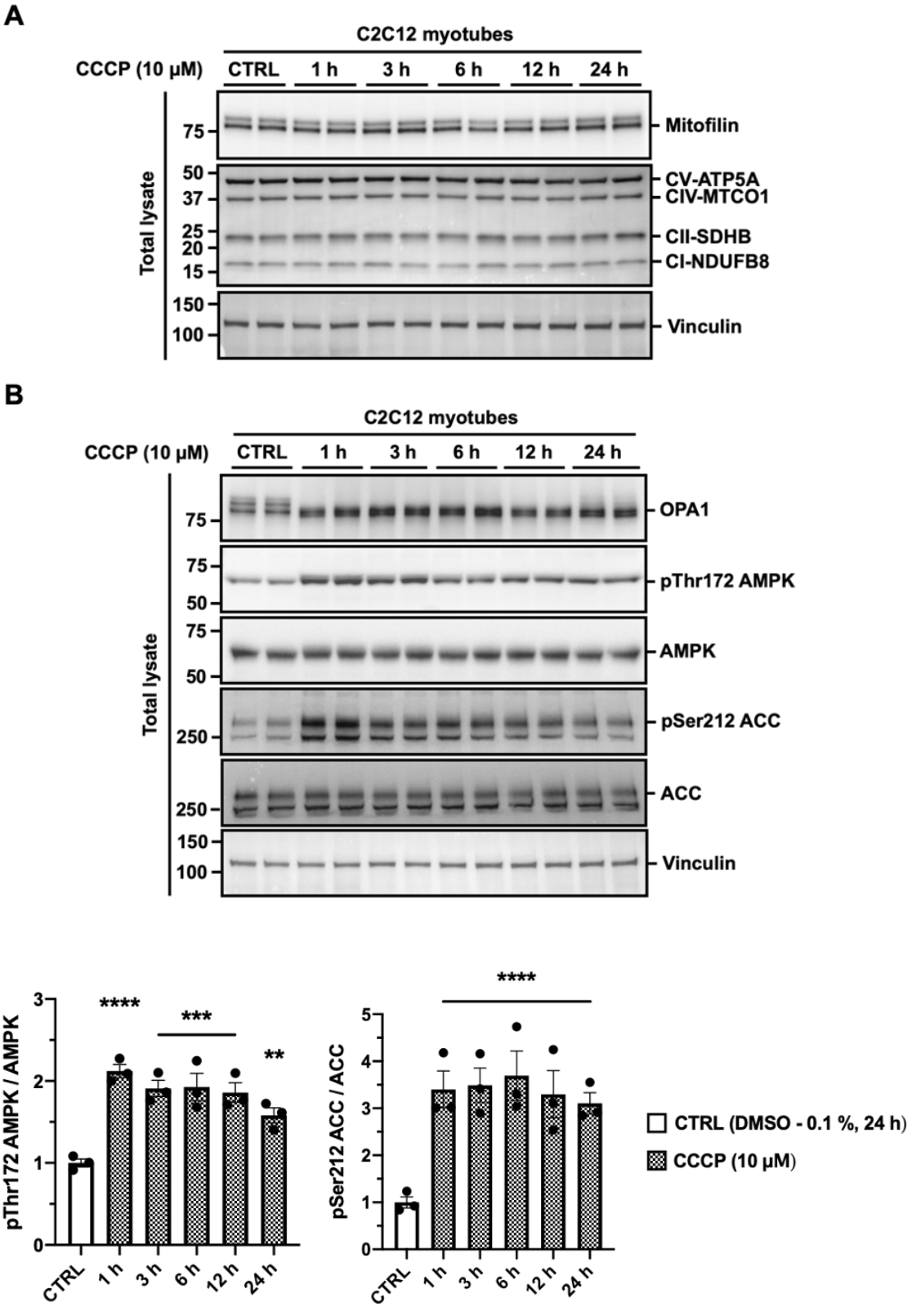
A
C2C12 myotubes
CCCP (10 µM)
CTRL
1 h
3 h
6 h
12 h
24 h
Total lysate
75
50
37
25
20
15
150
100
Mitofilin
CV-ATP5A
CIV-MTCO1
CII-SDHB
CI-NDUFB8
Vinculin
B
C2C12 myotubes
CCCP (10 µM)
CTRL
1 h
3 h
6 h
12 h
24 h
Total lysate
OPA1
pThr172 AMPK
AMPK
pSer212 ACC
ACC
Vinculin
pThr172 AMPK / AMPK
pSer212 ACC / ACC
****
***
**
****
CTRL (DMSO - 0.1 %, 24 h)
CCCP (10 µM)

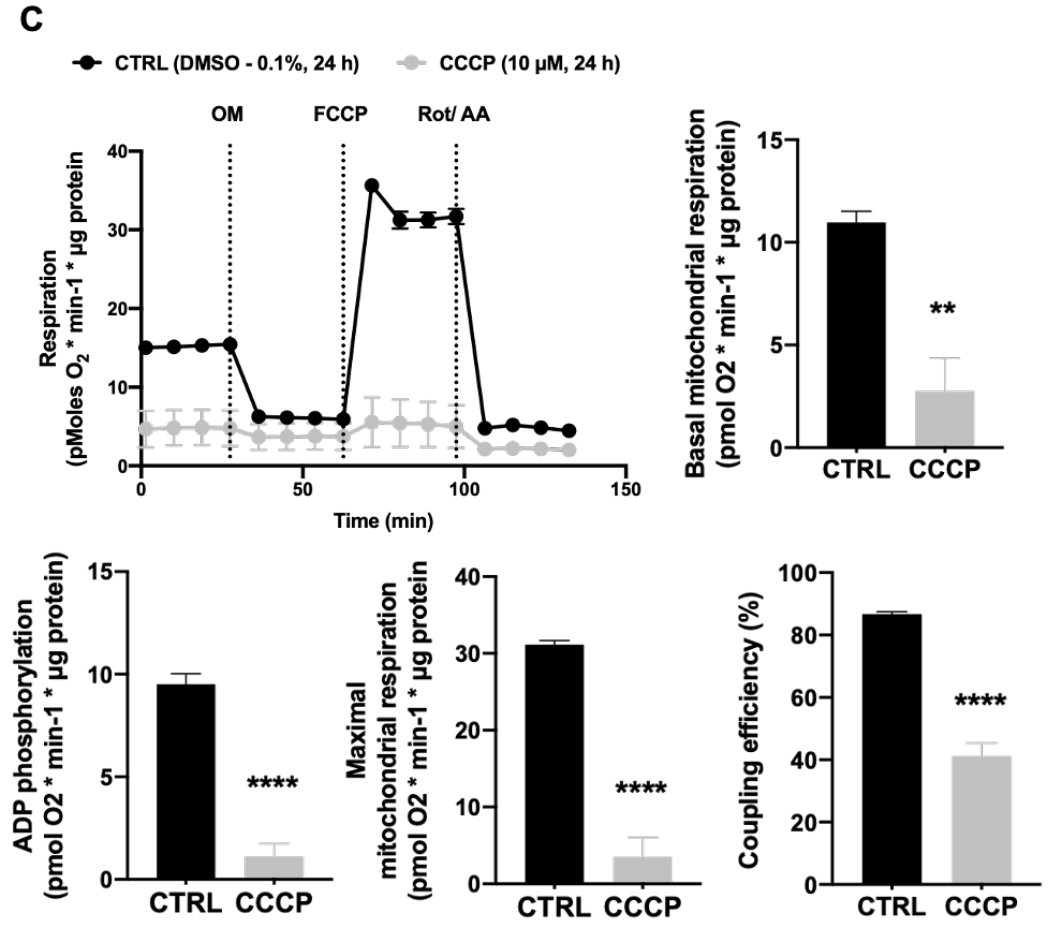

Figure 4.2 CCCP treatment does not reduce markers of mitochondrial protein content in skeletal muscle cells despite inducing mitochondrial membrane depolarisation and impairing mitochondrial respiration. (A) Markers of mitochondrial content are unaltered following CCCP treatment for up to 24 h. C2C12 myotubes were treated with DMSO (0.1%, 24 h) as a vehicle control (CTRL) or 10 µM of CCCP for up to 24 h. Total lysates were analysed by SDS-PAGE and western blotting with the indicated antibodies. (B) CCCP treatment induces mitochondrial membrane depolarisation and cellular energy stress in C2C12 myotubes. C2C12 myotubes were treated with DMSO (0.1%, 24 h) as a vehicle control (CTRL) or 10 µM of CCCP for up to 24 h. Total lysates were analysed by SDS-PAGE and western blotting with the indicated antibodies. Representative images and quantification of n = 3 independent experiments are shown. Data are expressed as means ± SEM; **P < .01, ***P < .001, ****P < .0001 compared to CTRL. C, Real-time effects of 24 h CCCP pre-treatment on rates of respiration in C2C12 myotubes. C2C12 myotubes were pre-treated with DMSO (0.1%, 24 h) as a vehicle control (CTRL) or CCCP (10 µM, 24 h). Oxygen consumption rate was assessed using the Seahorse XFe24 extracellular flux analyser. Basal

mitochondrial respiration was calculated using rates of oxygen consumption measured prior to the addition of oligomycin (OM). ADP phosphorylation respiration was calculated using rates of oxygen consumption sensitive to oligomycin. Maximal mitochondrial respiration was calculated using rates oxygen consumption following uncoupling with carbonyl cyanide- 4-(trifluoromethoxy) phenylhydrazone (FCCP). Coupling efficiency of oxidative phosphorylation was calculated as the percentage of respiration linked to ATP synthesis. Data were normalized to total protein content and corrected for non-mitochondrial respiration as assessed by the amount of oxygen consumption remaining after the addition of rotenone (Rot) and antimycin A (AA). Data are expressed as mean ± SEM from 1 experimental replicate with four wells per group; **P < .01, ****P < .0001 compared to CTRL.

4.4.3 CCCP treatment induces PINK1 kinase activity and Parkin E3 ligase activity in skeletal muscle cells

Phosphorylation of Ub at Ser 65 and CISD1 ubiquitylation represent intracellular readouts of PINK1 kinase activity (69-71) and Parkin E3 ligase activity (75, 173) respectively. In order to explore endogenous PINK1 kinase and Parkin E3 ligase activities, we used immobilised haloalkane dehalogenase (HALO)-tagged-UBA^{UBQLN1} tetramers to capture ubiquitylated proteins in whole cell lysates (162). Phosphorylation of Ub at Ser 65 and ubiquitylation of CISD1, were increased after 6, 12, and 24 hours of CCCP treatment (Figure 4.3), consistent with research demonstrating Parkin E3 ligase activity to be regulated by PINK1 activation (73). These data demonstrate that endogenous PINK1 kinase and Parkin E3 ligase activities are functional in skeletal muscle cells, although their activation requires prolonged (≥6 h) CCCP treatment.

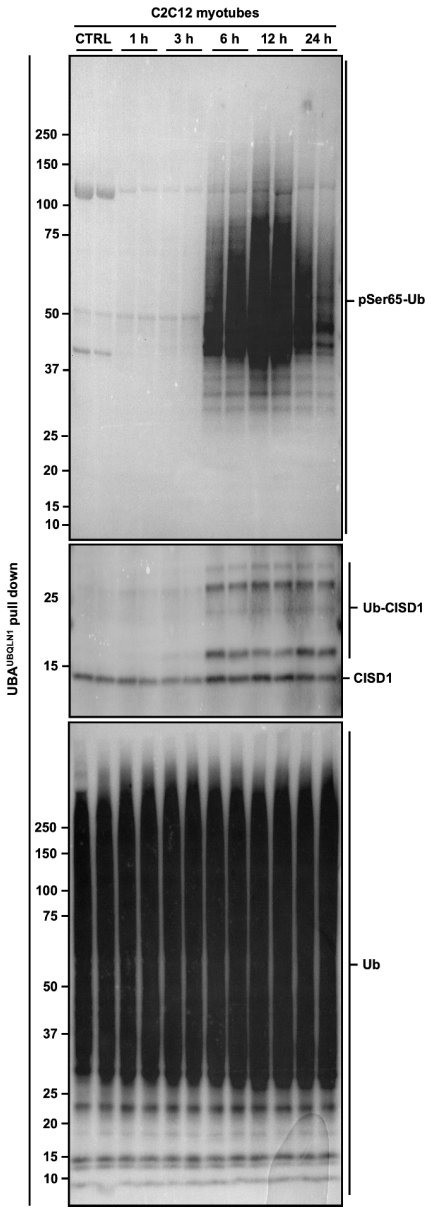

Figure 4.3 CCCP treatment induces endogenous PINK1 kinase activity and Parkin E3 ligase activity in skeletal muscle cells. C2C12 myotubes were treated with DMSO (0.1%, 24 h) as a vehicle control (CTRL) or 10 μM of CCCP for up to 24 h. Total lysates were incubated with ubiquitin-binding resins derived from his-halo-ubiquilin1 UBA domain tetramer (UBA^{UBQLN1}). Captured ubiquitylated proteins were subject to SDS-PAGE and western blotting with antibodies specific to: phospho-Ser65 ubiquitin (pSer65 Ub, to determine intracellular PINK1 kinase activity), CDGSH iron sulphur domain 1 (CISD1, to determine intracellular Parkin E3 ligase activity toward its substrate) and total ubiquitin (Ub, to verify ubiquitin enrichment). Representative images of n = 3 independent experiments with two technical replicates per passage for each timepoint are shown.

4.4.4 CCCP treatment induces phosphorylation of TBK1 in a PINK1-Parkin independent manner

TANK-binding kinase 1 (TBK1) is thought to be pivotal for the activation of autophagy receptors such as: OPTN, NDP52, and SQSTM1/ p62 (78, 80-82, 84, 165). Recent work has suggested that TBK1 phosphorylation at Ser 172 and its activation (83) upon mitochondrial depolarisation, requires PINK1-Parkin signalling (78, 84). However, we observed increased TBK1 phosphorylation at Ser 172 at all time points from 1 to 24 hours after CCCP treatment (Figure 4.4 A). Given that TBK1 phosphorylation precedes the activation of PINK1 and Parkin (Figure 4.3), these data suggest that TBK1 activation is independent of PINK1-Parkin activity in skeletal muscle cells. To verify that phosphorylation endogenous TBK1 in response to CCCP treatment does not require the PINK-Parkin signalling pathway, we employed PINK1KO HeLa cells. HeLa cells lack Parkin expression (174), and so, performing experiments on PINK1 KO HeLa cells would abolish the signalling effects of both PINK1 and Parkin. Strikingly, we still observed TBK1 phosphorylation at Ser 172 in PINK1 KO HeLa cells after 1 and 6 hours of CCCP treatment (Figure 4.4 B), indicating that TBK1 is acutely activated following mitochondrial depolarisation in a PINK1-Parkin independent manner. Knock out (KO) of PINK1 was confirmed via western blotting (Figure 4.4 B). In addition, lack of PINK1 activity was confirmed by an undetectable level of phosphorylated Ub after captured ubiquitylated proteins were subjected to SDS-PAGE and western blotting (Figure 4.4 C).

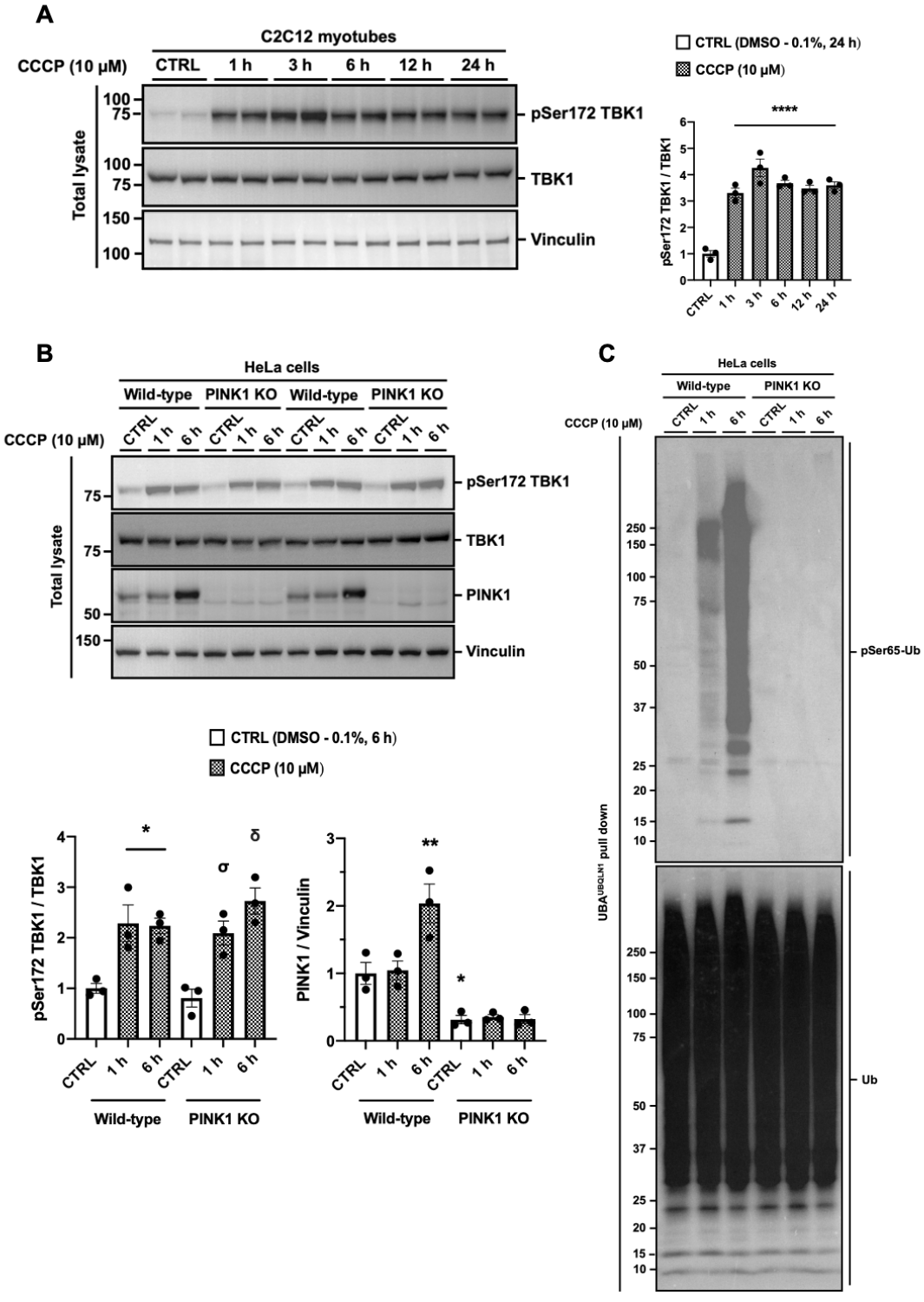

Figure 4.4 CCCP treatment induces phosphorylation of endogenous TBK1 in a PINK1-Parkin independent manner. (A) TBK1 phosphorylation increases acutely during CCCP treatment. C2C12 myotubes were treated with DMSO (0.1%) as a vehicle control (CTRL) or 10 μM of CCCP for up to 24 h. (B) CCCP-induced TBK1 phosphorylation is independent of PINK1 and Parkin. HeLa wild type and

PINK1 knockout (KO) cells were treated with DMSO (0.1%) as a vehicle control (CTRL) or CCCP (10 μM) for 1 and 6 h. Lysates were analysed by SDS-PAGE and western blotting with the indicated antibodies. Representative images of n = 3 independent experiments are shown. For the quantification of PINK1/ Vinculin, PINK1 KO CTRL is significantly reduced compared to wild-type CTRL. PINK1 KO 1 h & 6 h timepoints are not statistically different from PINK1 KO CTRL. Data are expressed as means ± SEM; *P < .05, **P < .01, ****P < .0001 compared to wild-type CTRL and $^{\sigma}$P < 0.01, $^{\delta}$P < 0.001 compared to PINK1 KO CTRL (C) Verification of HeLa PINK1 knockout cells. Ubiquitin was enriched from the total lysates of HeLa wild type and PINK1 KO cells with ubiquitin-binding resins derived from his-halo-ubiquilin1 UBA domain tetramer (UBA^{UBQLN1}). Captured ubiquitylated proteins were subject to SDS-PAGE and western blotting with an antibody specific to phospho-Ser65 ubiquitin (pSer65 Ub, to determine intracellular PINK1 kinase activity).

4.4.5 AMPK activation by 991 induces mitophagy and promotes mitochondrial fission via phosphorylation of MFF in skeletal muscle cells

Recent work has suggested that mitochondrial fission may spare healthy mitochondria from modification by the PINK1-Parkin signalling pathway, rather than preparing cells for the clearing of damaged mitochondrial fragments (170). Nevertheless, evidence suggests that AMPK-mediated mitochondrial fission is partly regulated via phosphorylation of MFF (168, 169). This led us to hypothesise that activation of AMPK may also induce mitophagy following mitochondrial fission. To test this, we used a small-molecule AMPK activator, 991, to specifically activate AMPK in skeletal muscle cells (175, 176) and found that a 2 h treatment with 991 increases mitophagy by 23% (Figure 4.5 A & B), similar to the effect of CCCP (Figure 4.1 A & B). Moreover, 991 treatment promotes fragmentation of the mitochondrial network (indicated by the increase in circularity and the decline in Feret's diameter) (Figure 4.5 A & B). Consistently, we show a robust increase in MFF phosphorylation at Ser146 (equivalent to Ser 172 in human

MFF) in response to 991 (Figure 4.6 A). We also observed increased MFF phosphorylation at Ser 146 in C2C12 myotubes following CCCP treatment from 1 to 24 hours (Figure 4.6 B), in parallel with AMPK activation as indicated by the phosphorylation status of its substrate ACC (Figure 4.2 B). Finally, we employed AMPK α1/α2 deficient HEK293 cells generated using CRISPR-Cas9 technology. Using this cell line, we confirmed that MFF Ser172 phosphorylation is AMPK dependent (Figure 4.6 C).

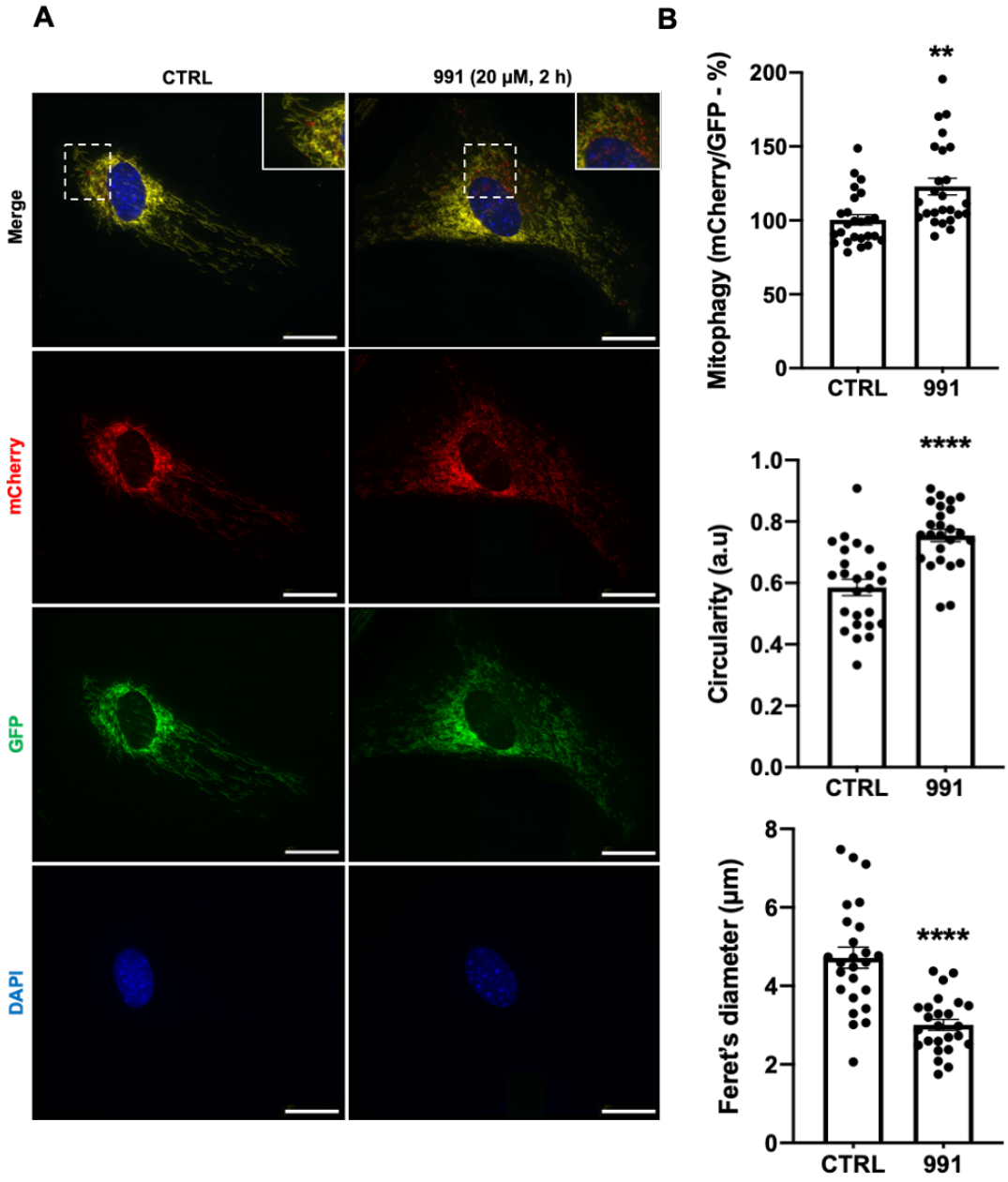

Figure 4.5 AMPK activation induces mitophagy and promotes mitochondrial fission in skeletal muscle cells. (A) Representative images illustrating AMPK activator 991 treatment induces mitophagy and mitochondrial fission in C2C12 myoblasts. C2C12 myoblasts stably expressing mCherry-GFP $FIS1_{101-152}$ were serum starved for 4 h prior to the treatment of DMSO (0.1%) as a vehicle control (CTRL) or 991 (a specific AMPK activator; 20 μM, 2h). Red puncta appearing in the merged image indicate sites of mitophagy. Scale bars = 20 μm. (B) Quantification of mitophagy (mCherry/GFP), circularity and Feret's diameter (n = 25 per group). Cells treated as in Figure 5A. Each data point represents one myoblast; mean ± SEM, **P < .01, ****P < .0001.

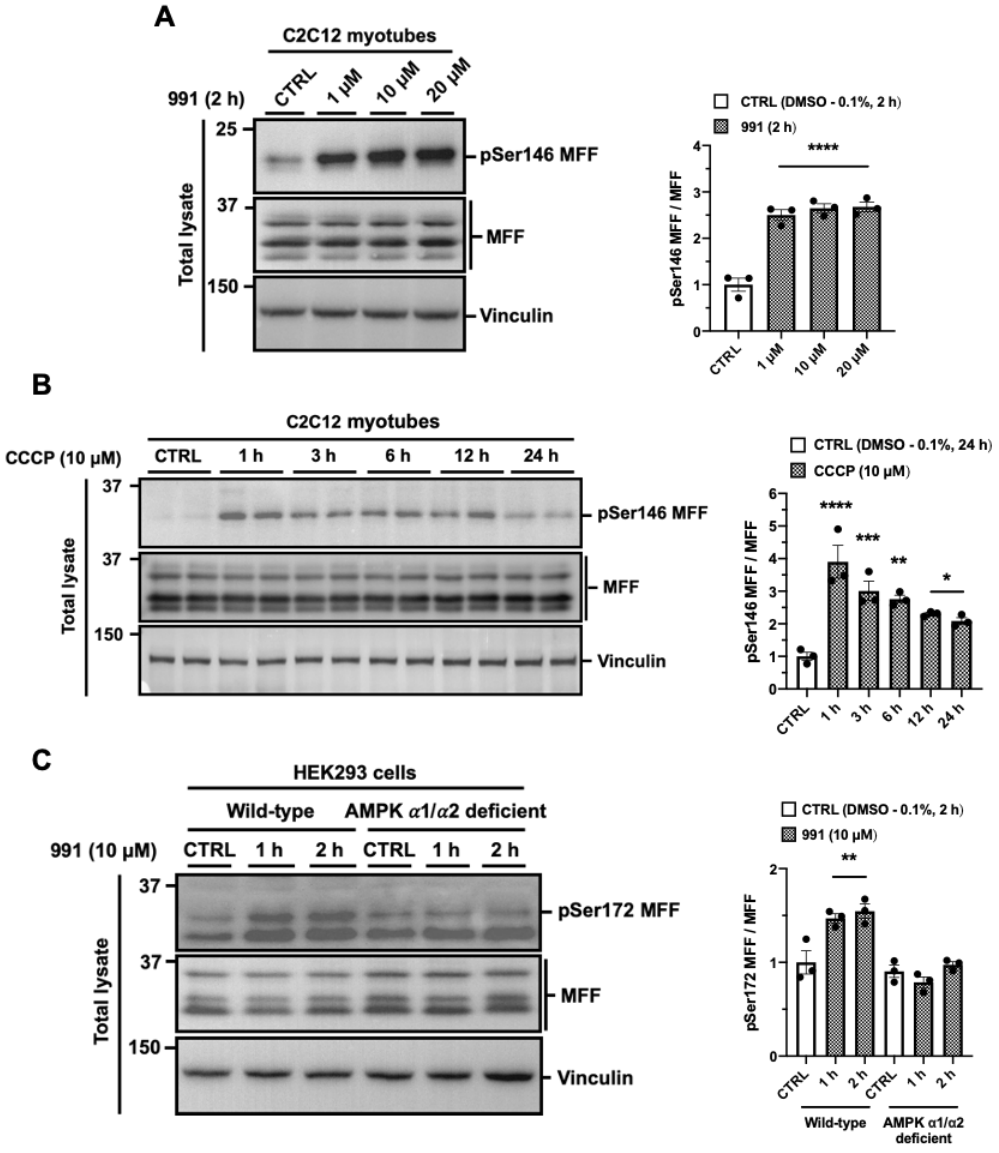

Figure 4.6 AMPK activation is responsible for MFF phosphorylation at Ser 146 in skeletal muscle cells. (A) 991 treatment induces MFF phosphorylation in skeletal muscle cells. C2C12 myotubes were serum starved for 4 h prior to the treatment of DMSO (0.1%) as a vehicle control (CTRL) or AMPK activator 991 at the indicated concentrations for 2 h. (B) CCCP treatment induces MFF phosphorylation. C2C12 myotubes were treated with DMSO (0.1%, 24 h) as a vehicle control (CTRL) or 10 μM of CCCP for up to 24 h. (C) 991-induced MFF phosphorylation is diminished in AMPK α1/α2 deficient cells. HEK293 wild type and AMPK α1/α2 deficient cells were treated with DMSO (0.1%) as a vehicle control (CTRL) or AMPK activator 991 (10 μM) for 1 h and 2 h. Cells were serum starved for 2 h prior to treatment. Total lysates were analysed by SDS-PAGE and western blotting with the indicated antibodies. Representative images of n = 3 independent experiments are shown. Data are expressed as means ± SEM; *P < .05, **P < .01, ***P < .001, ****P < .0001 compared to CTRL.

4.4.6 AMPK activation by 991 induces endogenous TBK1 activation in a PINK1- Parkin independent manner in skeletal muscle cells

AMPK activates ULK1 through direct phosphorylation at various sites (177-179). Importantly, ULK1 phosphorylation at Ser 555 regulates its activation and translocation to mitochondria (52, 59, 177, 180). Recent work in adipose tissue suggested a role for TBK1 and demonstrated that AICAR-mediated AMPK activation-induced TBK1 phosphorylation at Ser 172 via ULK1 (181). Given that 1 hour of CCCP treatment activates both AMPK and TBK1 in C2C12 myotubes (Figures 4.2 B and 4.4 A), we hypothesized that the rapid activation of TBK1 may be AMPK dependent. Interestingly, we found that 991 treatment induces TBK1 phosphorylation at Ser 172, as well as ULK1 phosphorylation at Ser 555, in a dose dependent manner (Figure 4.7 A). As expected, phosphorylation of AMPK and ACC were also increased following 991 treatment (Figure 4.7 B) (176). To demonstrate that TBK1 phosphorylation is AMPK dependent, we employed HEK293 AMPK α1/α2 deficient cells and found that TBK1 phosphorylation

was attenuated following AMPK activation by 991 (Figure 4.7 C). These data indicate that TBK1 phosphorylation is AMPK dependent. Interestingly, after confirming AMPK α1/α2 deficiency (Figure 4.7 C), we observed low levels of ACC phosphorylation at Ser 212 and ULK1 phosphorylation at Ser 555 in AMPK α1/α2 deficient cells following 991 treatment (Figure 4.7 C). Because phosphorylated ACC and ULK1 at Ser 212 and Ser 555 are direct AMPK substrates, these data suggest that other AMPK subunits, namely β and γ, may be capable of phosphorylating downstream AMPK targets when α1 and α2 subunits are deficient. Finally, we demonstrated that AMPK-mediated TBK1 phosphorylation in response to 991 treatment was independent of mitochondrial membrane depolarization and PINK1-Parkin activity by showing that long OPA1 isoforms are not truncated, and an absence of Ub phosphorylation and CISD1 ubiquitylation (Figure 4.7 D). Taken together, these data suggest that AMPK regulates the activation of TBK1 in skeletal muscle cells, and that this occurs in a PINK1-Parkin independent manner.

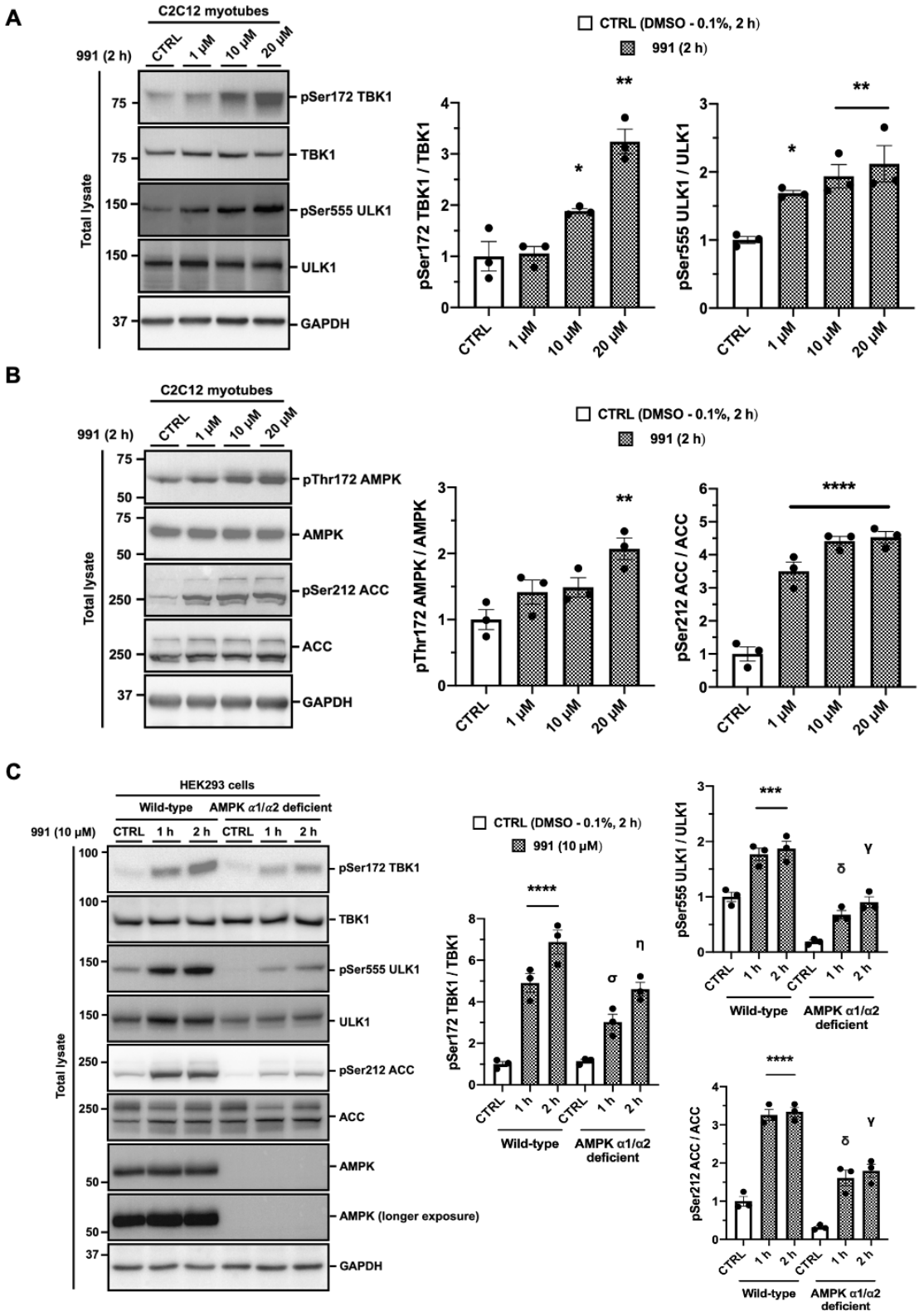
A
C2C12 myotubes
991 (2 h)
CTRL
1 μM
10 μM
20 μM
Total lysate
75
pSer172 TBK1
75
TBK1
150
pSer555 ULK1
150
ULK1
37
GAPDH
CTRL (DMSO - 0.1%, 2 h)
991 (2 h)
pSer172 TBK1 / TBK1
pSer555 ULK1 / ULK1
B
C2C12 myotubes
991 (2 h)
75
pThr172 AMPK
50
75
AMPK
50
250
pSer212 ACC
250
ACC
37
GAPDH
CTRL (DMSO - 0.1%, 2 h)
991 (2 h)
pThr172 AMPK / AMPK
pSer212 ACC / ACC
C
HEK293 cells
Wild-type
AMPK α1/α2 deficient
991 (10 μM)
CTRL
1 h
2 h
Total lysate
100
pSer172 TBK1
100
TBK1
150
pSer555 ULK1
150
ULK1
250
pSer212 ACC
250
ACC
50
AMPK
50
AMPK (longer exposure)
37
GAPDH
CTRL (DMSO - 0.1%, 2 h)
991 (10 μM)
pSer172 TBK1 / TBK1
pSer555 ULK1 / ULK1
pSer212 ACC / ACC
Wild-type
AMPK α1/α2 deficient

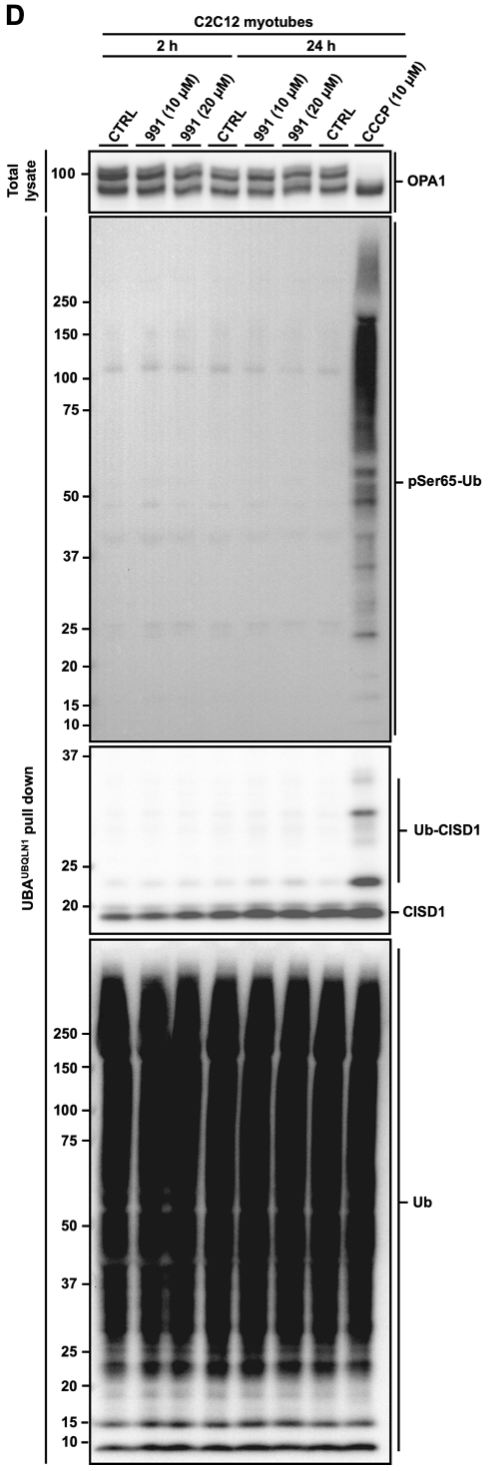

Figure 4.7 AMPK activation by 991 induces TBK1 activation in a PINK1-Parkin independent manner. (A) 991 treatment induces TBK1 phosphorylation in C2C12 myotubes. C2C12 myotubes were serum starved for 4 h prior to the treatment of DMSO (0.1%) as a vehicle control (CTRL) or AMPK activator 991 at the indicated concentrations for 2 h. (B) 991 activates AMPK signalling in C2C12

myotubes. Cells treated as in Figure 5A. (C) 991-induced TBK1 phosphorylation is diminished in AMPK α1/α2 deficient cells. HEK293 wild type and AMPK α1/α2 deficient cells were treated with DMSO (0.1%) as a vehicle control (CTRL) or AMPK activator 991 (10 μM) for 1 h and 2 h. Cells were serum starved for 2 h prior to treatment. (D) AMPK activation does not induce PINK1-Parkin signalling in skeletal muscle cells. C2C12 myotubes were serum starved for 4 h prior to the treatment of DMSO (0.1%) as a vehicle control (CTRL) or AMPK activator 991 at the indicated concentration for 2 and 24 h. As negative and positive controls, C2C12 myotubes were treated with DMSO (0.1%, 24 h, lane 7) or CCCP (10 μM, 24 h, lane 8), respectively, without serum starvation. For ubiquitin pulldown, total lysates were incubated with ubiquitin-binding resins derived from his-halo-ubiquilin1 UBA domain tetramer (UBA^{UBQLN1}). Ubiquitin enriched extracts were analysed by SDS-PAGE and western blotting with antibodies specific to: phospho-Ser65 ubiquitin (pSer65 Ub, to determine intracellular PINK1 kinase activity), CDGSH iron sulphur domain 1 (CISD1, to determine intracellular Parkin E3 ligase activity toward its substrate) and total ubiquitin (Ub, to verify ubiquitin enrichment). Representative images of n = 3 independent experiments are shown. Data are expressed as means ± SEM; *P < .05, **P < .01, ***P < .001, ****P < .0001 compared to CTRL. $^{\sigma}P < 0.05$, $^{\delta}P < 0.0001$ compared to wild type 1 h. $^{\eta}P < 0.05$, $^{\gamma}P < 0.0001$ compared to wild type 2 h.

4.5 Discussion

The rationale for this study stemmed from our lack of current knowledge concerning the molecular mechanisms that underpin mitophagy in skeletal muscle. Much of the research that informs our understanding of the mechanisms governing mitophagy has been conducted in immortalised mammalian cells harbouring systems that stably express non-native PINK1 and/ or Parkin (42, 46, 69, 71, 75, 81, 84, 91, 166, 167). In skeletal muscle, our understanding of mitophagy, and how it changes in response to physiological stimuli such as exercise and aging, has been largely informed by indirect assessments of mitophagy (129-131) rather than measuring mitophagy directly. Therefore, the main objective of this investigation was to directly measure mitophagy alongside its

endogenous molecular mechanisms in skeletal muscle cells. The key questions we sought to answer were: (a) whether the PINK1-Parkin signalling pathway is functionally active; (b) how AMPK is involved in the regulation of mitophagy; and (c) whether it cooperates with PINK1-Parkin signalling. Our results demonstrate that the PINK1-Parkin signalling pathway does operate in skeletal muscle cells, but its activation requires prolonged mitochondrial depolarisation. We also demonstrate that AMPK activation stimulates mitochondrial fission via phosphorylation of MFF in skeletal muscle cells. Interestingly, in muscle cells, we found that AMPK activation stimulates TBK1 activation in a PINK1-Parkin independent manner. To measure mitophagy directly, we harnessed the "mito-QC" construct to generate a stable mitophagy reporter skeletal muscle cell line. The use of this tool allowed us to assess the occurrence of mitophagy and mitochondrial morphology in response to mitochondrial depolarisation and AMPK activation.

The recent development of different tractable tools has made direct assessment of mitophagy in both cells and rodents feasible (48, 50, 114-117). Here, we transfer a fluorescent, binary-based mitophagy reporter construct previously developed by Allen and colleagues (114) into an immortalised mouse skeletal muscle (C2C12) cell line. After generating a C2C12 "mito-QC" cell line capable of stably expressing the mitophagy reporter construct (mCherry-GFP-mtFIS1$_{101-152}$), we show that CCCP treatment for 24 hours significantly increases mitophagy by 18% in skeletal muscle cells (Figure 4.1). Unexpectedly, we observed no change in markers of mitochondrial protein content. Several studies have shown a marked reduction of mitochondrial content using microscopy and western blotting following treatment with CCCP (42, 91, 167). However, these investigations use cells that stably express Parkin which is thought to induce non-native activation of its E3 ligase activity, particularly when fused with an exogenous tag

at the N-terminus of Parkin (182). Interestingly, Rakovic and colleagues (183) have shown Parkin overexpression to be required for a significant reduction in levels of mitochondrial proteins and mitochondrial mass following treatment with depolarising agents, such as carbonyl cyanide-4-(trifluoromethoxy)phenylhydrazone (FCCP) or valinomycin. Our results are consistent with those of Rakovic and colleagues (183) who also demonstrated that levels of mitochondrial proteins in neuroblastoma SH-SY5Y cells expressing only endogenous Parkin to remain unchanged. However, unlike Rakovic et al (183), we observed a significant increase in mitophagy following treatment with CCCP (Figure 4.1 B), albeit in the C2C12 mito-QC skeletal muscle cell line developed here. In this instance, it is worth noting the importance of the methodological optimisation required for the detection of mitophagy. For example, when piloting our experiments on glass coverslips, we noticed poor cell adherence, particularly upon drug treatment. Therefore, we suggest the use of imaging dishes with a tissue culture treated polymer for improved cell adherence during microscopy. Finally, the C2C12 "mito-QC" muscle cell line we have established may serve as a useful tool for future studies to monitor mitophagy in skeletal muscle cells in real-time. Moreover, given the recent finding that acute exercise induces mitophagy in mouse skeletal muscle (58) our C2C12 "mito-QC" muscle cell line may help to explore this further by using electrical stimulation as a means to mimic muscle contraction.

Studying endogenous ubiquitylation events is challenging because of the lack of experimental tools sensitive enough for detection. Unlike protein phosphorylation where the use of phospho-specific antibodies is common, similar tools for studying protein ubiquitylation are yet to be developed. Moreover, when using western blotting to study protein ubiquitylation, signal often appears diffuse and stretches from low to high

molecular weight ranges making detection more difficult. Even though Ub is the substrate of PINK1 and Parkin is a Ub E3 ligase, to our knowledge, their intracellular activities are yet to be studied with endogenous levels of expression in skeletal muscle. To facilitate the study of endogenous PINK1-Parkin signalling, we employed a specific Ub pull-down technique. Using this technique, it was possible to unequivocally demonstrate the covalent attachment of poly-Ub chains to the proteins of interest (184). First, we captured all the ubiquitylated proteins in cell lysates using Halo-tagged TUBEs, which consist of tandem UBA domain repeats of the protein Ubiquilin-1. After gel electrophoresis and protein transfer, membranes were probed with antibodies raised against our proteins of interest (Figures 4.3, 4.4 C and 4.7 D). This method allowed us to demonstrate endogenous PINK1-Parkin signalling to be functional in skeletal muscle cells, despite their activation requiring prolonged (≥6 hours) CCCP treatment (Figure 4.3). More specifically, we observed a marked increase in phosphorylated Ub at Ser 65 in C2C12 myotubes treated with CCCP for 6 h and this increased further after 12 h. However, following 24 h of CCCP treatment, phosphorylation of Ub at Ser 65 was visibly reduced compared to 12 h, indicating a decline in PINK1 kinase activity. Given the high toxicity of CCCP, we speculate that treatment of C2C12 myotubes beyond 12 h may activate signalling molecules involved with cell death and apoptosis, which in turn, could supress PINK1 kinase activity. Interestingly ubiquitylation of the OMM protein CISD1, indicative of Parkin E3 ligase activity, did not subside after 24 h of CCCP treatment, perhaps suggesting PINK1-independent regulation of Parkin's E3 ligase activity at this timepoint. Overall, these data clearly demonstrate successful application of a Ub pull-down technique in skeletal muscle to monitor PINK1 kinase and Parkin E3 ligase activity. In future studies, this method will not only be useful for studying endogenous PINK1-

Parkin activity but could also be used to provide insight into ubiquitylation status in a wide range of tissues.

TBK1 is now known to be an important signalling node that operates as part of a positive feedback loop, helping to orchestrate efficient mitophagy through its association with autophagy receptors, such as OPTN, NDP52, and SQSTM1/ p62 (78, 80-82, 84, 165). Although the role of TBK1 in mitophagy is subject to ongoing research, one of its identified functions is to enhance the binding capacity of OPTN with poly-Ub chains (81). Thereafter, OPTN and other autophagy receptors are thought to link cargo to autophagosomal membranes via binding to LC3 family proteins (164). Recent studies have suggested that TBK1 activation following phosphorylation at Ser 172 (83) requires both PINK1 and Parkin activity in response to mitochondrial depolarisation (78, 84, 166). However, we found that under endogenous condition activation of TBK1 is independent of both PINK1 and Parkin activation (Figure 4.4 B). This first became evident after we observed that TBK1 was phosphorylated (Figure 4.4 A) prior to activation of PINK1 and Parkin following CCCP treatment (Figure 4.3). To verify this, we went on to demonstrate TBK1 phosphorylation following CCCP treatment was unchanged in both wild type and PINK1 KO HeLa cells (Figure 4.4 B). Taken together, these data indicate that endogenous TBK1 is acutely activated following mitochondrial depolarisation in a PINK1-Parkin independent manner.

Mitochondrial fission plays a key role in mitophagy, preparing cells for the clearing of damaged mitochondrial fragments (169) while preserving healthy mitochondria from the unchecked actions of the PINK1-Parkin signalling pathway (170). It has recently been established that recruitment of the GTPase dynamin-related protein 1 (DRP1) is essential for mitochondrial fission (185). MFF is a key receptor of DRP1 (186) and evidence

suggests that AMPK directly phosphorylates MFF at Ser 146 in order to promote mitochondrial fission (168, 169). In accordance with previous research, we observed MFF phosphorylation following CCCP treatment (Figure 4.6 B) was similar to that of phosphorylated AMPK at Thr 172 and ACC at Ser 212 (Figure 4.2 B). We also showed a robust increase in MFF phosphorylation at Ser 146 following 991 treatment in skeletal muscle cells. Using AMPK α1/α2 HEK293 deficient cells, we confirmed that MFF phosphorylation at Ser 146 is AMPK dependent (Figure 4.6 C). In addition to this, we demonstrated the mitochondrial network to become more circular and less elongated following CCCP (Figure 4.1 B) and 991 (Figure 4.5 B) treatments, suggesting mitochondrial fission. Taken together, these data provide evidence that AMPK activation plays an important role in promoting mitochondrial fission in skeletal muscle cells by phosphorylating MFF.

To further probe the mechanistic basis through which AMPK initiates mitophagy, we treated mito-QC skeletal muscle cells for 2 hours with 991 (Figure 4.5). Interestingly, we found that AMPK activation induces mitophagy on its own (Figure 4.5 B) without the need for PINK1-Parkin activity (Figure 4.7 D). It is worth mentioning that after serum starvation, but prior to 991 treatment, we observed increases in red puncta, illustrating mitophagy in mito-QC skeletal muscle cells (Figure 4.5 A; CTRL). Unexpectedly, we observed a dose dependent increase in TBK1 activation following 991 treatment, suggesting that TBK1 phosphorylation may be mediated by AMPK. Moreover, phosphorylation of TBK1 increased across a 24 h time course of CCCP treatment (Figure 4.4 A), in parallel with ACC (Figure 4.2 B) and MFF phosphorylation (Figure 4.6 B). These data further support the hypothesis that TBK1 phosphorylation is controlled by AMPK. Finally, we confirm this hypothesis, by showing that TBK1 phosphorylation was

dramatically reduced in HEK293 AMPK α1/α2 deficient cells. Previous research in adipose tissue has suggested that TBK1 is not a direct target of AMPK with ULK1 acting as an intermediate kinase responsible for TBK1 phosphorylation (181). In agreement with Zhao and colleagues (181), we observed similar patterns of AMPK, ULK1, and TBK1 phosphorylation in wild type and AMPK α1/α2 deficient cells following 991 treatment, supporting the notion that AMPK-dependent TBK1 phosphorylation may be mediated via ULK1.

4.6 Limitations & future directions

Although our findings clearly demonstrate the induction of mitophagy (~20%) in C2C12 mito-QC myoblasts in response to both CCCP treatment and AMPK activation by 911, it is important for these experiments to be repeated. This is because we were unable to perform CCCP and 991 treatments several times over multiple passages. Repeating these experiments will ensure that our findings are reproducible. In doing so, we recommend employing a time course approach to help dissect the sequence of AMPK-dependent and PINK1-Parkin-dependent mitophagy in skeletal muscle cells. More specifically, by replicating the CCCP treatment time course performed in this study (0, 1, 3, 6, 12 and 24 hours) and measuring mitophagy (mCherry/ GFP) at each timepoint, it will be possible to determine whether activation of PINK1-Parkin signalling coincides with mitophagy. Because our data shows that PINK1 kinase and Parkin E3 ligase are activated after 6 hours of CCCP treatment (Figure 4.3), a significant increase in mitophagy (assessed via mCherry/GFP) at this time point would suggest induction of PINK1-Parkin-mediated mitophagy. Furthermore, detection of mitophagy before 6 h would indicate induction of PINK1-Parkin independent mitophagy. Given that CCCP treatment indirectly activates AMPK after 1 h (Figure 4.2 B) and specific activation of AMPK by 991 induces

mitophagy (Figure 4.5 A & B), we hypothesise that AMPK may drive mitophagy in skeletal muscle cells after 1 and 3 hours of CCCP treatment. Thus, using this approach, it may be possible to demonstrate sequential activation of AMPK-dependent and PINK1-Parkin-dependent mitophagy following CCCP treatment in skeletal muscle cells.

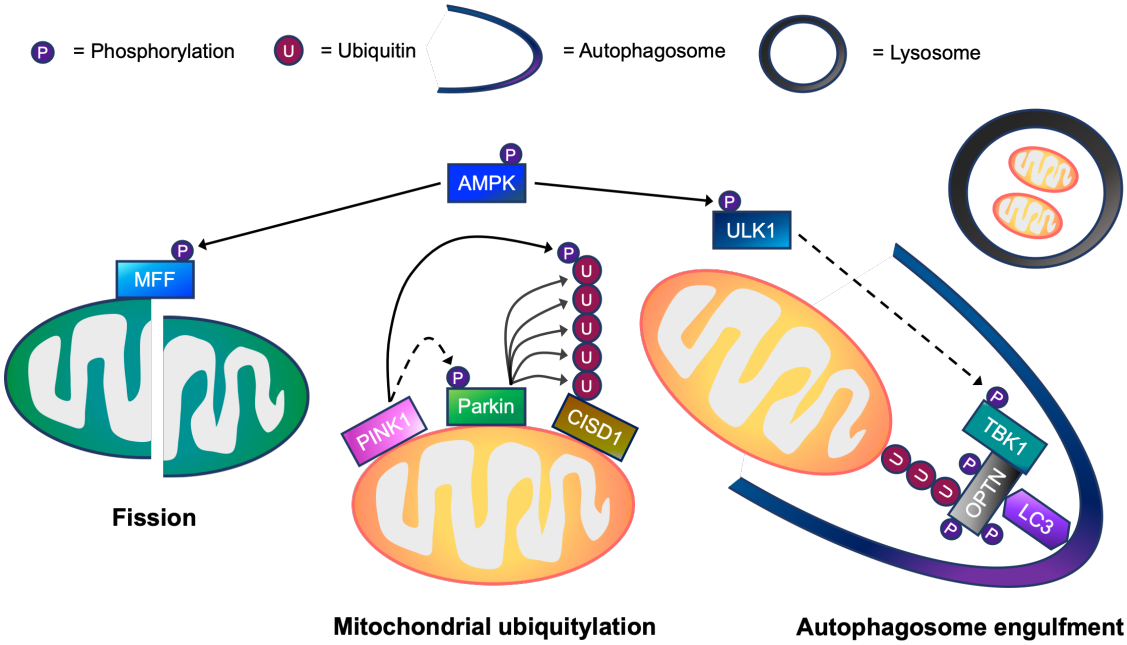

Figure 4.8 A working model of the mechanisms regulating mitophagy processing in skeletal muscle cells. In response to cellular energy stress, (1) AMP-activated protein kinase (AMPK) activation initially promotes mitochondrial fission via direct phosphorylation of mitochondrial fission factor (MFF). This allows the separation of healthy and depolarized mitochondria. In depolarized mitochondria, (2) PTEN-induced kinase 1 (PINK1) accumulates on the outer mitochondrial membrane (OMM) and phosphorylates both ubiquitin (Ub) and Parkin. (3) This is suggested to promote the recruitment of Parkin E3 ubiquitin ligase to the OMM. Parkin then ubiquitylates OMM proteins including CDGSH iron sulphur domain 1 (CISD1), facilitating mitochondrial ubiquitylation. Meanwhile, (4) AMPK activation leads to TBK1 phosphorylation possibly via ULK1, which in turn, is thought to translocate to the mitochondria. (5) The activation of TBK1 is proposed to enhance the binding capacity of autophagy receptors (eg, optineurin, OPTN) to ubiquitylated mitochondria, facilitating autophagosome engulfment. (6) Subsequently, the autophagosome fuses with the lysosome for mitochondrial degradation. → = signalling thought to occur in skeletal muscle. ⇢ = assumption based on signalling events in non-muscle cell lines.

4.7 Conclusion

Based on the findings in the present study and existing literature, we propose a working model of endogenous mechanisms that regulate mitophagy in skeletal muscle cells activated and phosphorylates MFF, which in turn, functions as a receptor for DRP1-mediated fission. Fission helps to separate healthy and depolarised mitochondria, with PINK1 and Parkin signalling being activated in the latter. First, PINK1 accumulates on the OMM and subsequently phosphorylates both the Ub, and the Ub-like domain of Parkin. This phosphorylation promotes the recruitment of Parkin to the OMM and helps to fully activate the Parkin Ub E3 ligase activity. Parkin then ubiquitylates a number of OMM proteins, such as CISD1, facilitating mitochondrial ubiquitylation. In contrast to previous research, we found the phosphorylation and activation of TBK1 was independent of both PINK1 and Parkin activity. Instead, our data suggests that TBK1 phosphorylation is mediated by AMPK, possibly via ULK1. The phosphorylation of TBK1 enhances the binding of autophagy receptors, such as OPTN, with poly-Ub chains emanating from depolarised mitochondria. This promotes selective mitochondrial autophagy in skeletal muscle. In summary, our results support the hypothesis that AMPK drives mitophagy by enhancing mitochondrial fission and mitochondrial autophagosomal engulfment via TBK1 phosphorylation independently of PINK1 and Parkin. Thus, this study improves our understanding of the mechanisms that govern mitophagy in skeletal muscle.

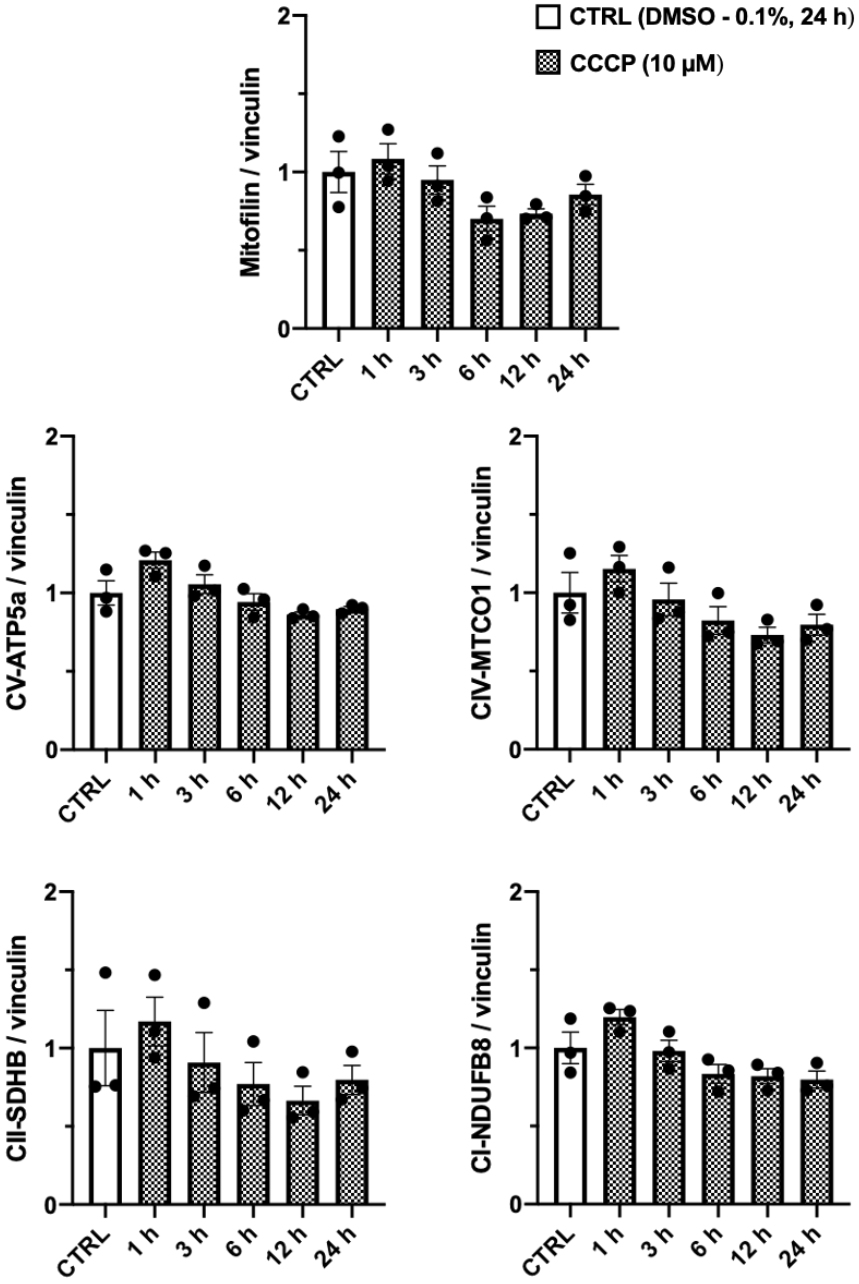

Supplementary Figure 4.9: Quantification of Figure 4.2A - CCCP treatment does not reduce markers of mitochondrial protein content in skeletal muscle cells. Markers of mitochondrial content are unaltered following CCCP treatment for up to 24 h. C2C12 myotubes were treated with DMSO (0.1%, 24 h) as a vehicle control (CTRL) or 10 µM CCCP for up to 24 h. Total lysates were analyzed by SDS-PAGE and western blotting. Representative images of n = 3 independent experiments are shown.

Supplementary Table 4.10 – List of antibodies used			
Antibody	**Source**	**Catalogue Number**	**Concentration**
ACC	Cell Signaling Technology	3676	1:1000
pSer79 ACC equivalent to mouse skeletal muscle ACC2 at Ser 212	Cell Signaling Technology	3661	1:1000
AMPKα	Cell Signaling Technology	2532	1:1000
pThr172 AMPKα	Cell Signaling Technology	2535	1:1000
CISD1	Proteintech	16006-1-AP	1:5000
GAPDH	Cell Signaling Technology	5174	1:5000
Mitofilin	Proteintech	10179-1-AP	1:1000
MFF	Cell Signaling Technology	84580	1:5000
pSer146 MFF equivalent to human at Ser 172	Cell Signaling Technology	49281	1:1000
OPA1	BD Biosciences	612606	1:1000
OXPHOS	Abcam	ab110413	1:1000
TBK1	Cell Signaling Technology	3504	1:500
PINK1 human residues 125–539	Dundee Cell Products		1:500
pSer172 TBK1	Cell Signaling Technology	5483	1:500
Ubiquitin	Biolegend	P4D1	1:2000
pSer65 Ubiquitin	Sigma-Aldrich	ABS1513-I	1:1000
ULK1	Cell Signaling Technology	4773	1:1000
pSer555 ULK1	Cell Signaling Technology	5869	1:1000
Vinculin	Abcam	ab73412	1:2000
Mouse IgG, HRP-linked	Cell Signaling Technology	7076	1:10 000
Rabbit IgG, HRP-linked	Cell Signaling Technology	7074	1:10 000

CHAPTER 5

REGUALTORY ROLES OF PINK1-PARKIN AND AMPK IN SKELETAL MUSCLE MITOPHAGY

5 Regulatory roles of PINK1-Parkin and AMPK in skeletal muscle mitophagy

Alex P. Seabright[1], Yu-Chiang Lai[1,2,3,4]

1. School of Sport, Exercise and, Rehabilitation Sciences, University of Birmingham, Birmingham, UK
2. Institute of Metabolism and Systems Research, University of Birmingham, Birmingham, UK
3. Mitochondrial Profiling Centre, University of Birmingham, Birmingham, UK
4. MRC Versus Arthritis Centre for Musculoskeletal Ageing Research, University of Birmingham, Birmingham, UK

Seabright AP & Lai YC. Regulatory roles of PINK1-Parkin and AMPK in skeletal muscle mitophagy. Frontiers in Physiology, 2020 (Under review).

5.1 Abstract

The selective removal of damaged mitochondria, also known as mitophagy, is an important mechanism that regulates mitochondrial quality control. Evidence suggests that mitophagy is adversely affected in aged skeletal muscle, and this is thought to contribute towards the age-related decline of muscle health. While our knowledge of the molecular mechanisms that regulate mitophagy are derived mostly from work in non-muscle cells, whether these mechanisms are conferred in muscle under physiological conditions has not been thoroughly investigated. Recent findings from our laboratory and those of others have made several novel contributions to this field. Herein, we consolidate current literature, including our recent work, while evaluating how mitophagy is regulated both in muscle and non-muscle cells through the steps of mitochondrial fission, ubiquitylation and autophagosomal engulfment. During mitophagy in non-muscle cells, mitochondrial depolarisation activates PINK1-Parkin signalling to elicit mitochondrial ubiquitylation. TANK-binding kinase 1 (TBK1) then activates autophagy receptors, which in turn, tether ubiquitylated mitochondria to autophagosomes prior to lysosomal degradation. In skeletal muscle, evidence supporting the involvement of PINK1-Parkin signalling in mitophagy is lacking. Instead, 5'-AMP-activated protein kinase (AMPK) is emerging as a critical regulator. Mechanistically, AMPK activation promotes mitochondrial fission before enhancing autophagosomal engulfment of damaged mitochondria possibly via TBK1. While TBK1 may be a point of convergence between PINK1-Parkin and AMPK signalling in muscle, the critical question that remains is whether mitochondrial ubiquitylation is required for mitophagy. In future, improving understanding of molecular processes that regulate mitophagy in muscle will help to develop novel strategies to promote healthy ageing.

5.2 Introduction

Skeletal muscle mitochondria are indispensable organelles that supply energy, in the form of ATP, to match metabolic and locomotive demands. To maintain optimal functioning in skeletal muscle, it is critical to remove damaged mitochondria through selective autophagy, known as mitophagy (187). While mitochondrial quality control is regulated by several mechanisms, including both mitochondrial biogenesis and mitophagy, evidence suggests that the latter is impaired during ageing (140). At present, it is not possible to directly assess skeletal muscle mitophagy in humans. However, evidence suggests that skeletal muscle mitochondria accrue protein damage (141) and become functionally impaired (142-145) during human ageing. The accumulation of damaged and dysfunctional mitochondria reported in these studies is consistent with the notion that mitochondrial clearance via mitophagy is compromised in aged muscle.

Much of our knowledge regarding mitophagy and its molecular mechanisms is derived from work in immortalised, non-muscle cells lines. In these cells, it has become clear that ubiquitin-dependent, receptor-dependent and cardiolipin-dependent mechanisms are capable of regulating mitophagy (57). Although signalling molecules such as, BNIP3, NIX/ BNIP3L, FUNDC1, BCL2-L-13 and FKBP8 are implicated in receptor-dependent mitophagy, as is cardiolipin in cardiolipin-dependent mitophagy (125), these are beyond the scope of this review. However, what is known about ubiquitin-dependent mitophagy in non-muscle cells is that it is comprised of four key steps: mitochondrial fission, ubiquitylation, autophagosomal engulfment and degradation. Execution of these steps in sequence promotes efficient mitophagy (see Figure 1). Firstly, healthy and damaged mitochondria need to be separated via fission. Once separated, damaged mitochondria are marked with ubiquitin chains that act as a recognition signal for autophagy receptors.

Autophagy receptors then tether ubiquitylated mitochondria to autophagic membranes, enabling autophagosomes to engulf damaged mitochondria. Finally, autophagosomes fuse with lysosomes for mitochondrial degradation.

From a mechanistic perspective, dynamin-related protein 1 (DRP1), mitochondrial fission factor (MFF), mitochondrial fission 1 protein (FIS1) and mitochondrial dynamics proteins 49/51 (MID49/51) have been shown to regulate the process of mitochondrial fission (24, 188). Moreover, several E3 ubiquitin ligases, such as Parkin (75, 76), MARCH5 (103) and MUL1 (85) are known to ubiquitylate outer mitochondrial membrane (OMM) proteins. Five autophagy receptors named: next to BRCA1 gene 1 protein (NBR1) nuclear dot protein 52 (NDP52), optineurin (OPTN), sequestosome-1 (SQSTM1/p62) and tax1-binding protein 1 (TAX1BP1) recognise ubiquitylated mitochondria and facilitate autophagosomal engulfment prior to mitochondrial degradation (77). Due to its high relevance in many human diseases (189), multiple signalling pathways are proposed to regulate the aforementioned components in order to orchestrate the four step mitophagy process (190). However, in skeletal muscle, our understanding of mitophagy and the molecular mechanisms underlying each of its four steps has not been thoroughly explored.

Transmission electron microscopy (TEM) is the gold standard technique for detecting mitophagy occurrence because it enables direct visualisation of mitochondria inside autophagic and lysosomal membranes. However, it is not widely used in skeletal muscle, mainly because operating TEM requires a high degree of technical expertise (113). In recent years, a number of fluorescence-based mouse models (e.g. mito-QC (48), mt-Keima (50) and mitoTimer (117) have been developed to measure mitophagy in vivo. These, groundbreaking, innovations have enabled researchers to produce quantitative

data in order to evaluate the level of mitophagy in skeletal muscle as well as in a range of other tissues and cell types. In the absence of these tools, the majority of research in skeletal muscle has assessed mitophagy signalling markers, such as Parkin and BCL2 interacting protein 3 (BNIP3) to indicate mitophagy (156, 157, 191-193). However, by measuring these signalling markers alone, it is difficult to make reliable conclusions about mitophagy.

In order to advance understanding of mitophagy in skeletal muscle, we recently generated a stable C2C12 "mito-QC" cell line to study mitophagy (152). This cell line also facilitates the assessment of mitochondrial morphology, including mitochondrial fission/ fusion events. In terms of the underlying signalling mechanisms, the PINK1-Parkin signalling axis is known to be the classical pathway that regulates: mitochondrial fission; ubiquitylation; and autophagosomal engulfment, during mitophagy. However, the vast majority of work investigating PINK1-Parkin signalling, has been conducted in cells that overexpress exogenous proteins to amplify ubiquitin signals (42, 46, 69, 71, 75, 81, 84, 166). To circumvent this, we employed a tandem ubiquitin binding entity (TUBE) pull-down technique to enrich ubiquitin, allowing us to assess endogenous ubiquitylation status (152). Interestingly, AMPK is also emerging as a key regulator of mitophagy via its involvement in mitochondrial fission and autophagosomal engulfment.

In this review we aim to integrate our recent findings into the current literature and evaluate how mitophagy is regulated in skeletal muscle through the steps of mitochondrial fission, ubiquitylation and autophagosomal engulfment. Firstly, we will discuss the involvement of PINK1-Parkin signalling in mitochondrial fission, ubiquitylation and autophagosomal engulfment. Afterwards, we will explore the role of AMPK in

mitochondrial fission and autophagosomal engulfment. Finally, we will highlight some of the important questions that are yet to be answered within the field.

5.3 PINK1-Parkin-mediated mitophagy

The PTEN induced kinase 1 (PINK1)-Parkin signalling axis is considered to be the classical mitophagy pathway. This signalling pathway has been studied extensively in the context of neurodegeneration because mutations in human PINK1 (PARK6) (60, 61) and Parkin (PARK2) (62) are assumed to be causative for early-onset Parkinson's disease. In addition, abnormal mitophagy processing is thought to contribute towards the pathophysiology of Parkinson's disease (63). Because of this, some studies have attempted to measure PINK1 or Parkin in skeletal muscle at the protein level to understand mitophagy (129, 153, 154, 156, 157, 191-193). However, the abundance of a protein does not reflect its enzymatic activity. Therefore, whether the PINK1-Parkin signalling is crucial in the regulation of skeletal muscle mitophagy has not been thoroughly examined. In the next few sections, we will discuss the involvement of the PINK1-Parkin signalling pathway in mitophagy including the steps of mitochondrial fission, ubiquitylation and autophagosomal engulfment.

5.3.1 PINK1-Parkin-mediated mitophagy in non-muscle cell lines

What we have learnt from studies using non-muscle cell lines is that under basal conditions, PINK1 is continuously degraded through the N-end-rule pathway (64). Conversely, insults such as: a) the loss of the mitochondrial membrane potential (42, 46); b) excessive production of reactive oxygen species (ROS) (65, 66); and, c) mutations in mitochondrial DNA (mtDNA) (67), can activate PINK1 kinase activity. PINK1 then phosphorylates and activates Parkin's ubiquitin E3 ligase activity, which labels damaged

mitochondria with ubiquitin prior to autophagosomal engulfment and mitochondrial degradation. A detailed mechanistic summary of the PINK1-Parkin signalling pathway in mitophagy in non-muscle cell lines is provided elsewhere (15, 68).

5.3.2 PINK1-Parkin-mediated mitophagy in skeletal muscle

Whether PINK1 and Parkin are involved in skeletal muscle mitophagy has only been investigated in a few studies. In mitochondria isolated from skeletal muscle, PINK1 protein content is reported to be increased in patients with spinal and bulbar muscular atrophy (SBMA) (153). In the same study, indirect measurements of mitophagy (co-localisation of LC3 and ATPase) were also elevated (153), suggesting that the PINK1-mediated mitophagy may be activated under conditions of severe pathological stress in human skeletal muscle. Using mitophagic flux analysis in mice, Chen and colleagues (130) observed LC3-II flux in mitochondrial enriched skeletal muscle lysates to be attenuated following endurance exercise in Parkin knock-out (KO) mice (130). These data suggest that Parkin is required for exercise-induced mitophagy. However, because mitophagy was not directly measured by both of these studies, the reliability of the conclusions is limited. On the other hand, using the pMitoTimer reporter alongside pLAMP1-YFP to visualise mitolysosomes, Laker and colleagues (58) have shown that acute endurance exercise induces mitophagy in skeletal muscle. Interestingly, using an identical exercise stimulus, subsequent work from the same group demonstrated PINK1 not to present in mitochondria enriched muscle lysates (154), indicating that exercise induced mitophagy that occurs in a PINK1-independent manner. Consistently data from PINK1 KO mice on a mito-QC background indicate that under healthy, rested conditions, PINK1 is not required for mitophagy in skeletal muscle (49). Thus, in studies that measure

mitophagy directly, there is very little evidence to support the involvement of the PINK1-Parkin signalling pathway in skeletal muscle mitophagy.

5.3.3 PINK1-Parkin mediated mitochondrial fission

5.3.3.1 Non-muscle cells lines

Mitochondrial fission is a prerequisite step that separates damaged mitochondrial fragments for subsequent degradation (169, 170). Evidence suggests that both PINK1 and Parkin are able to regulate mitochondrial fission. In rat hippocampal neurons, overexpression of both PINK1 and Parkin induces fission, whereas knockdown of PINK1 has the opposite effect (194). Yang and colleagues (195) have also shown that PINK1 knockdown increases the number of long tubular mitochondria, and this effect is suppressed by the overexpression of DRP1 or FIS1. In another study using COS-7 cells, overexpression of an inactive DRP1 variant (DRP1 K38A) significantly attenuated the pro-fission effects of individual PINK1 and Parkin overexpression (196). Collectively, these data suggest that PINK1 and Parkin regulate DRP1-mediated mitochondrial fission.

5.3.3.2 Skeletal muscle

Recent work conducted by Favaro and colleagues (197) revealed that mitochondrial volume is not significantly altered in DRP1-deficient muscle, but the average size of individual organelles is greater. These data indicate that DRP1 deletion induces fusion of the mitochondrial network, resulting in larger, but fewer mitochondria. Despite these findings, our understanding of the signalling events that precede DRP1-mediated mitochondrial fission has not been thoroughly explored. Therefore, whether PINK1 and/ or Parkin activate DRP1-mediated mitochondrial fission in skeletal muscle requires further investigation.

5.3.4 PINK1-Parkin-mediated mitochondrial ubiquitylation

5.3.4.1 Non-muscle cells lines

Labelling damaged mitochondria with ubiquitin molecules is an important step that helps to recruit autophagy receptors for autophagosomal engulfment (77). The reason why PINK1-Parkin signalling is a critical mediator of mitophagy is because activation of Parkin's ubiquitin E3 ligase activity leads to mitochondrial ubiquitylation (198). In response to mitochondrial depolarisation, PINK1 is stabilised and activated on the outer mitochondrial membrane (OMM). PINK1 then phosphorylates ubiquitin (69-71), which in turn, recruits Parkin to the OMM (46). Furthermore, binding of phospho-ubiquitin to Parkin (72) along with PINK1-mediated Parkin phosphorylation, maximally activates Parkin E3 ligase activity (73, 74). This enables Parkin to label damaged mitochondrial by ubiquitylating OMM proteins, such as: CDGSH iron sulphur domain 1 (CISD1); mitofusin-1/2 (MFN-1/2); translocase of outer membrane 70 kDa subunit (TOM70); mitochondrial fission 1 protein (FIS1); and, voltage-dependent anion channel 1 (VDAC1) (75, 76).

5.3.4.2 Skeletal muscle

While the PINK1-Parkin signalling pathway is the most widely studied mechanism of mitochondrial ubiquitylation, the necessity of this pathway for mitophagy in skeletal muscle is currently undefined. This is primarily due to the lack of appropriate tools to study the activities of PINK1 kinase and Parkin E3 ligase. The main reason why there are so few studies investigating the role of PINK1 in skeletal muscle mitophagy is because many of the commercially available antibodies are insensitive or unspecific when detecting endogenous PINK1 (158). Furthermore, because Parkin is reported to

translocate to mitochondria for both mitophagy (42) and mitochondrial biogenesis (159-161) simply measuring mitochondrial Parkin content does not determine which process Parkin is involved in. Thus, developing tools to assess the activities of PINK1 kinase and Parkin E3 ligase will help to improve our understanding of the role of PINK1-Parkin signalling in skeletal muscle mitophagy.

We recently implemented a tandem ubiquitin binding entity (TUBE) pulldown technique to enrich ubiquitin and simultaneously capture all the ubiquitylated proteins in skeletal muscle cells (152). Following SDS-PAGE and protein transfer, we then used antibodies specific to phosphorylated ubiquitin at Ser 65 and CISD1 to measure intracellular PINK1 kinase activity and Parkin E3 ligase activity, respectively (152). In this experiment, we found that endogenous activities of PINK1 kinase and Parkin E3 ligase were increased following CCCP-induced mitochondrial depolarisation in C2C12 muscle cells (152). These data provide the first evidence to suggest that PINK1-Parkin signalling can be activated in skeletal muscle. Interestingly, these findings also indicate that the activation of PINK1 and Parkin requires very severe stimulation, which is unlikely to occur under physiological conditions.

So far, no study has been able to clearly demonstrate that mitochondrial ubiquitylation occurs in skeletal muscle. Since mitochondrial ubiquitylation is a critical step for the recognition of damaged mitochondria in the lead up to their degradation, we suggest that TUBE ubiquitin enrichment techniques be used to address this question.

5.3.5 PINK1-Parkin-mediated autophagosomal engulfment

5.3.5.1 Non-muscle cells lines

Activation Parkin E3 ligase activity labels damaged mitochondria with ubiquitin, helping to recruit autophagy receptors for autophagosomal engulfment. The formation of poly-ubiquitin chains on damaged mitochondria leads to the recruitment of autophagy receptors, including NBR1, NDP52, OPTN, SQSTM1/p62 and TAX1BP1 (77). Because these autophagy receptors possess a ubiquitin-binding domain as well as a LC3-interacting region (LIR) motif, they have the capacity to link ubiquitylated mitochondria to autophagosomal LC3. Mechanistically, NDP52 and OPTN are the essential receptors for mitophagy with some contribution from TAX1BP1, whereas NBR1 and p62 are dispensable (78, 84). The binding capacity of OPTN with poly-ubiquitin chains is enhanced by TBK1 which phosphorylates OPTN at multiple serine residues (81). In the other study, Vargas and colleagues (82) have also shown that TBK1 activation promotes NDP52-mediated recruitment of the ULK1 complex during autophagosomal engulfment. Importantly, studies have also shown that TBK1 activation following its phosphorylation at Ser 172 (83) requires the activation of PINK1-Parkin signalling, which in turn, generates poly-ubiquitin chains on depolarised mitochondria (78, 84). Based on these reports, it is clear that TBK1 plays a critical role in autophagosomal engulfment of damaged mitochondria via its association with OPTN and NDP52.

5.3.5.2 Skeletal muscle

In skeletal muscle, however, recent work from our laboratory suggests that TBK1 phosphorylation and activation is independent of both PINK1 and Parkin activation (152). Using a time course experiment, we observed that TBK1 phosphorylation occurs prior to the activation of PINK1 kinase and Parkin E3 ligase activity. We also demonstrated that TBK1 phosphorylation occurs normally in PINK1 knockout HeLa cells following CCCP treatment. We suspect that the disparity between our data and findings generated in non-muscle cell lines may be due to the use of overexpression systems employed in other studies. HeLa cells lack native Parkin expression (174). Stably expressing non-native Parkin, has been shown to induce artificial activation of its E3 ligase activity, particularly when fused with exogenous tags at its N-terminus (182). Thus, we believe that in skeletal muscle TBK1 is acutely activated following mitochondrial depolarisation in a PINK1-Parkin independent manner. However, this conclusion also raises the question as to which other E3 ligases, excluding Parkin, elicit mitochondrial ubiquitylation to promote autophagy receptor recognition and interaction with autophagic membranes.

5.3.6 A summary of PINK-Parkin signalling pathway in skeletal muscle mitophagy

So far, evidence supporting the involvement of PINK1-Parkin signalling in the molecular regulation of skeletal muscle mitophagy is scarce. This is mainly due to lack of tools to study endogenous PINK1-Parkin signalling. In future, employing techniques to enrich ubiquitin (e.g. TUBE pulldown technique), will help to identify physiological conditions that activate PINK1-Parkin signalling as well as determining whether mitochondrial ubiquitylation in skeletal muscle is required for mitophagy.

5.4 AMPK-mediated mitophagy

5.4.1 AMPK in skeletal muscle

The energy sensing kinase 5'-AMP-activated protein kinase (AMPK) is a master regulator of metabolism (199). AMPK becomes activated in response to rising AMP levels following ATP hydrolysis. Upon its activation, AMPK promotes glucose and fatty acid utilisation (199) while inhibiting pro-growth signals (200), thus restoring ATP levels. Because AMPK senses changes in ATP levels, and mitochondria resynthesise ATP, it is not surprising that and AMPK regulates mitochondrial biology to help maintain cellular energy homeostasis. For example, AMPK has been shown to phosphorylate and activate peroxisome proliferator-activated receptor gamma coactivator 1-alpha (PGC1α) (201) which in turn, promotes mitochondrial biogenesis. Interestingly, others have also reported that AMPK controls mitochondrial fission (169) and is capable of orchestrating the selective removal of damaged mitochondria in mitophagy (58).

5.4.2 AMPK-mediated mitophagy in non-muscle cell lines

Egan and colleagues (52) first revealed that AMPK is involved in mitophagy. In their study, not only did cells expressing non-phosphorylatable ULK1 mutants contain more mitochondria, but a higher proportion of these mitochondria were enlarged with altered cristae. Others have subsequently shown that AMPK-mediated phosphorylation of ULK1 at Ser 555 regulates its activation and translocation to mitochondria for its involvement in mitophagy (52, 59). These early studies indicate that AMPK-mediated phosphorylation of ULK1 facilitates mitophagy.

5.4.3 AMPK-mediated mitophagy in skeletal muscle

AMPK-mediated mitophagy in skeletal muscle was first demonstrated by Laker and colleagues (58). In this study, mice expressing a muscle-specific dominant-negative form of the catalytic α2 subunit of AMPK (dnTG) showed no transient elevation in mitophagy 6 h after a bout of treadmill running unlike wild-type mice (58). Importantly, mitophagy was measured directly in these mice via pMitoTimer and pLAMP1-YFP to visualise on-going sites of mitophagy. In the same study, Laker and colleagues (58) also demonstrated ULK1, a direct substrate of AMPK, to be required for exercise-induced mitophagy using muscle-specific ULK1 KO mice (58). In support of these findings, we recently demonstrated elevated levels of mitophagy in skeletal muscle cells stably expressing the mito-QC reporter following specific, pharmacological activation of AMPK (152). Furthermore, we also observed a dose-dependent increase in ULK1 phosphorylation at Ser 555, a phospho-site that controls its translocation to mitochondria for its involvement in mitophagy (52, 59), in response to pharmacological AMPK activation.

5.4.4 AMPK-mediated mitochondrial fission

5.4.4.1 Non-muscle cells lines

The process of mitochondrial fission is a critical step during mitophagy as it helps to separate healthy and damaged mitochondrial fragments. AMPK's involvement in mitochondrial fission was first suggested by the Sakamoto laboratory, who used a proteomic approach to reveal that mitochondrial fission factor (MFF) is an AMPK substrate (168). Later, Toyama and colleagues (169) used AMPK α1/α2 double knockout U2OS cells with specific (A769662 & AICAR) AMPK activators to demonstrate that AMPK activation induces mitochondrial fission. Along with mitochondrial fission

protein 1 (FIS1) and mitochondrial dynamics proteins 49/51 (MID49/51), MFF functions as a key receptor for the dynamin-related protein 1 (DRP1) on the outer mitochondrial membrane (OMM) (24, 188). Following its activation and translocation to the mitochondria, DRP1 wraps around mitochondrial constriction sites to enable scission. Interestingly, Toyama and colleagues (169) also showed that AMPK-mediated phosphorylation of MFF at Ser 155 and 172 is required for DRP1 recruitment to the OMM. These findings indicate that AMPK-mediated phosphorylation of MFF induces DRP1 translocation to mitochondria to facilitate mitochondrial scission.

5.4.4.2 Skeletal muscle

In agreement with observations made in non-muscle cell lines mentioned above, we have shown that AMPK activation by 991 induces phosphorylation of MFF and promotes the accumulation of smaller, fragmented mitochondria, indicating fission (152). To the best of our knowledge this is the first study showing that MFF phosphorylation in skeletal muscle is AMPK dependent. Furthermore, although phosphorylation of DRP1 at Ser 616 is known to promote DRP1-mediated mitochondrial scission (202), Laker and colleagues (58) have shown that AMPK is not responsible for exercise-induced phosphorylation of DRP1 at this site. Collectively, our data alongside the work of Taguchi and colleagues (202) suggest that assessing the phosphorylation status of both MFF and DRP1 can be used as a marker to indicate mitochondrial fission. However, it is important to note that while phosphorylation of MFF has been shown to mediate the recruitment of DRP1 to the OMM in non-muscle cell lines (24, 188), this phenomenon has not been verified in skeletal muscle.

5.4.5 AMPK and mitochondrial ubiquitylation

5.4.5.1 Non-muscle cells lines

As mentioned previously, labelling of damaged mitochondria with ubiquitin is essential to recruit autophagy receptors for autophagosomal engulfment. To us, it is surprising that AMPK reportedly activates both PINK1 kinase and Parkin E3 ligase activity through phosphorylation. Wang and colleagues (203) showed that AMPKα2 phosphorylates PINK1 at Ser 495. This AMPK-mediated PINK1 phosphorylation induces its kinase activity, which leads to increased Parkin phosphorylation at Ser 65 in cardiomyocytes (203). In the other study, Lee and colleagues (204) showed that AMPK can also phosphorylate Parkin Ser 9 to induce Parkin's ubiquitin E3 ligase activity towards its substrate, RIPK3. These studies suggest possible interplay between AMPK and PINK1-Parkin signalling. However, evidence demonstrating that AMPK activation leads to mitochondrial ubiquitylation and/ or Parkin-mediated OMM protein ubiquitylation is lacking.

5.4.5.2 Skeletal muscle

By taking advantage of TUBE ubiquitin enrichment, we recently demonstrated that the intracellular activities of PINK1 kinase and Parkin E3 ligase are not increased following AMPK activator treatment in skeletal muscle cells, despite significant induction of mitophagy (152). We also showed no detectable mitochondrial depolarisation under these conditions, suggesting that PINK1-Parkin signalling is not activated (152). Although our data suggests that PINK1-Parkin signalling is not required for AMPK-mediated mitophagy, we have not yet tested whether mitochondrial ubiquitylation occurs under these conditions. Given that all five of the aforementioned autophagy receptors that

facilitate autophagosomal engulfment have ubiquitin binding domains (77), determining whether mitochondrial ubiquitylation is required for autophagy receptor recognition is the next critical question that should be addressed. If it is confirmed that mitochondrial ubiquitylation is required for mitophagy, it is important to determine which E3 ubiquitin ligases, other than Parkin, are responsible for this process.

5.4.6 AMPK and autophagosomal engulfment

5.4.6.1 Non-muscle cells lines

OPTN and NDP52 are the principle autophagy receptors that tether ubiquitylated mitochondria to autophagic membranes via their ubiquitin binding and LC3 interacting domains, respectively (78, 84). As previously mentioned, TBK1 activation is required to facilitate autophagosomal engulfment of ubiquitylated mitochondria by activating OPTN and NDP52. Interestingly, a recent study suggests that AMPK is able to activate TBK1 via ULK1 in adipose tissue. However, in this study, AMPK-mediated phosphorylation and activation TBK1 was not investigated in the context of mitophagy.

5.4.6.2 Skeletal muscle

While investigating the signalling mechanisms underlying skeletal muscle mitophagy, we observed similar phosphorylation patterns of both AMPK and TBK1 in response to indirect and specific AMPK activation (152). To validate the cause-effect relationship between AMPK and TBK1, we used CRISPR-Cas9 generated AMPK α1/α2 knockout cells to demonstrate that TBK1 phosphorylation is AMPK dependent (152). These data suggest that activation of AMPK promotes autophagosomal engulfment via TBK1 activation. Referring back to the findings of Zhao and colleagues in adipocytes, we believe that AMPK activates TBK1 via ULK1-mediated phosphorylation (181).

Although these data suggest that AMPK-ULK1-TBK1 signalling occurs in skeletal muscle cells, the functional relevance of TBK1 in autophagosomal engulfment of damaged mitochondria is yet to be determined.

5.4.7 A summary of AMPK-mediated mitophagy in skeletal muscle

AMPK is emerging as a major regulator of mitophagy in skeletal muscle. Mechanistically, AMPK activation promotes mitochondrial fission before enhancing autophagosomal engulfment of damaged mitochondria possibly via TBK1. Further research is needed to verify the functional relevance AMPK-mediated TBK1 activation in autophagosomal engulfment of damaged mitochondria and therefore skeletal muscle mitophagy.

5.5 Mitophagy is not homogeneous between tissues

As mentioned previously, many studies have used immortalised cells lines derived from various tissue types to help dissect the molecular mechanisms that underpin mitophagy (42, 46, 52, 114, 152, 155, 183). Some of these studies have used cells made to overexpress non-native proteins, such as Parkin (42, 46, 69, 71, 75, 81, 84, 166). Evidence suggests that studying mitophagy in cells that overexpress Parkin may misrepresent mitophagy under endogenous conditions (183). However, while this may be true, it is also important to note that when mitophagy is assessed in vivo, it is not homogeneous between tissues. Recently, the Ganley laboratory demonstrated that levels of mitophagy in skeletal muscle taken from mito-QC mice under resting conditions were similar to that of cardiac muscle, more than the spleen, but less than the liver and kidneys (48). Subsequently, the same group have shown that highly metabolic tissues, such as neural and retinal cells exhibit differential levels of mitophagy under resting conditions (49). While it is not

known why levels of mitophagy differ between cells and tissues, in vivo experiments such as these rule out the potential artefacts of non-native protein expression. Furthermore, because mitophagy occurrence is different between tissues (48), even in those of high metabolic demand (49), the molecular mechanisms controlling mitophagy in various tissues may also be different. Thus, as our knowledge of mitophagy progresses, it is important not to assume that the molecular mechanisms regulating mitophagy in certain cells and tissues are the same everywhere else.

5.6 A working model of mitophagy in skeletal muscle

In this review, we summarise the molecular mechanisms that regulate skeletal muscle mitophagy in four key steps: mitochondrial fission, ubiquitylation, autophagosomal engulfment and degradation (see Figure 1). We reveal that AMPK plays a vital role in the coordination of mitophagy and controls molecular mechanisms associated with mitochondrial fission via MFF and autophagosomal engulfment via ULK1 and TBK1. On the other hand, such evidence supporting the activation and involvement of PINK1-Parkin signalling in mitochondrial ubiquitylation during mitophagy in skeletal muscle under physiological conditions is currently lacking. While TBK1 may be a point of convergence between AMPK and PINK1-Parkin signalling during mitophagy, the critical question that remains is whether mitochondrial ubiquitylation is required for mitophagy in muscle. Gaining a deeper understanding of molecular mechanisms that control mitophagy in skeletal muscle will help to identify important signalling molecules that regulate this process. Such knowledge can then be used to help develop novel therapies, including pharmacological strategies, to combat defective mitophagy in muscle and thus promote healthy ageing.

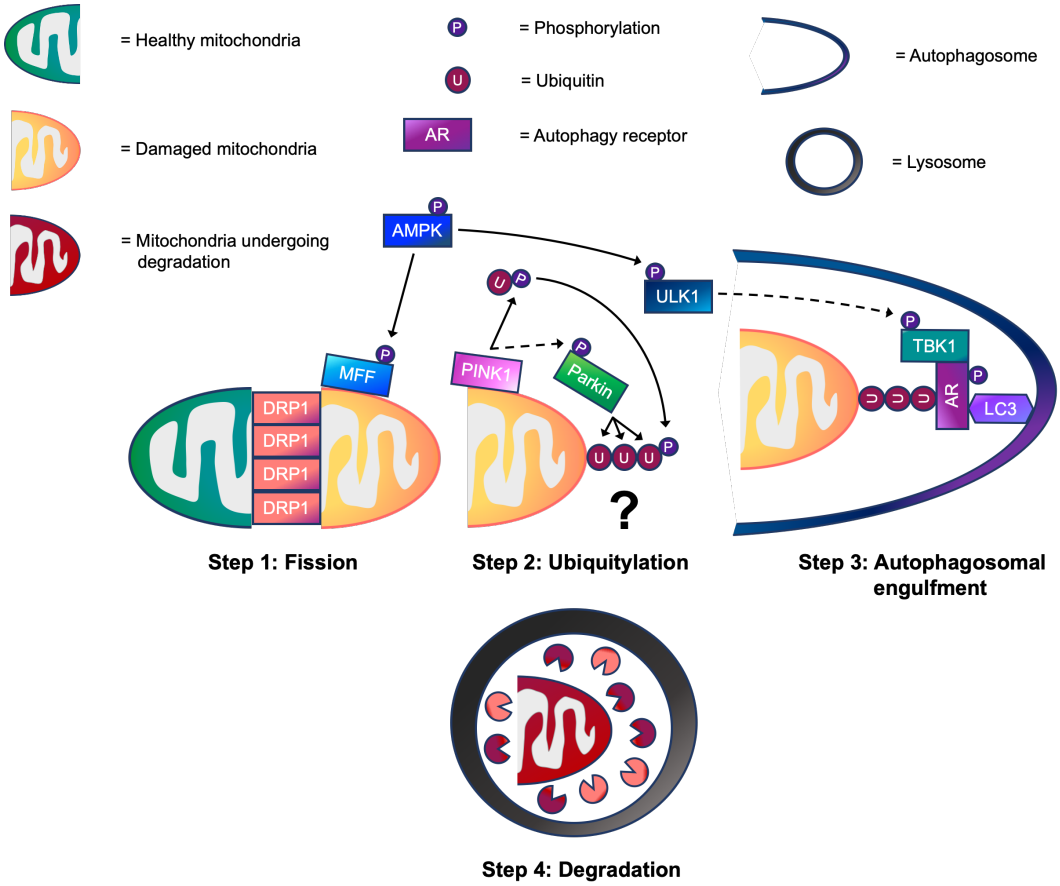

Figure 5.1 A working model of the four step mitophagy process in skeletal muscle. Step 1: Activation of 5'-AMP-activated protein kinase (AMPK) promotes mitochondrial fission via phosphorylation of MFF. This helps to recruit dynamin-related protein 1 (DRP1) to the outer mitochondrial membrane (OMM), enabling it to wrap around mitochondrial constriction sites to carry out scission, separating healthy and damaged mitochondria. Step 2: While the physiological conditions needed to activate PINK1-Parkin signalling for mitophagy in skeletal muscle are unknown, our data shows that PINK1 accumulates on the OMM where it phosphorylates ubiquitin following CCCP-induced mitochondrial depolarisation. This promotes the recruitment of Parkin E3 ubiquitin ligase to the OMM, which in turn, facilitates PINK1-mediated Parkin phosphorylation. Next, Parkin flags damaged mitochondria by ubiquitylating OMM proteins. (?) Despite our knowledge of these events, whether mitochondrial ubiquitylation is required for mitophagy in skeletal muscle is a critical question that warrants future investigation. Step 3: Meanwhile, AMPK also phosphorylates and activates ULK1. This enables the ULK1 complex to translocate to the mitochondria for its involvement in autophagosomal engulfment. ULK1 is suggested to phosphorylate and activate TANK-binding kinase 1 (TBK1). During autophagosomal

engulfment, TBK1 activates autophagy receptors, such as optineurin (OPTN) and nuclear dot protein 52 (NDP52) that tether ubiquitylated mitochondria to autophagosomes. Step 4: Lastly, the autophagosomes fuse with the lysosomes for the degradation of damaged mitochondrial fragments via cathepsin proteases. → = Signalling that occurs in skeletal muscle. ⇢ = Assumption based on signalling events in non-muscle cell lines.

5.7 Future directions

As highlighted throughout this review, crucial questions remain unanswered within this field are: 1) whether the step of mitochondrial ubiquitylation is required for mitophagy in skeletal muscle; and, 2) under what physiological conditions is PINK1-Parkin signalling is activated for mitophagy. To help address the question outlined above, we recommend employing the TUBE ubiquitin enrichment technique described in this review to help facilitate the assessment of mitochondrial ubiquitylation, as well as PINK1 kinase and Parkin E3 ligase activities. Furthermore, using a newly developed fluorescence-based mouse model, such as mito-QC (48) will enable quantifiable analysis of lysosome-dependent mitochondrial degradation to be made. In parallel, it would also be interesting to study mitochondrial fission and autophagosomal engulfment alongside their respective signalling markers (e.g. MFF, DRP1, ULK1 and TBK1) that are highlighted in this review.

CHAPTER 6

FINAL REMARKS

6.1 Main findings

The primary aim of this thesis was to investigate the molecular signalling mechanisms that regulate mitophagy in skeletal muscle. Aberrant skeletal muscle mitophagy has been implicated in the age-related decline of skeletal muscle health. Thus, gaining a deeper understanding of molecular mechanisms that control mitophagy in skeletal muscle will help to identify important signalling molecules that can be targeted in future pharmacological interventions to promote healthy ageing.

Previous research has identified PINK1-Parkin and AMPK to be important signalling molecules that induce mitophagy. In parallel, several fluorescence-based tools have been developed over the past decade to facilitate the study of mitophagy. While these innovations have vastly improved understanding of mitophagy in non-muscle cell lines, our knowledge in skeletal muscle lags well behind. From the outset, it was clear that by harnessing newly developed fluorescence-based reporter 'mito-QC' to study mitophagy in skeletal muscle cells, it would be possible to make useful contributions to this field. As a result, the specific objectives of this thesis in the context of skeletal muscle were to:

1) Develop a C2C12 cell line that stably expresses mito-QC.

2) Determine whether endogenous PINK1-Parkin signalling is functionally active.

3) Determine whether pharmacological activation of AMPK induces mitophagy.

4) Identify downstream AMPK substrates that help to facilitate mitophagy.

5) Determine whether AMPK cooperates with PINK1-Parkin signalling.

After successfully generating a stable C2C12 mito-QC skeletal muscle cell line, and a ubiquitin pull-down technique to study endogenous PINK1 kinase and Parkin E3 ligase activity (Chapter 3; Figure 3.1 & 3.2), several important findings were made.

Firstly, we show that the endogenous activities of PINK1 kinase and Parkin E3 ligase can be simulated in skeletal muscle cells. However, such activation requires prolonged (≥ 6 h), non-physiological stimulation with the mitochondrial depolarising agent carbonyl cyanide m-chlorophenyl hydrazine (CCCP) (Chapter 4.; Figure 4.3). These data clearly demonstrate that endogenous PINK1-Parkin signalling remains functionally active in skeletal muscle. Interestingly, our observations in Chapter 4 (Figure 4.3) do not match what has been found in in immortalised, non-muscle cell lines (42, 46, 84, 166). A plausible explanation for these differences is that non-muscle cell lines, such as HeLa cells, are often made to harbour systems that stably express non-native PINK1 and/or Parkin (42, 46, 69, 71, 75, 81, 82, 84, 91, 166, 167). Stably expressing non-native proteins, such as Parkin, can induce artificial activation of its E3 ligase activity, particularly when fused with exogenous tags at the N-terminus (182). Following the integration of our findings into current literature in Chapter 5, it appears that PINK1-Parkin signalling plays a lesser role in the orchestration of skeletal muscle mitophagy. This hypothesis is supported by in vivo data which suggests that PINK1 is dispensable for skeletal muscle mitophagy under basal conditions (49) and in response to acute endurance-type exercise (154). Because activation of PINK1-Parkin signalling induces mitochondrial ubiquitylation, the critical question that has not yet been tested in this field is whether mitochondrial ubiquitylation is required for skeletal muscle mitophagy.

Importantly, the findings contained within this thesis demonstrate that pharmacological activation of AMPK induces mitophagy in skeletal muscle cells stably expressing mito-

QC (Chapter 4; Figure 4.5). From a mechanistic perspective, data within this thesis also verifies MFF and TBK1 as AMPK substrates (Chapter 4; Figure 4.6 & 4.7). In non-muscle cell lines, both MFF (169) and TBK1 (78, 80-82, 84) are thought to play a pivotal role in the orchestration of mitophagy. Consequently, based on our findings and the current literature, we propose a working model of AMPK-mediated mitophagy (Chapter 5; Figure 5.1). Briefly, activation of AMPK promotes mitochondrial fission via the phosphorylation of MFF as a means to separate healthy and damaged mitochondria. Meanwhile, activated AMPK also upregulates molecular signals associated with autophagosomal engulfment of damaged mitochondrial fragments, via the phosphorylation and activation of ULK1 and TBK1. Activated TBK1 is suggested to enhance the binding capacity of autophagy receptors, such as optineurin, to help tether ubiquitylated mitochondria to the autophagosome. Subsequently, the autophagosome fuses with the lysosome facilitating the degradation of damaged mitochondria.

Lastly, the findings contained within this thesis suggest a lack of cooperation between AMPK and PINK1-Parkin signalling during the coordination of skeletal muscle mitophagy. Strikingly, prolonged treatment of skeletal muscle cells with AMPK activator 991 was not sufficient to depolarise the mitochondrial membrane or induce the activities of endogenous PINK1 and Parkin (Chapter 4; Figure 4.7 D).

6.2 Limitations

A major limitation of this thesis the sole use of C2C12 skeletal muscle cells to study skeletal muscle mitophagy. Although cell-based models of skeletal muscle, such as C2C12 can be used to provide important molecular insights into muscle specific signalling they do not fully represent mature skeletal muscle tissue. This is because mature skeletal muscle tissue is comprised not only of muscle cells, but nerves, blood vessels, smooth muscle cells, fibroblasts, and immune cells. These cell types contribute to the various functions of muscle. However, their presence means the structural composition and metabolic needs of mature skeletal muscle tissue are different to those cultured skeletal muscle cells. Because of these differences, it is important to consider that findings made in cultured skeletal muscle cells may not be conferred in mature skeletal muscle tissue.

Another notable limitation of the present thesis and one that lacks physiological relevance is its heavy reliance upon pharmacological treatments of cultured skeletal muscle cells. More specifically, AMPK activator 991 was used to activate AMPK while CCCP was primarily employed to depolarise the mitochondrial membrane and stimulate PINK1-Parkin activity. Although it was possible to address the objectives of the present thesis using these drugs, our initial approach was to activate AMPK using electrical pulse stimulation (EPS) (C-Pace EP; IonOptix, Milton, MA, USA). In differentiated C2C12 skeletal muscle cells, EPS has been shown to induce phosphorylation of AMPK at Thr 172 (205), the primary mechanism responsible for AMPK activation (206). Based on these data, we sought to activate AMPK via EPS with the eventual aim of determining whether EPS-mediated AMPK activation alters levels of mitophagy in C2C12 cells stably expressing mito-QC. Unfortunately, despite the testing of numerous EPS protocols, we

could not reproduce the changes previously reported by Evers-van Gogh and colleagues (205) in EPS-mediated AMPK Thr 172 phosphorylation.

Another limitation of the present thesis is the lack of in vivo data. Despite the recent development of mito-QC knock in mouse model by Dr. Ian Ganley's laboratory at the University of Dundee (48) and, through collaboration, transportation of frozen embryos to the Biomedical Services Unit (BMSU) at the University of Birmingham, it was not possible to perform experiments using this tool. The reason for this is that obtaining a UK Home Office project license and generating a stable mouse colony from frozen embryos was too costly. To overcome this setback, and to continue in the pursuit of in vivo data, analysis of powdered skeletal muscle biopsies taken from human subjects was due to take place earlier this year (March - June 2020). Samples were obtained by Dr Gareth Wallis' laboratory in the School of Sport, Exercise and Rehabilitation Sciences at the University of Birmingham. In exchange for analytical expertise, Dr Wallis kindly agreed to share some of the samples he had collected. Based on our findings in cell culture and given the types of analysis can be performed using powdered muscle tissue, the questions we sought to answer were whether exhaustive endurance-type exercise induces mitochondrial ubiquitylation and/or the activities of PINK1 kinase and Parkin E3 ligase. Our intention was to address this question using the ubiquitin pull-down technique established within this thesis (Chapter 3; Figure 3.2). However, because the COVID-19 pandemic, we were unable to undertake this work due to the extended closure of the University.

Although the data contained within this thesis suggests that AMPK mediates MFF and TBK1 phosphorylation, this experiment was not performed in muscle cells or tissue. Access to AMPK α1/α2 skeletal muscle-specific knock out mice would have made it possible to address this shortfall. However, despite multiple efforts, we could not get hold

of skeletal muscle tissue or primary cells from these animals. In addition to this, within the present thesis, we did not determine functional relevance of either MFF or TBK1 in skeletal muscle mitophagy.

Finally, whether levels of skeletal muscle mitophagy are elevated prior to the activation of endogenous PINK1 kinase and Parkin E3 ligase was not tested in the present thesis. A useful experiment to address this knowledge gap would be to use the CCCP treatment time course previously described (Chapter 4; Figure 4.3) on skeletal muscle cells stably expressing mito-QC. Importantly, this experiment would determine whether activation of endogenous PINK1 kinase and Parkin E3 ligase after 6, 12 and 24 h of CCCP treatment (Chapter 4; Figure 4.3) coincides with a significant change in levels of mitophagy.

6.3 Conclusion

Overall, this thesis contributes novel data towards our understanding of the molecular mechanisms that regulate mitophagy in skeletal muscle. Notably, the findings within this thesis verify previous work by demonstrating that pharmacological activation of AMPK drives mitophagy in skeletal muscle. However, the greatest advancement made by this thesis is that it starts to dissect the molecular signals that control mitochondrial fission and autophagosomal engulfment in the lead up to mitochondrial degradation. From a mechanistic perspective, we show that AMPK promotes mitochondrial fission and autophagosomal engulfment of damaged mitochondria possibly via MFF and TBK1 phosphorylation respectively. Furthermore, this thesis also demonstrates that while it is possible to stimulate endogenous PINK1 kinase and Parkin E3 ligase activity in muscle, such activation requires prolonged, non-physiological stimulation. Alongside current literature our observations are consistent with the notion that the PINK1-Parkin signalling

axis likely plays a lesser in the orchestration of in skeletal muscle mitophagy under physiological conditions. Finally, we propose a working model of mitophagy in skeletal muscle through the steps of: mitochondrial fission, ubiquitylation, autophagosomal engulfment and degradation.

CHAPTER 7

REFERENCES

1. Sagan L. On the origin of mitosing cells. J Theor Biol. 1967;14(3):255-74.

2. Bonen L, Cunningham RS, Gray MW, Doolittle WF. Wheat embryo mitochondrial 18S ribosomal RNA: evidence for its prokaryotic nature. Nucleic Acids Res. 1977;4(3):663-71.

3. Schwartz RM, Dayhoff MO. Origins of prokaryotes, eukaryotes, mitochondria, and chloroplasts. Science (New York, NY). 1978;199(4327):395-403.

4. Yang D, Oyaizu Y, Oyaizu H, Olsen GJ, Woese CR. Mitochondrial origins. Proceedings of the National Academy of Sciences of the United States of America. 1985;82(13):4443-7.

5. Palade GE. An electron microscope study of the mitochondrial structure. J Histochem Cytochem. 1953;1(4):188-211.

6. Sjostrand FS. Electron microscopy of mitochondria and cytoplasmic double membranes. Nature. 1953;171(4340):30-2.

7. Mannella CA, Marko M, Penczek P, Barnard D, Frank J. The internal compartmentation of rat-liver mitochondria: tomographic study using the high-voltage transmission electron microscope. Microsc Res Tech. 1994;27(4):278-83.

8. Kirkwood SP, Munn EA, Brooks GA. Mitochondrial reticulum in limb skeletal muscle. Am J Physiol. 1986;251(3 Pt 1):C395-402.

9. Spinelli JB, Haigis MC. The multifaceted contributions of mitochondria to cellular metabolism. Nat Cell Biol. 2018;20(7):745-54.

10. De Stefani D, Rizzuto R, Pozzan T. Enjoy the Trip: Calcium in Mitochondria Back and Forth. Annu Rev Biochem. 2016;85:161-92.

11. Weinberg SE, Chandel NS. Targeting mitochondria metabolism for cancer therapy. Nature chemical biology. 2015;11(1):9-15.

12. Shadel GS, Horvath TL. Mitochondrial ROS signaling in organismal homeostasis. Cell. 2015;163(3):560-9.

13. Wang C, Youle RJ. The role of mitochondria in apoptosis*. Annu Rev Genet. 2009;43:95-118.

14. Bohovych I, Chan SS, Khalimonchuk O. Mitochondrial protein quality control: the mechanisms guarding mitochondrial health. Antioxid Redox Signal. 2015;22(12):977-94.

15. Pickles S, Vigie P, Youle RJ. Mitophagy and Quality Control Mechanisms in Mitochondrial Maintenance. Curr Biol. 2018;28(4):R170-r85.

16. Pfanner N. Protein sorting: recognizing mitochondrial presequences. Curr Biol. 2000;10(11):R412-5.

17. Tang JX, Thompson K, Taylor RW, Oláhová M. Mitochondrial OXPHOS Biogenesis: Co-Regulation of Protein Synthesis, Import, and Assembly Pathways. Int J Mol Sci. 2020;21(11).

18. Eisner V, Picard M, Hajnóczky G. Mitochondrial dynamics in adaptive and maladaptive cellular stress responses. Nat Cell Biol. 2018;20(7):755-65.

19. Mishra P, Chan DC. Metabolic regulation of mitochondrial dynamics. The Journal of cell biology. 2016;212(4):379-87.

20. Westermann B. Bioenergetic role of mitochondrial fusion and fission. Biochim Biophys Acta. 2012;1817(10):1833-8.

21. Westermann B. Mitochondrial fusion and fission in cell life and death. Nat Rev Mol Cell Biol. 2010;11(12):872-84.

22. Hoppins S, Lackner L, Nunnari J. The machines that divide and fuse mitochondria. Annu Rev Biochem. 2007;76:751-80.

23. Smirnova E, Griparic L, Shurland DL, van der Bliek AM. Dynamin-related protein Drp1 is required for mitochondrial division in mammalian cells. Mol Biol Cell. 2001;12(8):2245-56.

24. Loson OC, Song Z, Chen H, Chan DC. Fis1, Mff, MiD49, and MiD51 mediate Drp1 recruitment in mitochondrial fission. Mol Biol Cell. 2013;24(5):659-67.

25. Kraus F, Ryan MT. The constriction and scission machineries involved in mitochondrial fission. J Cell Sci. 2017;130(18):2953-60.

26. Youle RJ, van der Bliek AM. Mitochondrial fission, fusion, and stress. Science (New York, NY). 2012;337(6098):1062-5.

27. Sugiura A, McLelland GL, Fon EA, McBride HM. A new pathway for mitochondrial quality control: mitochondrial-derived vesicles. Embo J. 2014;33(19):2142-56.

28. Lewis MR, Lewis WH. MITOCHONDRIA IN TISSUE CULTURE. Science (New York, NY). 1914;39(1000):330-3.

29. Ashford TP, Porter KR. Cytoplasmic components in hepatic cell lysosomes. The Journal of cell biology. 1962;12(1):198-202.

30. Clark SL, Jr. Cellular differentiation in the kidneys of newborn mice studies with the electron microscope. J Biophys Biochem Cytol. 1957;3(3):349-62.

31. Novikoff AB, Essner E. Cytolysomes and mitochondrial degeneration. The Journal of cell biology. 1962;15(1):140-6.

32. De Duve C. The lysosome. Sci Am. 1963;208:64-72.

33. De Duve C, Wattiaux R. Functions of lysosomes. Annu Rev Physiol. 1966;28:435-92.

34. Beaulaton J, Lockshin RA. Ultrastructural study of the normal degeneration of the intersegmental muscles of Anthereae polyphemus and Manduca sexta (Insecta, Lepidoptera) with particular reference of cellular autophagy. J Morphol. 1977;154(1):39-57.

35. Decker RS, Wildenthal K. Lysosomal alterations in hypoxic and reoxygenated hearts. I. Ultrastructural and cytochemical changes. Am J Pathol. 1980;98(2):425-44.

36. Heynen MJ, Verwilghen RL. A quantitative ultrastructural study of normal rat erythroblasts and reticulocytes. Cell Tissue Res. 1982;224(2):397-408.

37. Lemasters JJ. Selective mitochondrial autophagy, or mitophagy, as a targeted defense against oxidative stress, mitochondrial dysfunction, and aging. Rejuvenation Res. 2005;8(1):3-5.

38. Scott SV, Klionsky DJ. Delivery of proteins and organelles to the vacuole from the cytoplasm. Current opinion in cell biology. 1998;10(4):523-9.

39. Kanki T, Wang K, Cao Y, Baba M, Klionsky DJ. Atg32 is a mitochondrial protein that confers selectivity during mitophagy. Dev Cell. 2009;17(1):98-109.

40. Sandoval H, Thiagarajan P, Dasgupta SK, Schumacher A, Prchal JT, Chen M, et al. Essential role for Nix in autophagic maturation of erythroid cells. Nature. 2008;454(7201):232-5.

41. Schweers RL, Zhang J, Randall MS, Loyd MR, Li W, Dorsey FC, et al. NIX is required for programmed mitochondrial clearance during reticulocyte maturation. Proceedings of the National Academy of Sciences of the United States of America. 2007;104(49):19500-5.

42. Narendra D, Tanaka A, Suen DF, Youle RJ. Parkin is recruited selectively to impaired mitochondria and promotes their autophagy. Journal of Cell Biology. 2008;183(5):795-803.

43. Geisler S, Holmström KM, Skujat D, Fiesel FC, Rothfuss OC, Kahle PJ, et al. PINK1/Parkin-mediated mitophagy is dependent on VDAC1 and p62/SQSTM1. Nat Cell Biol. 2010;12(2):119-31.

44. Geisler S, Holmström KM, Treis A, Skujat D, Weber SS, Fiesel FC, et al. The PINK1/Parkin-mediated mitophagy is compromised by PD-associated mutations. Autophagy. 2010;6(7):871-8.

45. Matsuda N, Sato S, Shiba K, Okatsu K, Saisho K, Gautier CA, et al. PINK1 stabilized by mitochondrial depolarization recruits Parkin to damaged mitochondria and activates latent Parkin for mitophagy. The Journal of cell biology. 2010;189(2):211-21.

46. Narendra DP, Jin SM, Tanaka A, Suen DF, Gautier CA, Shen J, et al. PINK1 is selectively stabilized on impaired mitochondria to activate Parkin. PLoS Biol. 2010;8(1):e1000298.

47. Vives-Bauza C, Zhou C, Huang Y, Cui M, de Vries RL, Kim J, et al. PINK1-dependent recruitment of Parkin to mitochondria in mitophagy. Proceedings of the National Academy of Sciences of the United States of America. 2010;107(1):378-83.

48. McWilliams TG, Prescott AR, Allen GF, Tamjar J, Munson MJ, Thomson C, et al. mito-QC illuminates mitophagy and mitochondrial architecture in vivo. The Journal of cell biology. 2016;214(3):333-45.

49. McWilliams TG, Prescott AR, Montava-Garriga L, Ball G, Singh F, Barini E, et al. Basal Mitophagy Occurs Independently of PINK1 in Mouse Tissues of High Metabolic Demand. Cell metabolism. 2018;27(2):439-49.e5.

50. Sun N, Yun J, Liu J, Malide D, Liu C, Rovira, II, et al. Measuring In Vivo Mitophagy. Molecular cell. 2015;60(4):685-96.

51. Lee JJ, Sanchez-Martinez A, Zarate AM, Benincá C, Mayor U, Clague MJ, et al. Basal mitophagy is widespread in Drosophila but minimally affected by loss of Pink1 or parkin. The Journal of cell biology. 2018;217(5):1613-22.

52. Egan DF, Shackelford DB, Mihaylova MM, Gelino S, Kohnz RA, Mair W, et al. Phosphorylation of ULK1 (hATG1) by AMP-activated protein kinase connects energy sensing to mitophagy. Science (New York, NY). 2011;331(6016):456-61.

53. Liu L, Feng D, Chen G, Chen M, Zheng Q, Song P, et al. Mitochondrial outer-membrane protein FUNDC1 mediates hypoxia-induced mitophagy in mammalian cells. Nat Cell Biol. 2012;14(2):177-85.

54. Wu W, Tian W, Hu Z, Chen G, Huang L, Li W, et al. ULK1 translocates to mitochondria and phosphorylates FUNDC1 to regulate mitophagy. EMBO reports. 2014;15(5):566-75.

55. Georgakopoulos ND, Wells G, Campanella M. The pharmacological regulation of cellular mitophagy. Nature chemical biology. 2017;13(2):136-46.

56. Heytler PG. uncoupling of oxidative phosphorylation by carbonyl cyanide phenylhydrazones. I. Some characteristics of m-Cl-CCP action on mitochondria and chloroplasts. Biochemistry. 1963;2:357-61.

57. Villa E, Marchetti S, Ricci JE. No Parkin Zone: Mitophagy without Parkin. Trends in cell biology. 2018;28(11):882-95.

58. Laker RC, Drake JC, Wilson RJ, Lira VA, Lewellen BM, Ryall KA, et al. Ampk phosphorylation of Ulk1 is required for targeting of mitochondria to lysosomes in exercise-induced mitophagy. Nat Commun. 2017;8(1):548.

59. Tian W, Li W, Chen Y, Yan Z, Huang X, Zhuang H, et al. Phosphorylation of ULK1 by AMPK regulates translocation of ULK1 to mitochondria and mitophagy. FEBS Lett. 2015;589(15):1847-54.

60. Valente EM, Bentivoglio AR, Dixon PH, Ferraris A, Ialongo T, Frontali M, et al. Localization of a novel locus for autosomal recessive early-onset parkinsonism, PARK6, on human chromosome 1p35-p36. Am J Hum Genet. 2001;68(4):895-900.

61. Valente EM, Brancati F, Ferraris A, Graham EA, Davis MB, Breteler MM, et al. PARK6-linked parkinsonism occurs in several European families. Ann Neurol. 2002;51(1):14-8.

62. Kitada T, Asakawa S, Hattori N, Matsumine H, Yamamura Y, Minoshima S, et al. Mutations in the parkin gene cause autosomal recessive juvenile parkinsonism. Nature. 1998;392(6676):605-8.

63. Whitworth AJ, Pallanck LJ. PINK1/Parkin mitophagy and neurodegeneration-what do we really know in vivo? Curr Opin Genet Dev. 2017;44:47-53.

64. Yamano K, Youle RJ. PINK1 is degraded through the N-end rule pathway. Autophagy. 2013;9(11):1758-69.

65. Xiao B, Deng X, Lim GGY, Xie S, Zhou ZD, Lim KL, et al. Superoxide drives progression of Parkin/PINK1-dependent mitophagy following translocation of Parkin to mitochondria. Cell Death Dis. 2017;8(10):e3097.

66. Xiao B, Goh JY, Xiao L, Xian H, Lim KL, Liou YC. Reactive oxygen species trigger Parkin/PINK1 pathway-dependent mitophagy by inducing mitochondrial recruitment of Parkin. The Journal of biological chemistry. 2017;292(40):16697-708.

67. Suen DF, Narendra DP, Tanaka A, Manfredi G, Youle RJ. Parkin overexpression selects against a deleterious mtDNA mutation in heteroplasmic cybrid cells. Proceedings

of the National Academy of Sciences of the United States of America. 2010;107(26):11835-40.

68. McWilliams TG, Muqit MM. PINK1 and Parkin: emerging themes in mitochondrial homeostasis. Current opinion in cell biology. 2017;45:83-91.

69. Kane LA, Lazarou M, Fogel AI, Li Y, Yamano K, Sarraf SA, et al. PINK1 phosphorylates ubiquitin to activate Parkin E3 ubiquitin ligase activity. The Journal of cell biology. 2014;205(2):143-53.

70. Kazlauskaite A, Kondapalli C, Gourlay R, Campbell DG, Ritorto MS, Hofmann K, et al. Parkin is activated by PINK1-dependent phosphorylation of ubiquitin at Ser65. The Biochemical journal. 2014;460(1):127-39.

71. Koyano F, Okatsu K, Kosako H, Tamura Y, Go E, Kimura M, et al. Ubiquitin is phosphorylated by PINK1 to activate parkin. Nature. 2014;510(7503):162-6.

72. Wauer T, Simicek M, Schubert A, Komander D. Mechanism of phospho-ubiquitin-induced PARKIN activation. Nature. 2015;524(7565):370-4.

73. Kondapalli C, Kazlauskaite A, Zhang N, Woodroof HI, Campbell DG, Gourlay R, et al. PINK1 is activated by mitochondrial membrane potential depolarization and stimulates Parkin E3 ligase activity by phosphorylating Serine 65. Open biology. 2012;2(5):120080.

74. Kazlauskaite A, Martinez-Torres RJ, Wilkie S, Kumar A, Peltier J, Gonzalez A, et al. Binding to serine 65-phosphorylated ubiquitin primes Parkin for optimal PINK1-dependent phosphorylation and activation. EMBO reports. 2015;16(8):939-54.

75. Chan NC, Salazar AM, Pham AH, Sweredoski MJ, Kolawa NJ, Graham RL, et al. Broad activation of the ubiquitin-proteasome system by Parkin is critical for mitophagy. Human molecular genetics. 2011;20(9):1726-37.

76. Sarraf SA, Raman M, Guarani-Pereira V, Sowa ME, Huttlin EL, Gygi SP, et al. Landscape of the PARKIN-dependent ubiquitylome in response to mitochondrial depolarization. Nature. 2013;496(7445):372-6.

77. Yamano K, Matsuda N, Tanaka K. The ubiquitin signal and autophagy: an orchestrated dance leading to mitochondrial degradation. EMBO reports. 2016;17(3):300-16.

78. Lazarou M, Sliter DA, Kane LA, Sarraf SA, Wang C, Burman JL, et al. The ubiquitin kinase PINK1 recruits autophagy receptors to induce mitophagy. Nature. 2015;524(7565):309-14.

79. Chen Q, Sun L, Chen ZJ. Regulation and function of the cGAS-STING pathway of cytosolic DNA sensing. Nat Immunol. 2016;17(10):1142-9.

80. Matsumoto G, Shimogori T, Hattori N, Nukina N. TBK1 controls autophagosomal engulfment of polyubiquitinated mitochondria through p62/SQSTM1 phosphorylation. Human molecular genetics. 2015;24(15):4429-42.

81. Richter B, Sliter DA, Herhaus L, Stolz A, Wang C, Beli P, et al. Phosphorylation of OPTN by TBK1 enhances its binding to Ub chains and promotes selective autophagy of damaged mitochondria. Proceedings of the National Academy of Sciences of the United States of America. 2016;113(15):4039-44.

82. Vargas JNS, Wang C, Bunker E, Hao L, Maric D, Schiavo G, et al. Spatiotemporal Control of ULK1 Activation by NDP52 and TBK1 during Selective Autophagy. Molecular cell. 2019;74(2):347-62.e6.

83. Larabi A, Devos JM, Ng SL, Nanao MH, Round A, Maniatis T, et al. Crystal structure and mechanism of activation of TANK-binding kinase 1. Cell Rep. 2013;3(3):734-46.

84. Heo JM, Ordureau A, Paulo JA, Rinehart J, Harper JW. The PINK1-PARKIN Mitochondrial Ubiquitylation Pathway Drives a Program of OPTN/NDP52 Recruitment and TBK1 Activation to Promote Mitophagy. Molecular cell. 2015;60(1):7-20.

85. Yun J, Puri R, Yang H, Lizzio MA, Wu C, Sheng ZH, et al. MUL1 acts in parallel to the PINK1/parkin pathway in regulating mitofusin and compensates for loss of PINK1/parkin. Elife. 2014;3:e01958.

86. Braschi E, Zunino R, McBride HM. MAPL is a new mitochondrial SUMO E3 ligase that regulates mitochondrial fission. EMBO reports. 2009;10(7):748-54.

87. Prudent J, Zunino R, Sugiura A, Mattie S, Shore GC, McBride HM. MAPL SUMOylation of Drp1 Stabilizes an ER/Mitochondrial Platform Required for Cell Death. Molecular cell. 2015;59(6):941-55.

88. Puri R, Cheng XT, Lin MY, Huang N, Sheng ZH. Mul1 restrains Parkin-mediated mitophagy in mature neurons by maintaining ER-mitochondrial contacts. Nat Commun. 2019;10(1):3645.

89. Li J, Qi W, Chen G, Feng D, Liu J, Ma B, et al. Mitochondrial outer-membrane E3 ligase MUL1 ubiquitinates ULK1 and regulates selenite-induced mitophagy. Autophagy. 2015;11(8):1216-29.

90. Ambivero CT, Cilenti L, Main S, Zervos AS. Mulan E3 ubiquitin ligase interacts with multiple E2 conjugating enzymes and participates in mitophagy by recruiting GABARAP. Cell Signal. 2014;26(12):2921-9.

91. Villa E, Proïcs E, Rubio-Patiño C, Obba S, Zunino B, Bossowski JP, et al. Parkin-Independent Mitophagy Controls Chemotherapeutic Response in Cancer Cells. Cell Rep. 2017;20(12):2846-59.

92. Zhang J, Ney PA. Role of BNIP3 and NIX in cell death, autophagy, and mitophagy. Cell Death Differ. 2009;16(7):939-46.

93. Matsushima M, Fujiwara T, Takahashi E, Minaguchi T, Eguchi Y, Tsujimoto Y, et al. Isolation, mapping, and functional analysis of a novel human cDNA (BNIP3L) encoding a protein homologous to human NIP3. Genes Chromosomes Cancer. 1998;21(3):230-5.

94. Birgisdottir Å B, Lamark T, Johansen T. The LIR motif - crucial for selective autophagy. J Cell Sci. 2013;126(Pt 15):3237-47.

95. Hanna RA, Quinsay MN, Orogo AM, Giang K, Rikka S, Gustafsson Å B. Microtubule-associated protein 1 light chain 3 (LC3) interacts with Bnip3 protein to selectively remove endoplasmic reticulum and mitochondria via autophagy. The Journal of biological chemistry. 2012;287(23):19094-104.

96. Novak I, Kirkin V, McEwan DG, Zhang J, Wild P, Rozenknop A, et al. Nix is a selective autophagy receptor for mitochondrial clearance. EMBO reports. 2010;11(1):45-51.

97. Zhu Y, Massen S, Terenzio M, Lang V, Chen-Lindner S, Eils R, et al. Modulation of serines 17 and 24 in the LC3-interacting region of Bnip3 determines pro-survival mitophagy versus apoptosis. The Journal of biological chemistry. 2013;288(2):1099-113.

98. Rogov VV, Suzuki H, Marinković M, Lang V, Kato R, Kawasaki M, et al. Phosphorylation of the mitochondrial autophagy receptor Nix enhances its interaction with LC3 proteins. Sci Rep. 2017;7(1):1131.

99. Gao F, Chen D, Si J, Hu Q, Qin Z, Fang M, et al. The mitochondrial protein BNIP3L is the substrate of PARK2 and mediates mitophagy in PINK1/PARK2 pathway. Human molecular genetics. 2015;24(9):2528-38.

100. Zhang T, Xue L, Li L, Tang C, Wan Z, Wang R, et al. BNIP3 Protein Suppresses PINK1 Kinase Proteolytic Cleavage to Promote Mitophagy. The Journal of biological chemistry. 2016;291(41):21616-29.

101. Chen G, Han Z, Feng D, Chen Y, Chen L, Wu H, et al. A regulatory signaling loop comprising the PGAM5 phosphatase and CK2 controls receptor-mediated mitophagy. Molecular cell. 2014;54(3):362-77.

102. Wu H, Xue D, Chen G, Han Z, Huang L, Zhu C, et al. The BCL2L1 and PGAM5 axis defines hypoxia-induced receptor-mediated mitophagy. Autophagy. 2014;10(10):1712-25.

103. Chen Z, Liu L, Cheng Q, Li Y, Wu H, Zhang W, et al. Mitochondrial E3 ligase MARCH5 regulates FUNDC1 to fine-tune hypoxic mitophagy. EMBO reports. 2017;18(3):495-509.

104. Murakawa T, Yamaguchi O, Hashimoto A, Hikoso S, Takeda T, Oka T, et al. c. Nat Commun. 2015;6:7527.

105. Murakawa T, Okamoto K, Omiya S, Taneike M, Yamaguchi O, Otsu K. A Mammalian Mitophagy Receptor, Bcl2-L-13, Recruits the ULK1 Complex to Induce Mitophagy. Cell Rep. 2019;26(2):338-45.e6.

106. Edlich F, Lücke C. From cell death to viral replication: the diverse functions of the membrane-associated FKBP38. Curr Opin Pharmacol. 2011;11(4):348-53.

107. Bhujabal Z, Birgisdottir Å B, Sjøttem E, Brenne HB, Øvervatn A, Habisov S, et al. FKBP8 recruits LC3A to mediate Parkin-independent mitophagy. EMBO reports. 2017;18(6):947-61.

108. Saita S, Shirane M, Nakayama KI. Selective escape of proteins from the mitochondria during mitophagy. Nat Commun. 2013;4:1410.

109. Yoo SM, Yamashita SI, Kim H, Na D, Lee H, Kim SJ, et al. FKBP8 LIRL-dependent mitochondrial fragmentation facilitates mitophagy under stress conditions. Faseb j. 2020;34(2):2944-57.

110. Maguire JJ, Tyurina YY, Mohammadyani D, Kapralov AA, Anthonymuthu TS, Qu F, et al. Known unknowns of cardiolipin signaling: The best is yet to come. Biochim Biophys Acta Mol Cell Biol Lipids. 2017;1862(1):8-24.

111. Chu CT, Ji J, Dagda RK, Jiang JF, Tyurina YY, Kapralov AA, et al. Cardiolipin externalization to the outer mitochondrial membrane acts as an elimination signal for mitophagy in neuronal cells. Nat Cell Biol. 2013;15(10):1197-205.

112. Kagan VE, Jiang J, Huang Z, Tyurina YY, Desbourdes C, Cottet-Rousselle C, et al. NDPK-D (NM23-H4)-mediated externalization of cardiolipin enables elimination of depolarized mitochondria by mitophagy. Cell Death Differ. 2016;23(7):1140-51.

113. McWilliams TG, Ganley IG. Investigating Mitophagy and Mitochondrial Morphology In Vivo Using mito-QC: A Comprehensive Guide. Methods Mol Biol. 2019;1880:621-42.

114. Allen GF, Toth R, James J, Ganley IG. Loss of iron triggers PINK1/Parkin-independent mitophagy. EMBO reports. 2013;14(12):1127-35.

115. Katayama H, Kogure T, Mizushima N, Yoshimori T, Miyawaki A. A sensitive and quantitative technique for detecting autophagic events based on lysosomal delivery. Chem Biol. 2011;18(8):1042-52.

116. Hernandez G, Thornton C, Stotland A, Lui D, Sin J, Ramil J, et al. MitoTimer: a novel tool for monitoring mitochondrial turnover. Autophagy. 2013;9(11):1852-61.

117. Wilson RJ, Drake JC, Cui D, Zhang M, Perry HM, Kashatus JA, et al. Conditional MitoTimer reporter mice for assessment of mitochondrial structure, oxidative stress, and mitophagy. Mitochondrion. 2019;44:20-6.

118. Terskikh A, Fradkov A, Ermakova G, Zaraisky A, Tan P, Kajava AV, et al. "Fluorescent timer": protein that changes color with time. Science (New York, NY). 2000;290(5496):1585-8.

119. Verkhusha VV, Chudakov DM, Gurskaya NG, Lukyanov S, Lukyanov KA. Common pathway for the red chromophore formation in fluorescent proteins and chromoproteins. Chem Biol. 2004;11(6):845-54.

120. Yarbrough D, Wachter RM, Kallio K, Matz MV, Remington SJ. Refined crystal structure of DsRed, a red fluorescent protein from coral, at 2.0-A resolution. Proceedings of the National Academy of Sciences of the United States of America. 2001;98(2):462-7.

121. Biazik J, Yla-Anttila P, Vihinen H, Jokitalo E, Eskelinen EL. Ultrastructural relationship of the phagophore with surrounding organelles. Autophagy. 2015;11(3):439-51.

122. Hailey DW, Rambold AS, Satpute-Krishnan P, Mitra K, Sougrat R, Kim PK, et al. Mitochondria supply membranes for autophagosome biogenesis during starvation. Cell. 2010;141(4):656-67.

123. Hamasaki M, Furuta N, Matsuda A, Nezu A, Yamamoto A, Fujita N, et al. Autophagosomes form at ER-mitochondria contact sites. Nature. 2013;495(7441):389-93.

124. Wong YC, Ysselstein D, Krainc D. Mitochondria-lysosome contacts regulate mitochondrial fission via RAB7 GTP hydrolysis. Nature. 2018;554(7692):382-6.

125. Rodger CE, McWilliams TG, Ganley IG. Mammalian mitophagy - from in vitro molecules to in vivo models. Febs j. 2018;285(7):1185-202.

126. Katayama H, Hama H, Nagasawa K, Kurokawa H, Sugiyama M, Ando R, et al. Visualizing and Modulating Mitophagy for Therapeutic Studies of Neurodegeneration. Cell. 2020;181(5):1176-87.e16.

127. Ghoda L, Sidney D, Macrae M, Coffino P. Structural elements of ornithine decarboxylase required for intracellular degradation and polyamine-dependent regulation. Mol Cell Biol. 1992;12(5):2178-85.

128. Gilon T, Chomsky O, Kulka RG. Degradation signals for ubiquitin system proteolysis in Saccharomyces cerevisiae. Embo J. 1998;17(10):2759-66.

129. Carter HN, Kim Y, Erlich AT, Zarrin-khat D, Hood DA. Autophagy and mitophagy flux in young and aged skeletal muscle following chronic contractile activity. J Physiol-London. 2018;596(16):3567-84.

130. Chen CCW, Erlich AT, Crilly MJ, Hood DA. Parkin is required for exercise-induced mitophagy in muscle: impact of aging. Am J Physiol Endocrinol Metab. 2018;315(3):E404-e15.

131. Chen CCW, Erlich AT, Hood DA. Role of Parkin and endurance training on mitochondrial turnover in skeletal muscle. Skelet Muscle. 2018;8(1):10.

132. Parousis A, Carter HN, Tran C, Erlich AT, Mesbah Moosavi ZS, Pauly M, et al. Contractile activity attenuates autophagy suppression and reverses mitochondrial defects in skeletal muscle cells. Autophagy. 2018;14(11):1886-97.

133. Vainshtein A, Tryon LD, Pauly M, Hood DA. Role of PGC-1alpha during acute exercise-induced autophagy and mitophagy in skeletal muscle. Am J Physiol Cell Physiol. 2015;308(9):C710-9.

134. Moulis M, Vindis C. Methods for Measuring Autophagy in Mice. Cells. 2017;6(2).

135. Zurlo F, Larson K, Bogardus C, Ravussin E. Skeletal muscle metabolism is a major determinant of resting energy expenditure. J Clin Invest. 1990;86(5):1423-7.

136. Cruz-Jentoft AJ, Bahat G, Bauer J, Boirie Y, Bruyère O, Cederholm T, et al. Sarcopenia: revised European consensus on definition and diagnosis. Age Ageing. 2019;48(4):601.

137. Janssen I, Heymsfield SB, Ross R. Low relative skeletal muscle mass (sarcopenia) in older persons is associated with functional impairment and physical disability. J Am Geriatr Soc. 2002;50(5):889-96.

138. Janssen I, Shepard DS, Katzmarzyk PT, Roubenoff R. The healthcare costs of sarcopenia in the United States. J Am Geriatr Soc. 2004;52(1):80-5.

139. Romanello V, Sandri M. Mitochondrial Quality Control and Muscle Mass Maintenance. Front Physiol. 2015;6:422.

140. Drake JC, Yan Z. Mitophagy in maintaining skeletal muscle mitochondrial proteostasis and metabolic health with ageing. The Journal of physiology. 2017;595(20):6391-9.

141. Beltran Valls MR, Wilkinson DJ, Narici MV, Smith K, Phillips BE, Caporossi D, et al. Protein carbonylation and heat shock proteins in human skeletal muscle: relationships to age and sarcopenia. The journals of gerontology Series A, Biological sciences and medical sciences. 2015;70(2):174-81.

142. Conley KE, Jubrias SA, Esselman PC. Oxidative capacity and ageing in human muscle. The Journal of physiology. 2000;526 Pt 1(Pt 1):203-10.

143. Short KR, Bigelow ML, Kahl J, Singh R, Coenen-Schimke J, Raghavakaimal S, et al. Decline in skeletal muscle mitochondrial function with aging in humans. Proceedings of the National Academy of Sciences of the United States of America. 2005;102(15):5618-23.

144. Tonkonogi M, Fernström M, Walsh B, Ji LL, Rooyackers O, Hammarqvist F, et al. Reduced oxidative power but unchanged antioxidative capacity in skeletal muscle from aged humans. Pflugers Arch. 2003;446(2):261-9.

145. Trounce I, Byrne E, Marzuki S. Decline in skeletal muscle mitochondrial respiratory chain function: possible factor in ageing. Lancet. 1989;1(8639):637-9.

146. Ryu D, Mouchiroud L, Andreux PA, Katsyuba E, Moullan N, Nicolet-Dit-Felix AA, et al. Urolithin A induces mitophagy and prolongs lifespan in C. elegans and increases muscle function in rodents. Nature medicine. 2016;22(8):879-88.

147. Montava-Garriga L, Singh F, Ball G, Ganley IG. Semi-automated quantitation of mitophagy in cells and tissues. Mech Ageing Dev. 2020;185:111196.

148. Abdelmoez AM, Sardón Puig L, Smith JAB, Gabriel BM, Savikj M, Dollet L, et al. Comparative profiling of skeletal muscle models reveals heterogeneity of transcriptome and metabolism. Am J Physiol Cell Physiol. 2020;318(3):C615-c26.

149. Kim YY, Um JH, Yoon JH, Kim H, Lee DY, Lee YJ, et al. Assessment of mitophagy in mt-Keima Drosophila revealed an essential role of the PINK1-Parkin pathway in mitophagy induction in vivo. Faseb j. 2019;33(9):9742-51.

150. Nisr RB, Shah DS, Ganley IG, Hundal HS. Proinflammatory NFkB signalling promotes mitochondrial dysfunction in skeletal muscle in response to cellular fuel overloading. Cell Mol Life Sci. 2019;76(24):4887-904.

151. Peker N, Donipadi V, Sharma M, McFarlane C, Kambadur R. Loss of Parkin impairs mitochondrial function and leads to muscle atrophy. Am J Physiol Cell Physiol. 2018;315(2):C164-c85.

152. Seabright AP, Fine NHF, Barlow JP, Lord SO, Musa I, Gray A, et al. AMPK activation induces mitophagy and promotes mitochondrial fission while activating TBK1 in a PINK1-Parkin independent manner. Faseb j. 2020;34(5):6284-301.

153. Borgia D, Malena A, Spinazzi M, Desbats MA, Salviati L, Russell AP, et al. Increased mitophagy in the skeletal muscle of spinal and bulbar muscular atrophy patients. Human molecular genetics. 2017;26(6):1087-103.

154. Drake JC, Laker RC, Wilson RJ, Zhang M, Yan Z. Exercise-induced mitophagy in skeletal muscle occurs in the absence of stabilization of Pink1 on mitochondria. Cell Cycle. 2019;18(1):1-6.

155. Fu T, Xu Z, Liu L, Guo Q, Wu H, Liang X, et al. Mitophagy Directs Muscle-Adipose Crosstalk to Alleviate Dietary Obesity. Cell Rep. 2018;23(5):1357-72.

156. Leermakers PA, Kneppers AEM, Schols A, Kelders M, de Theije CC, Verdijk LB, et al. Skeletal muscle unloading results in increased mitophagy and decreased mitochondrial biogenesis regulation. Muscle Nerve. 2019;60(6):769-78.

157. Leermakers PA, Schols A, Kneppers AEM, Kelders M, de Theije CC, Lainscak M, et al. Molecular signalling towards mitochondrial breakdown is enhanced in skeletal muscle of patients with chronic obstructive pulmonary disease (COPD). Sci Rep. 2018;8(1):15007.

158. Walsh TG, van den Bosch MTJ, Lewis KE, Williams CM, Poole AW. Loss of the mitochondrial kinase PINK1 does not alter platelet function. Sci Rep. 2018;8(1):14377.

159. Kuroda Y, Mitsui T, Kunishige M, Shono M, Akaike M, Azuma H, et al. Parkin enhances mitochondrial biogenesis in proliferating cells. Human molecular genetics. 2006;15(6):883-95.

160. Leduc-Gaudet JP, Reynaud O, Hussain SN, Gouspillou G. Parkin overexpression protects from ageing-related loss of muscle mass and strength. The Journal of physiology. 2019;597(7):1975-91.

161. Stevens DA, Lee Y, Kang HC, Lee BD, Lee YI, Bower A, et al. Parkin loss leads to PARIS-dependent declines in mitochondrial mass and respiration. Proceedings of the National Academy of Sciences of the United States of America. 2015;112(37):11696-701.

162. Lai YC, Kondapalli C, Lehneck R, Procter JB, Dill BD, Woodroof HI, et al. Phosphoproteomic screening identifies Rab GTPases as novel downstream targets of PINK1. Embo J. 2015;34(22):2840-61.

163. Hood DA, Memme JM, Oliveira AN, Triolo M. Maintenance of Skeletal Muscle Mitochondria in Health, Exercise, and Aging. Annu Rev Physiol. 2019;81:19-41.

164. Chu CT. Mechanisms of selective autophagy and mitophagy: Implications for neurodegenerative diseases. Neurobiology of disease. 2019;122:23-34.

165. Wild P, Farhan H, McEwan DG, Wagner S, Rogov VV, Brady NR, et al. Phosphorylation of the Autophagy Receptor Optineurin Restricts Salmonella Growth. Science (New York, NY). 2011;333(6039):228-33.

166. Heo JM, Ordureau A, Swarup S, Paulo JA, Shen K, Sabatini DM, et al. RAB7A phosphorylation by TBK1 promotes mitophagy via the PINK-PARKIN pathway. Sci Adv. 2018;4(11):eaav0443.

167. Van Humbeeck C, Cornelissen T, Hofkens H, Mandemakers W, Gevaert K, De Strooper B, et al. Parkin interacts with Ambra1 to induce mitophagy. Movement Disord. 2011;26:S29-S.

168. Ducommun S, Deak M, Sumpton D, Ford RJ, Nunez Galindo A, Kussmann M, et al. Motif affinity and mass spectrometry proteomic approach for the discovery of cellular AMPK targets: identification of mitochondrial fission factor as a new AMPK substrate. Cell Signal. 2015;27(5):978-88.

169. Toyama EQ, Herzig S, Courchet J, Lewis TL, Jr., Loson OC, Hellberg K, et al. Metabolism. AMP-activated protein kinase mediates mitochondrial fission in response to energy stress. Science (New York, NY). 2016;351(6270):275-81.

170. Burman JL, Pickles S, Wang CX, Sekine S, Vargas JNS, Zhang Z, et al. Mitochondrial fission facilitates the selective mitophagy of protein aggregates. Journal of Cell Biology. 2017;216(10):3231-47.

171. Fogarty S, Ross FA, Vara Ciruelos D, Gray A, Gowans GJ, Hardie DG. AMPK Causes Cell Cycle Arrest in LKB1-Deficient Cells via Activation of CAMKK2. Mol Cancer Res. 2016;14(8):683-95.

172. Affourtit C, Brand MD. Measuring mitochondrial bioenergetics in INS-1E insulinoma cells. Methods in enzymology. 2009;457:405-24.

173. Ordureau A, Sarraf SA, Duda DM, Heo JM, Jedrychowski MP, Sviderskiy VO, et al. Quantitative proteomics reveal a feedforward mechanism for mitochondrial PARKIN translocation and ubiquitin chain synthesis. Molecular cell. 2014;56(3):360-75.

174. Denison SR, Wang F, Becker NA, Schule B, Kock N, Phillips LA, et al. Alterations in the common fragile site gene Parkin in ovarian and other cancers. Oncogene. 2003;22(51):8370-8.

175. Bultot L, Jensen TE, Lai YC, Madsen AL, Collodet C, Kviklyte S, et al. Benzimidazole derivative small-molecule 991 enhances AMPK activity and glucose uptake induced by AICAR or contraction in skeletal muscle. Am J Physiol Endocrinol Metab. 2016;311(4):E706-E19.

176. Lai YC, Kviklyte S, Vertommen D, Lantier L, Foretz M, Viollet B, et al. A small-molecule benzimidazole derivative that potently activates AMPK to increase glucose transport in skeletal muscle: comparison with effects of contraction and other AMPK activators. Biochemical Journal. 2014;460:363-75.

177. Hoffman NJ, Parker BL, Chaudhuri R, Fisher-Wellman KH, Kleinert M, Humphrey SJ, et al. Global Phosphoproteomic Analysis of Human Skeletal Muscle Reveals a Network of Exercise-Regulated Kinases and AMPK Substrates. Cell metabolism. 2015;22(5):922-35.

178. Kim J, Kundu M, Viollet B, Guan KL. AMPK and mTOR regulate autophagy through direct phosphorylation of Ulk1. Nature Cell Biology. 2011;13(2):132-U71.

179. Shang L, Chen S, Du F, Li S, Zhao L, Wang X. Nutrient starvation elicits an acute autophagic response mediated by Ulk1 dephosphorylation and its subsequent dissociation from AMPK. Proceedings of the National Academy of Sciences of the United States of America. 2011;108(12):4788-93.

180. Bach M, Larance M, James DE, Ramm G. The serine/threonine kinase ULK1 is a target of multiple phosphorylation events. Biochemical Journal. 2011;440:283-91.

181. Zhao P, Wong KI, Sun X, Reilly SM, Uhm M, Liao Z, et al. TBK1 at the Crossroads of Inflammation and Energy Homeostasis in Adipose Tissue. Cell. 2018;172(4):731-43.e12.

182. Burchell L, Chaugule VK, Walden H. Small, N-terminal tags activate Parkin E3 ubiquitin ligase activity by disrupting its autoinhibited conformation. PLoS One. 2012;7(4):e34748.

183. Rakovic A, Shurkewitsch K, Seibler P, Grunewald A, Zanon A, Hagenah J, et al. Phosphatase and tensin homolog (PTEN)-induced putative kinase 1 (PINK1)-dependent ubiquitination of endogenous Parkin attenuates mitophagy: study in human primary fibroblasts and induced pluripotent stem cell-derived neurons. The Journal of biological chemistry. 2013;288(4):2223-37.

184. Emmerich CH, Cohen P. Optimising methods for the preservation, capture and identification of ubiquitin chains and ubiquitylated proteins by immunoblotting. Biochem Biophys Res Commun. 2015;466(1):1-14.

185. Fonseca TB, Sanchez-Guerrero A, Milosevic I, Raimundo N. Mitochondrial fission requires DRP1 but not dynamins. Nature. 2019;570(7761):E34-e42.

186. Liu R, Chan DC. The mitochondrial fission receptor Mff selectively recruits oligomerized Drp1. Mol Biol Cell. 2015;26(24):4466-77.

187. Gan Z, Fu T, Kelly DP, Vega RB. Skeletal muscle mitochondrial remodeling in exercise and diseases. Cell Res. 2018;28(10):969-80.

188. Otera H, Wang C, Cleland MM, Setoguchi K, Yokota S, Youle RJ, et al. Mff is an essential factor for mitochondrial recruitment of Drp1 during mitochondrial fission in mammalian cells. The Journal of cell biology. 2010;191(6):1141-58.

189. Bakula D, Scheibye-Knudsen M. MitophAging: Mitophagy in Aging and Disease. Front Cell Dev Biol. 2020;8:239.

190. Zimmermann M, Reichert AS. How to get rid of mitochondria: crosstalk and regulation of multiple mitophagy pathways. Biol Chem. 2017;399(1):29-45.

191. Balan E, Schwalm C, Naslain D, Nielens H, Francaux M, Deldicque L. Regular Endurance Exercise Promotes Fission, Mitophagy, and Oxidative Phosphorylation in Human Skeletal Muscle Independently of Age. Front Physiol. 2019;10:1088.

192. Brandt N, Gunnarsson TP, Bangsbo J, Pilegaard H. Exercise and exercise training-induced increase in autophagy markers in human skeletal muscle. Physiol Rep. 2018;6(7):e13651.

193. Schwalm C, Deldicque L, Francaux M. Lack of Activation of Mitophagy during Endurance Exercise in Human. Med Sci Sports Exerc. 2017;49(8):1552-61.

194. Yu W, Sun Y, Guo S, Lu B. The PINK1/Parkin pathway regulates mitochondrial dynamics and function in mammalian hippocampal and dopaminergic neurons. Human molecular genetics. 2011;20(16):3227-40.

195. Yang Y, Ouyang Y, Yang L, Beal MF, McQuibban A, Vogel H, et al. Pink1 regulates mitochondrial dynamics through interaction with the fission/fusion machinery. Proceedings of the National Academy of Sciences of the United States of America. 2008;105(19):7070-5.

196. Buhlman L, Damiano M, Bertolin G, Ferrando-Miguel R, Lombès A, Brice A, et al. Functional interplay between Parkin and Drp1 in mitochondrial fission and clearance. Biochim Biophys Acta. 2014;1843(9):2012-26.

197. Favaro G, Romanello V, Varanita T, Andrea Desbats M, Morbidoni V, Tezze C, et al. DRP1-mediated mitochondrial shape controls calcium homeostasis and muscle mass. Nat Commun. 2019;10(1):2576.

198. Lee JY, Nagano Y, Taylor JP, Lim KL, Yao TP. Disease-causing mutations in parkin impair mitochondrial ubiquitination, aggregation, and HDAC6-dependent mitophagy. The Journal of cell biology. 2010;189(4):671-9.

199. Garcia D, Shaw RJ. AMPK: Mechanisms of Cellular Energy Sensing and Restoration of Metabolic Balance. Molecular cell. 2017;66(6):789-800.

200. Inoki K, Zhu T, Guan KL. TSC2 mediates cellular energy response to control cell growth and survival. Cell. 2003;115(5):577-90.

201. Jäger S, Handschin C, St-Pierre J, Spiegelman BM. AMP-activated protein kinase (AMPK) action in skeletal muscle via direct phosphorylation of PGC-1alpha. Proceedings of the National Academy of Sciences of the United States of America. 2007;104(29):12017-22.

202. Taguchi N, Ishihara N, Jofuku A, Oka T, Mihara K. Mitotic phosphorylation of dynamin-related GTPase Drp1 participates in mitochondrial fission. The Journal of biological chemistry. 2007;282(15):11521-9.

203. Wang B, Nie J, Wu L, Hu Y, Wen Z, Dong L, et al. AMPKα2 Protects Against the Development of Heart Failure by Enhancing Mitophagy via PINK1 Phosphorylation. Circ Res. 2018;122(5):712-29.

204. Lee SB, Kim JJ, Han SA, Fan Y, Guo LS, Aziz K, et al. The AMPK-Parkin axis negatively regulates necroptosis and tumorigenesis by inhibiting the necrosome. Nat Cell Biol. 2019;21(8):940-51.

205. Evers-van Gogh IJ, Alex S, Stienstra R, Brenkman AB, Kersten S, Kalkhoven E. Electric Pulse Stimulation of Myotubes as an In Vitro Exercise Model: Cell-Mediated and Non-Cell-Mediated Effects. Sci Rep. 2015;5:10944.

206. Stein SC, Woods A, Jones NA, Davison MD, Carling D. The regulation of AMP-activated protein kinase by phosphorylation. The Biochemical journal. 2000;345 Pt 3(Pt 3):437-43.